Title
Chemical and Genetic Tools for Probing the Cooperativity of Molecular Chaperones

Author
Taylor, Isabelle

Publication Date
2018

Peer reviewed|Thesis/dissertation

Chemical and Genetic Tools for Probing the Cooperativity of Molecular Chaperones

by

Isabelle R. Taylor

DISSERTATION

Submitted in partial satisfaction of the requirements for the degree of

DOCTOR OF PHILOSOPHY

in

Chemistry and Chemical Biology

in the

GRADUATE DIVISION

of the

UNIVERSITY OF CALIFORNIA, SAN FRANCISCO

[redacted]

This thesis contains work adapted from, or as it appears in the following publications:

1. Li X, Shao H, Taylor IR, Gestwicki JE “Targeting allosteric control mechanisms of heat shock protein 70 (Hsp70)” *Curr Top Med Chem* (2016)
2. Taylor IR, Dunyak BM, Komiyama T, Shao H, Ran X, Assimon VA, Kalyanaraman C, Rauch JN, Jacobson MP, Zuiderweg ERP, Gestwicki JE “High throughput screen for inhibitors of protein-protein interactions in a reconstituted heat shock protein 70 (Hsp70) complex” *J Biol Chem* (2018)

Dedicated to my mom, Jane Bealer. She is the true detective of our family – everything I know about seeking the truth, I learned from her.

Acknowledgements

There is no way I will be able to thank everyone who has helped me get to this point, but there are several people who need to be recognized. I am fortunate enough to have completed my PhD in one of the most supportive labs at UCSF. For that, I have to thank my advisor, Jason Gestwicki. His patience, and the time he took throughout my years in the lab to find opportunities that would further my education and career, have been truly vital to my training as a scientist.

I would like to thank every member of the Gestwicki Lab, past and present. In particular, Xiaokai and Hao for their chemical expertise and ideas about Hsp70 (and Hsp60) inhibitors as highlighted in Chapter 1, Bryan for being my mentor in the early days and for getting me started on the work presented in Chapter 2, Victoria for being a great friend and collaborator on all things DnaK, and Tomoko for her amazing work on the high throughput screen described in Chapter 2. I would also like to thank Martin Kampmann, and the entire Kampmann lab, for their contributions and advice regarding functional genomics, without which Chapter 3 would not have been possible.

The program at UCSF, and our various collaborations have provided many resources that were essential to the completion of this PhD. However, there are certain external sources that were unsung “heroes” in this process, and they have to be acknowledged. I must thank David Bowie for the tunes, Oliver Sacks for the reading, BurgerMeister for the food, and the Walgreens on Stanyan for the Swedish Fish.

I have several friends to thank for their continued support, both scientific and emotional. Thank you to my CCB classmates – our weekly lunches were key to my survival through this program. Thank you to my friends from home: Christina, Bree,

Brooke, and Sara. And thank you to my Bard Team Chem family: Nicole, Madison, Eli, and Youseung. I am so proud of all of you.

Finally, I have to thank my family for their unconditional love and support: my parents for always believing in me, and my sister, Dana, for sending me so many pictures of puppies. I am so lucky to have you all in my life.

Chemical and Genetic Tools for Probing the Cooperativity of Molecular Chaperones

By Isabelle R. Taylor

Abstract:

The cytosol of the mammalian cell is a highly crowded environment, where all of the molecular processes necessary for sustaining life take place. In order to maintain a healthy balance of protein synthesis, folding, trafficking, and degradation in this environment, the cell relies heavily on a class of proteins known as molecular chaperones. These chaperones, such as the 70 and 90 kDa heat shock proteins (Hsp70 and Hsp90), are the most abundant proteins in the cell, and make up a highly interconnected, cooperative network of hundreds of individual members. Recent efforts have been made to explore chaperones as drug targets, due to their implications in various diseases, including cancer and neurodegeneration. However, these proteins have proven to be extremely difficult drug targets, in large part due to the complexity of their functions in a cell. It has become increasingly clear that before we can develop successful therapeutics for this system, there is a need for new tools to dissect the underlying biology of the chaperone network.

This thesis describes efforts from our group toward building a set of tools to study the cooperative nature of molecular chaperones. This cooperation exists on various levels, from the interdomain allostery of the Hsp70 protein itself, to this chaperone's interactions with its co-chaperones, and ultimately its role in the greater network of protein homeostasis (proteostasis). We carried out a high throughput ATPase screen to identify a new chemical scaffold for inhibiting the interaction of Hsp70 with its nucleotide

exchange factor class of co-chaperones. This inhibitor series was further optimized through synthetic diversification, and secondary biochemical assays. Additionally, we aimed to increase the power of established chemical probes by combining them with a chaperone-centric functional genomic platform, in the form of an shRNA screen. We screened a focused chaperone shRNA library in combination with chaperone inhibitors in various cell lines to identify targetable weaknesses in the proteostasis network. Ultimately, the work herein presents a starting point for the synthesis of new allosteric inhibitors of Hsp70, as well as novel targets for the development of advanced prostate cancer therapeutics.

Table of Contents

List of Tables

Chapter 3

List of Figures

Chapter 1

Chapter 2

Chapter 3

Chapter 4

Chapter 1: Targeting Allosteric Control Mechanisms in Heat Shock Protein 70 (Hsp70)

INTRODUCTION

Heat shock protein 70 (Hsp70) is a highly conserved chaperone that is broadly involved in protein homeostasis and quality control. This chaperone has been linked to molecular pathways of protein folding, trafficking, disaggregation, turnover and many other aspects of a protein's life cycle (1-4). Indeed, Hsp70 is a central "hub" of the larger protein homeostasis (*e.g.* proteostasis) network, which includes hundreds of chaperones, co-chaperones and related systems that, together, maintain the health of the proteome (5). There is a growing appreciation that the proteostasis network includes many untapped drug targets, a perspective enforced by recent clinical successes with proteasome inhibitors (6-8) and autophagy inducers (9). However, other possible targets in the network, including Hsp70, heat shock protein 90 (Hsp90) and proteins involved in the unfolded protein response (UPR), have proven more difficult to safely inhibit (10-12). These "challenging" targets are inexorably linked to each other as part of the broader proteostasis network, often making it difficult to anticipate the impact of perturbing a specific node (13). In this review, we focus on Hsp70 as a model for this type of target complexity and we highlight how recent examples of allosteric Hsp70 inhibition are illuminating both the challenges and opportunities.

Multi-Domain Allostery and Dynamics in Hsp70

Hsp70 is composed of a 45 kDa nucleotide-binding domain (NBD) that is attached to a 35 kDa substrate-binding domain (SBD). The NBD is composed of two lobes (I and II) that are further divided into four subdomains (IA, IIA, IB, IIB). In turn, the SBD is divided into a beta-sandwich domain (βSBD), which contains the substrate binding cleft, and an alpha-helical "lid" domain (αSBD) that regulates affinity for misfolded proteins (i.e.

"substrates"). The SBD and NBD are linked to each other through a short, hydrophobic linker. Hsp70 is highly conserved across prokaryotes and eukaryotes, with the prokaryotic ortholog termed DnaK. In eukaryotes, the major Hsp70 isoforms in the cytosol are termed Hsc70 and Hsp72, while BiP is found in the ER and mortalin/mtHsp70 in the mitochondria. For simplicity, we will often use the inclusive term "Hsp70" when referring to the conserved structural and biochemical properties of these chaperones.

The Hsp70 system has often served as a model for studying the allosteric mechanisms of multi-domain proteins because the NBD and SBD engage in well-defined, two-way cooperativity (14-16). The two domains are tightly docked to each other in the ATP-bound state, which causes the αSBD to remain "open" (**Figure 1.1**) (14,15). Hydrolysis uncouples the NBD from the SBD so that they now move independently in solution (17). In this state, the αSBD domain closes onto the βSBD, increasing the affinity for substrates (**Figure 1.1**). Thus, the net effect of ATP cycling is that the NBD and SBD are iteratively coupled and then decoupled, sampling the tight- and weak-binding states (18,19). The linker between the NBD and SBD is critical to this allosteric communication, as are a series of weak, intra-molecular contacts throughout the chaperone (14,20).

Another key to understanding Hsp70's biology is that it functions as part of a multi-protein complex in the cell. Members of the J protein class of co-chaperones use a conserved J domain to bind between the NBD and SBD, stimulating hydrolysis of ATP (**Figure 1.1**) (21). Likewise, members of the nucleotide exchange factor (NEF) family, such as Hsp105, Bag1, Bag2 and Bag3, bind to the IB and IIB subdomains of the NBD, stimulating local release of ADP and distal release of substrate from the SBD (22-25). Thus, a series of protein-protein interactions between Hsp70, J proteins and NEFs,

combine to regulate ATP and substrate cycling (**Figure 1.1**). In addition to these contacts, some Hsp70s interact with tetratricopeptide repeat (TPR) co-chaperones, including CHIP, HOP and PP5 (26). These contacts appear to have less of an impact on Hsp70's ATP/substrate cycling; rather, they recruit specific enzymatic functions to the complex (27). For example, CHIP is an E3 ubiquitin ligase involved in substrate turnover by the proteasome (28,29), while PP5 is a phosphatase that acts on Hsp70 substrates (30). Each of these TPR-domain co-chaperones binds to the C-terminal "EEVD" motif of Hsp70, such that only one can be bound at a given time. The substrates of Hsp70 include nearly all proteins with exposed hydrophobic regions (31), including short peptide segments and even partially folded proteins (3,32). This promiscuity allows Hsp70 to engage in many types of interactions, a necessity to maintain the global proteostasis network. Adding to this complexity, there are >10 Hsp70s, >45 J proteins and dozens of NEFs and TPR domain co-chaperones expressed in humans – creating a complicated web of possible multi-protein complexes.

In the absence of granular details about the connectivity of the proteostasis network, recent work has focused, instead, on developing broad classes of Hsp70 "inhibitors". These molecules are defined by their abilities to bind Hsp70 and interrupt its biochemical activities, such as ATP turnover, which can be readily measured *in vitro*. However, does chemical inhibition of ATP turnover directly correlate with chaperone functions, especially within the cytosol or ER lumen? This correlation is not clear (33). Rather these molecules are being used as chemical probes to empirically link specific biochemical mechanisms to cellular outcomes. This approach aims to produce pharmacological definitions of Hsp70 function. In other words, the molecules themselves

are being used to define the biology. Indeed, a similar pharmacological definition (*e.g.* partial agonists, inverse agonists, antagonists, *etc.*) approach has been time-tested in the study of GPCRs and ion channels (34).

Multiple Allosteric Binding Sites on Hsp70

In the cell, Hsp70 might be best considered the "core" of a dynamic, multi-protein sub-network composed of co-chaperones, nucleotides and substrates. Dramatic allosteric transitions and changes in protein-protein interaction partners accompany the motions of Hsp70 and these activities are powered by nucleotide turnover. In the face of this orchestrated complexity, it is not surprising that numerous inhibitors of Hsp70 have been discovered (35,36) or that many of these inhibitors have non-degenerate binding sites (37-42). In theory, Hsp70 is rich in possible allosteric regulatory sites and, as it transitions through an ATP hydrolysis cycle, these sites are expected to appear/disappear (16,27). In addition, binding to co-chaperones would be expected to "hide" some possible sites, while possibly revealing others.

In this review, we will focus on three of the classes of Hsp70 inhibitors, exemplified by MKT-077, VER-155008 and YK5 (**Figure 1.2**). We will discuss how emerging evidence suggests that they each disrupt Hsp70 function through a complex, "domino effect" on allostery, dynamics and protein-protein interactions. We discuss how each of these inhibitors, because of their distinct binding sites, might have both similar and different effects on Hsp70 biology. A major theme (or speculation) is that each Hsp70 inhibitor, because of its unique properties, might be expected to have some non-degenerate effects in cells and animals. By better understanding the molecular mechanisms of an inhibitor, we might be able to better select the "right tool for the job".

Allosteric Inhibitors Based on MKT-077

MKT-077, 1-ethyl-2-((*Z*)-((*E*)-3-ethyl-5-(3-methylbenzo[*d*]thiazol-2(3*H*)-ylidene)-4-oxothiazolidin-2-ylidene)methyl)pyridin-1-ium chloride, is a cationic rhodacyanine that was first discovered by Fuji Film (43). It was subsequently found to have promising anti-cancer (44,45) and anti-malarial activities (46). The major cellular targets of MKT-077 were identified as mortalin, the mitochondrial Hsp70, and Hsc70, a cytoplasmic isoform (44). It is likely that the delocalized cation of MKT-077 is responsible for the targeting of the compound to mortalin, although this localization appears to be incomplete (47).

MKT-077 has little cytotoxicity against either normal human fibroblasts or immortalized epithelial cells (48). This selectivity is thought to originate from increased dependence of cancer cells on Hsp70s, because of their elevated requirements for protein synthesis and high levels of oxidative stress (49). Based on its promising pre-clinical selectivity, MKT-077 was advanced into a Phase I clinical trial in patients with advanced solid tumors in the 1990s; however, the study was terminated due to renal toxicity in a subset of patients (50). Despite this setback, MKT-077 remains an interesting scaffold for studying Hsp70 structure-function.

To advance the utility of MKT-077 as a chemical probe, modifications have been introduced to improve its efficacy in various disease models. A single replacement of the ethyl group on the pyridinium nitrogen with a methyl group yielded YM-01 (**Figure 1.3**), which is more potent than MKT-077 in a number of cellular and animal systems, including cancer xenograft models (47,51), tau turnover assays (52), and polyglutamine-induced proteotoxicity models (53). This molecule had more exposure to the cytoplasmic isoforms of Hsp70, which might give rise to some of this efficacy (47). In addition, a neutral MKT-

077 derivative, YM-08, was developed to remove the pyridinium and improve blood-brain barrier permeability (54), but this molecule lost significant potency and will need to be re-optimized. More recent modifications to YM-01 have focused on improving microsomal stability and reducing renal toxicity, while retaining the pyridinium (55-57). JG-98, a next-generation of MKT-077 derivative, binds 60-fold tighter to Hsp70 than YM-01 (K_D ~ 86 nM) and its anti-proliferative activity is improved 3- to 20-fold in various cancer cell lines (EC_{50} ~ 0.3 - 4 μM) (Li, et al. (in revision)).

NMR titrations and docking calculations revealed that MKT-077 and its analogs bind within a highly conserved, hydrophobic pocket adjacent to the nucleotide-binding cleft (37). The enhanced affinity of JG-98 for Hsp70 appears to originate from favorable contacts with a deep pocket composed of residues T13, T14, K71, V146, Y149, E175 and T226 (**Figure 1.3**; **Figure 1.4a**). Those residues provided favorable hydrophobic interactions with the benzothiazole moiety, while providing electrostatic interactions with the delocalized cation. Interestingly, this binding site is not over-lapping with the nucleotide-binding cleft and docking studies suggest that both MKT-077 analogs and ADP can be bound simultaneously (Li *et al.* 2013).

Analogs of MKT-077 block the ATPase activity of Hsp70s *in vitro* and they also interrupt its ability to refold model substrates (53). How do they inhibit Hsp70 functions if they don't compete with nucleotide? One clue comes from NMR titration experiments, which reveal that MKT-077 and its analogs bind Hsc70 in the ADP-state, but not to the ATP-bound state or the apo conformation (37,57). The structures of Hsp70 isoforms in the ADP- (PDB: 3C7N) (58) and ATP-bound states (PDB: 4B9Q) (15) provide a compelling reason for this selectivity. The entrance to the MKT-077 binding pocket is

formed by Y149 and T226 when Hsp70 is in its “open”, ADP-bound state (**Figure 1.4a**). Upon binding of ATP; however, rotations in lobes I and II of the NBD dramatically re-organize the binding pocket, such that it “collapses”. Indeed, the former binding pocket becomes fully occupied by hydrophobic side chains (**Figure 1.4b**). In addition, the gate residues (*i.e.* Y149 and T226) swivel to block the entrance to the binding site (37). Thus, the binding site of MKT-077 analogs is only accessible in the ADP-bound state and these compounds appear to favor that specific conformer of Hsp70.

MKT-077 analogs allosterically inhibit interactions between Hsp70 and Bag domain proteins. What are the effects of stabilizing the ADP-bound state on Hsp70 structure-function? As mentioned above, nucleotides bind at the bottom of a deep cleft between lobes I and II and are coordinated by residues from all four subdomains (**Figure 1.4c**) (59). The ADP-bound state keeps the αSBD in the “closed” conformation, enhancing affinity for substrates (see **Figure 1.1**). Thus, one outcome of MKT-077 treatment is to promote the substrate-binding affinity of Hsp70 (53). Chemically disrupting the normal “catch-and-release” dynamics of Hsp70 then prevents re-folding of damaged substrates *in vitro* (60)(53), consistent with biochemical studies (33,61). Thus, binding of MKT-077 analogs has an impact on the *in vitro* chaperone functions of Hsp70 by altering its internal dynamics.

What about effects on co-chaperone binding? To explore this question, we used molecular dynamic (MD) simulations (62,63) to monitor how the NBD might change in response to MKT-077 and its analogs. MD trajectories suggested that the major consequence of compound binding is rotation of subdomain IIB, which is even more dramatic than the rotation that occurs in the ADP-bound state (PDB: 3C7N) (**Figure 1.4c**).

A major consequence of this rotation is that the residues at the IB and IIB subdomains are dramatically shifted. Specifically, the positions of residues E268, K271, S275 in subdomain IIB and T13, T14, and Y15 in subdomain IB are moved out of position. This movement is important because these residues are required for binding the Bag domain (64). Indeed, comparing the crystal structure of apo-Hsc70 bound to the Bag1M domain (PDB: 1HX1) with the compound-bound $Hsc70_{NBD}$ model (by aligning the Cα atoms of the IIA subdomain) shows that many of the key interactions are disrupted (**Figure 1.4d**). Electrostatic interactions between the Bag domain and Hsp70's NBD are normally mediated by E213, D225, R236, and Q245 in the Bag domain, which form hydrogen bonds with residues R261, R262, E283/Y294, and S286 in Hsc70 (**Figure 1.4d**) (64). Indeed, mutations in R262A and E283A (in Hsc70) or E213A, D225A, R236A, and Q245A (in Bag1) are known to disrupt binding (23)(64). Likewise, MKT-077 is predicted to cause major re-organization of residues R261, S286, and Y294 and dramatically perturb the hydrogen-bonding network (**Figure 1.4d**, right). Because the other Bag domains are thought to bind similarly to Bag1 (65), MKT-077 might be expected to broadly disrupt the Bag-Hsp70 interactions, a concept that has recently been experimentally confirmed (Li et al (in revision)) (51). Thus, although MKT-077 analogs bind >20Å away from the Hsp70-NEF interaction surface, they trap a conformer that disfavors this contact.

Allosteric inhibitors based on VER-155008

Pioneering work by medicinal chemists at Vernalis has produced a distinct chemical probe for Hsp70. Their strategy was to identify an ATP-competitive inhibitor, but the challenges in this approach are that Hsp70 has a tight affinity for ATP (K_D ~ nM) and the ATP-binding site is quite hydrophilic, especially compared to that of Hsp90 (66).

Despite these challenges, the Vernalis group screened an adenosine analog library using a fluorescence polarization (FP) assay (42) and expansion of an active hit yielded compound VER-155008 (**Figure 1.5a**). It was confirmed that VER-155008 competes with ATP for binding to Hsp70 with an IC_{50} of 0.5 μM, and it inhibits Hsp70- and Hsc70-mediated luciferase refolding *in vitro* (40,67). It also inhibits the growth of several human breast and colon cancer cell lines with GI_{50} values ranging from ~5 to 14 μM, and it induces degradation of suspected Hsp70 substrates, such as Her2 and Raf-1, in both HCT116 and BT474 cells. These activities might be expected from Hsp70 knockdowns (68). Although VER-155008 still requires further optimization to improve its potency and pharmacokinetic properties, the molecule provides another compelling test case of an Hsp70 inhibitor with a defined binding site.

VER-155008 binding approximates the ATP-bound state of the NBD. As mentioned above, ATP binding causes Hsp70's linker to be buried in the cleft between the IA and IIA subdomains, bringing the NBD and SBD closer together (14,69). The net effect of this motion is that substrate affinity in the βSBD is decreased and substrates can rapidly bind/release. Treatment with VER-155008 did not significantly impact substrate binding, except at high concentrations (40), suggesting that it might favor a more ATP-like state. Indeed, the structure of VER-155008-bound Hsc70 has been solved using both $Hsc70_{NBD}$/Bag-1 (by soaking) and $Hsp70_{NBD}$ alone (by co-crystallization) (40,42). In both cases, the NBD appears to be largely ATP-like. Specifically, the adenine moiety of VER-155008 overlays with ATP and the N^1 of the adenine ring forms a hydrogen bond with S275 (**Figure 1.5b**). The $O^{2'}$ of the ribose part makes a direct hydrogen bond with K271, whereas $O^{3'}$ forms a hydrogen bond with D234 via a water molecule. It is only the π-

stacking interactions between the side chain of R272 and the dichlorobenzene and the interactions between Y15 and the 4-cyano-benzyloxymethyl moieties that appear to differentiate the binding modes (**Figure 1.5c**). Thus, VER-155008, unlike MKT-077, appears to trap a largely ATP-like conformation of the Hsp70 protein. However, it is important to note that the compound-bound structure is not identical to the ATP-bound state. Rather, there are perturbations in the locations the subdomains, which position the IIB and IB midway between the "closed" and "open" states (**Figure 1.5d**).

Does VER-155008 affect co-chaperone binding to Hsp70? Binding to VER-155008 has only modest effects on the position of the key Bag-interacting residues in the IIB subdomain. Specifically, the interacting residues, such as R261, R262, E283, Y294 and S286, are nearly overlapping with those in the ATP-bound NBD (**Figure 1.5d**) (15,42). Thus, one would assume that VER-155008 would have minimal impact on NEF protein binding, although experimental evidence to support this conclusion is currently lacking. There is reason to believe that VER-155008 may affect the interactions between Hsp70s and J proteins. A number of studies have shown J proteins, such as DnaJ, bind tighter to Hsp70 in the ATP-bound state – when compared to the ADP-bound state (70-72). For example, disrupting ATP binding in prokaryotic Hsp70, using the D201N mutation, prevents binding to DnaJ (73). Thus, VER-155008 might be predicted to strengthen the interaction with J proteins. However, ATP analogs, ATPγS and AMP-PNP, are known to inhibit DnaJ interactions (70), so this hypothesis needs to be carefully tested. This outcome would be interesting because a different class of dihydropyrimidine-based Hsp70 inhibitors, exemplified by MAL3-101, selectively interrupts the interaction between Hsp70 and J proteins by binding directly to the interface in the IA and IIA subdomains

(38,74). The activity of MAL3-101 has been reviewed elsewhere (75,76). Briefly, this compound has anti-proliferative activity in a number of cancer cells (77), suggesting that the Hsp70 contact with J proteins might be an interesting drug target. However, VER-155008 also has anti-proliferative activity, so the role of J proteins remains mysterious. More systematic, side-by-side studies are needed to differentiate between different classes of Hsp70 inhibitors.

Allosteric Inhibitors Based on YK5.

Recently, Rodina *et al.* reported their discovery of a new druggable site in the NBD located between lobes IB and IIB (78). They identified this site after searching through approximately 25 available structures of Hsp70 paralogs in various nucleotide states. A superimposition of these structures most resembled the ADP-bound state, where the nucleotide-binding cleft of the NBD was in an "open" conformation. Searching for druggable pockets in this consensus state revealed a potential binding site that is distinct from the site bound by either MKT-077 or VER-155008. However, like MKT-077, this site is only available in the ADP-bound state because of rotations in lobes I and II. Exploration of this site revealed a potentially reactive cysteine at position 267 (the TAC^{267}ERAK sequence is shown in **Figure 1.6**) and this cysteine was then exploited in the rational design of a 2,5'-thiodipyrimide series featuring a terminal acrylamide, leading to the identification of compound YK5 (**Figure 1.6a**). YK5 was shown to selectively and irreversibly interact with Hsp70 in cancer cells, in particular with the cytosolic isoforms and not the mitochondrial or ER-resident isoforms (Grp75 and Grp78, respectively), where C267 is not conserved.

YK5 Inhibits Formation of the Hsp70-HOP complex, with Minor Effects on Other Co-Chaperones. In vitro, YK5 only modestly inhibits ATP hydrolysis by the combination of Hsc70, a J protein (DnaJA1) and a NEF (Hsp110), while having no significant effect on ATP turnover by the combination of Hsc70 and DnaJA1 alone (78). YK5 was shown to inhibit Hsc70-mediated refolding of denatured luciferase *in vitro*, suggesting that it does interfere with the productive interaction with substrates. These findings suggest that YK5 might have relatively minimal effects on the protein-protein interactions with J proteins or NEFs, while impacting substrate dynamics. However, the protein-protein interactions have not been measured directly, so this remains an open question.

After the discovery of YK5, more potent, irreversible inhibitors were developed that also exploit C267 (41). Derivatives of the 2,5'-thiodipyrimide and 5-(phenylthio)pyrimidine class were assembled and armed with an electrophilic acrylamide moiety. Importantly, these compounds bound irreversibly to Hsp70 in lysates, but they did not bind Hsp90. Treatment with YK5 significantly reduces the levels of oncogenic Hsp70/Hsp90 substrates, such as HER2 and Raf-1, presumably by destabilizing Hsp70 interactions. It was also shown that in breast cancer SKBr3 cell lysates, one derivative dose-dependently depleted the amount of Hsp70 bound to the TPR domain co-chaperone, HOP, with an IC_{50} value very similar to that needed to inhibit growth. The results of these experiments suggest that YK5 analogs employ a mechanism that involves disruption of the Hsp70-HOP-Hsp90 complex. In a companion paper, a new series of reversible inhibitors, lacking the acrylamide moiety, was developed (**Figure 1.6b**) (79). While taking a hit in potency across a panel of biological assays (by approximately one log unit), these non-covalent inhibitors were also shown to bind Hsp70 selectively, and appeared to potentially work

via similar mechanisms to their irreversible counterparts. Thus, covalent attachment is not required. It still isn't clear why binding of the molecules to the region around C267 might impact interactions between Hsp70 and HOP, which occur at the end of the disordered, C-terminal tail region (78).

Cysteine reactivity in Hsp70. One possible clue into the mechanism of YK5 comes from a series of studies focused on understanding redox signaling in Hsp70s. Miyata *et al.* found that methylene blue (MB) catalyzes the oxidation of another reactive cysteine in Hsp70, C306 (**Figure 1.6c**), an event which was predicted by both molecular modeling and mutagenesis to allow for the subsequent oxidation of C267 (80). Treatment with MB *in vitro* led to the decreased ability of Hsp70 to bind ATP, presumably by trapping a state that is not competent to bind nucleotide. Mutation of either cysteine to a serine was partially protective against this effect and the double mutant, C267/306S, was nearly fully protective. Thus, C267 appears to be a redox "sensor" for Hsp70 that couples oxidative stress to nucleotide binding affinity, a result supported by other studies (81). Interestingly, Cys267 is conserved among human cytosolic forms of Hsp70, but not the organellar forms, Grp75 or Grp78 (mortalin and BiP) (82), whereas C306 is only conserved in the stress induced isoform(80). Thus, Hsp70 does seem to rely on C267 as a stress sensor and YK5 analogs may take advantage of this natural mechanism to interfere with chaperone function.

CONCLUSIONS

Hsp70 is a dynamic, two-domain protein that functions in concert with its co-chaperones (16). The chaperone itself is highly mobile and there are many important contacts made between its NBD and SBD. In this ensemble of possible structures, a

compound might be expected to “trap” a subset of states as a consequence of its binding. In turn, this trapped state would be expected to communicate with the local network of protein-protein interactions (83). For example, the ATP-bound state is known to interact with J proteins and NEFs, while the ADP-bound state has tight affinity for substrates (22,84). Thus, binding of small molecules at two different sites might produce distinct effects on Hsp70 structure/function by favoring a specific conformer and shifting the ensemble of bound co-chaperones.

To explore this concept, we reviewed the literature around three distinct chemical inhibitors of Hsp70: MKT-077, VER-155008 and YK5. These molecules were chosen because they have been shown to be relatively specific for Hsp70 in cells and they each were known to bind a different site on the protein. MKT-077 appears to trap an ADP-like state, while VER-155008 favors an ATP-like state. Importantly, neither of these conformers are exactly the same as the natural nucleotide-bound state, at least by modeling and crystallography. The impact of these subtle variations is not fully clear, but these two molecules certainly provide probes to explore the relative effects of different Hsp70 conformers. YK5 was designed based on an ADP-bound structure, but experimental evidence and previous work on C267 suggest that YK5 might favor a conformer of Hsp70 that is not well-defined as either ATP- or ADP-bound. Oxidation of C267/306 dramatically reduces the affinity of Hsp70 for nucleotides, so one possibility is that YK5 could favor an apo-state, but this speculation is not yet tested. Regardless, MKT-077, VER-155008 and YK5 provide a suite of molecules with distinct binding sites and mechanisms.

What are the impacts of enforcing an Hsp70 conformer on chaperone functions? *In vitro*, MKT-077 and VER-155008 interrupt ATP cycling and refolding, while YK5 has a less dramatic effect. MKT-077 blocks Hsp70-NEF interactions, while VER-155008 and YK5 are expected to have a minor effect on this protein-protein interaction. Thus, *in vitro* measurements of Hsp70 biochemistry (*e.g.* ATP turnover, binding to co-chaperones) may "bin" the small molecules into distinct categories. However, side-by-side studies are severely lacking (40) and more work is needed to understand how many categories of Hsp70 inhibitors might be possible. These are early days.

Taking this speculative thought-process a step further, one might also assume that different Hsp70 inhibitors might have non-overlapping effects on Hsp70 function in the cell. This hypothesis is starting to be tested. For example, trapping the ADP-bound state with MKT-077 analogs appears to catalyze the degradation of some misfolded Hsp70 substrates, including polyglutamine-expanded androgen receptor (53) and tau (52), while having comparatively less effect on the undamaged versions (85). Likewise, some oncoproteins, including kinases, seem to require constant cycling of Hsp70 to avoid proteasomal degradation (85). Thus, any compound that interferes with cycling might have degenerate effects on the stability of these proteins. Indeed, treatment with VER-155008, YK5 and MKT-077 all destabilize some chaperone-dependent oncoproteins in cancer cells (57,67,78).

The Future of Hsp70 Inhibitor Research

The ultimate goals of Hsp70 inhibitor research are to: (a) learn how this chaperone is involved in disease and (b) produce clinical candidates for the sue in treating these diseases. In addition to the Hsp70 inhibitors discussed here, a number of others have

been identified. Unfortunately, none of these molecules has yet advanced to clinical trials (with the exception of MKT-077, which failed in Phase I). However, a number of series are in active pre-clinical development. The path for these molecules may be long and, in our opinion, the current compounds may ultimately be more useful as chemical probes than drugs. This conclusion is based, in part, on the complexity of the Hsp70 system and, as we have highlighted in this review, on the diversity of the possible mechanisms. Indeed, it seems prudent and important to develop and fully characterize a number of different tool compounds. Out of that process, the field might uncover the safest and most effective ways of using Hsp70 as a therapeutic target.

Another frontier area in the study of Hsp70 inhibitors is paralog specificity. As mentioned above, there are Hsp70 paralogs found in each cellular compartment (*e.g.* mitochondria, ER, *etc.*) and it is often not clear whether specific paralogs should be targeted or whether pan-Hsp70 inhibitors will be most effective. There needs to be significantly more work done to address this question, likely using a combination of paralog-specific inhibitors and genetics.

ACKNOWLEDGEMENTS

This work was prepared in collaboration with Xiaokai Li, Hao Shao, and Jason Gestwicki and was published as a review in *Curr Top Med Chem* (2016) (86).

The authors acknowledge the continued support of NIH (NS059690).

REFERENCES

1. Bukau, B., Weissman, J., and Horwich, A. (2006) Molecular Chaperones and Protein Quality Control. *Cell* **125**, 443-451
2. Hartl, F. U. (1996) Molecular chaperones in cellular protein folding. *Nature* **381**, 571-580
3. Hartl, F. U., Bracher, A., and Hayer-Hartl, M. (2011) Molecular chaperones in protein folding and proteostasis. *Nature* **475**, 324-332

4. Hartl, F. U., and Hayer-Hartl, M. (2002) Protein folding - Molecular chaperones in the cytosol: from nascent chain to folded protein. *Science* **295**, 1852-1858
5. Powers, E. T., Morimoto, R. I., Dillin, A., Kelly, J. W., and Balch, W. E. (2009) Biological and chemical approaches to diseases of proteostasis deficiency. in *Annu. Rev. Biochem.*, Annual Reviews, Palo Alto. pp 959-991
6. Adams, J., Palombella, V. J., Sausville, E. A., Johnson, J., Destree, A., Lazarus, D. D., Maas, J., Pien, C. S., Prakash, S., and Elliott, P. J. (1999) Proteasome inhibitors: A novel class of potent and effective antitumor agents. *Cancer Res.* **59**, 2615-2622
7. Kisselev, A. F., and Goldberg, A. L. (2001) Proteasome inhibitors: from research tools to drug candidates. *Chem. Biol.* **8**, 739-758
8. Adams, J. (2004) The proteasome: A suitable antineoplastic target. *Nat. Rev. Cancer* **4**, 349-360
9. Rubinsztein, D. C., Codogno, P., and Levine, B. (2012) Autophagy modulation as a potential therapeutic target for diverse diseases. *Nat. Rev. Drug Discov.* **11**, 709-730
10. Trepel, J., Mollapour, M., Giaccone, G., and Neckers, L. (2010) Targeting the dynamic HSP90 complex in cancer. *Nat. Rev. Cancer* **10**, 537-549
11. Evans, C. G., Chang, L., and Gestwicki, J. E. (2010) Heat Shock Protein 70 (Hsp70) as an emerging drug target. *J. Med. Chem.* **53**, 4585-4602
12. Hetz, C., Chevet, E., and Harding, H. P. (2013) Targeting the unfolded protein response in disease. *Nat. Rev. Drug Discov.* **12**, 703-719
13. Gestwicki, J. E., and Garza, D. (2012) Chapter 10 - Protein Quality Control in Neurodegenerative Disease. in *Progress in Molecular Biology and Translational Science* (David, B. T. ed.), Academic Press. pp 327-353
14. Zhuravleva, A., Clerico, Eugenia M., and Gierasch, Lila M. (2012) An interdomain energetic Tug-of-War creates the allosterically active state in Hsp70 molecular chaperones. *Cell* **151**, 1296-1307
15. Kityk, R., Kopp, J., Sinning, I., and Mayer, Matthias P. (2012) Structure and dynamics of the ATP-bound open conformation of Hsp70 chaperones. *Mol. Cell* **48**, 863-874
16. Zuiderweg, E. R. P., Bertelsen, E. B., Rousaki, A., Mayer, M. P., Gestwicki, J. E., and Ahmad, A. (2013) Allostery in the Hsp70 chaperone proteins. *Top. Curr. Chem.* **328**, 99-153
17. Bertelsen, E. B., Chang, L., Gestwicki, J. E., and Zuiderweg, E. R. P. (2009) Solution conformation of wild-type E. coli Hsp70 (DnaK) chaperone complexed with ADP and substrate. *Proc. Natl. Acad. Sci. U. S. A.* **106**, 8471-8476
18. Vogel, M., Bukau, B., and Mayer, M. P. (2006) Allosteric regulation of Hsp70 chaperones by a proline switch. *Mol. Cell* **21**, 359-367
19. Swain, J. F., Dinler, G., Sivendran, R., Montgomery, D. L., Stotz, M., and Gierasch, L. M. (2007) Hsp70 chaperone ligands control domain association via an allosteric mechanism mediated by the interdomain linker. *Mol. Cell* **26**, 27-39
20. Ung, P. M.-U., Thompson, A. D., Chang, L., Gestwicki, J. E., and Carlson, H. A. (2013) Identification of key Hinge residues important for nucleotide-dependent allostery in E. coli Hsp70/DnaK. *PLoS Comput. Biol.* **9**

21. Kampinga, H. H., and Craig, E. A. (2010) The HSP70 chaperone machinery: J proteins as drivers of functional specificity. *Nat. Rev. Mol. Cell Biol.* **11**, 579-592
22. Rauch, J. N., and Gestwicki, J. E. (2014) Binding of human nucleotide exchange factors to heat shock protein 70 (Hsp70) generates functionally distinct complexes *in vitro*. *J. Biol. Chem.* **289**, 1402-1414
23. Briknarova, K., Takayama, S., Brive, L., Havert, M. L., Knee, D. A., Velasco, J., Homma, S., Cabezas, E., Stuart, J., Hoyt, D. W., Satterthwait, A. C., Llinas, M., Reed, J. C., and Ely, K. R. (2001) Structural analysis of BAG1 cochaperone and its interactions with Hsc70 heat shock protein. *Nat. Struct. Mol. Biol.* **8**, 349-352
24. Xu, Z., Page, R. C., Gomes, M. M., Kohli, E., Nix, J. C., Herr, A. B., Patterson, C., and Misra, S. (2008) Structural basis of nucleotide exchange and client binding by the Hsp70 cochaperone Bag2. *Nat. Struct. Mol. Biol.* **15**, 1309-1317
25. Andréasson, C., Fiaux, J., Rampelt, H., Druffel-Augustin, S., and Bukau, B. (2008) Insights into the structural dynamics of the Hsp110–Hsp70 interaction reveal the mechanism for nucleotide exchange activity. *Proc. Natl. Acad. Sci. U. S. A.* **105**, 16519-16524
26. D'Andrea, L. D., and Regan, L. (2003) TPR proteins: the versatile helix. *Trends Biochem. Sci.* **28**, 655-662
27. Assimon, V. A., Gillies, A. T., Rauch, J. N., and Gestwicki, J. E. (2013) Hsp70 protein complexes as drug targets. *Curr. Pharm. Des.* **19**, 404-417
28. Petrucelli, L., Dickson, D., Kehoe, K., Taylor, J., Snyder, H., Grover, A., De Lucia, M., McGowan, E., Lewis, J., Prihar, G., Kim, J., Dillmann, W. H., Browne, S. E., Hall, A., Voellmy, R., Tsuboi, Y., Dawson, T. M., Wolozin, B., Hardy, J., and Hutton, M. (2004) CHIP and Hsp70 regulate tau ubiquitination, degradation and aggregation. *Hum. Mol. Genet.* **13**, 703-714
29. Qian, S.-B., McDonough, H., Boellmann, F., Cyr, D. M., and Patterson, C. (2006) CHIP-mediated stress recovery by sequential ubiquitination of substrates and Hsp70. *Nature* **440**, 551-555
30. Connarn, J. N., Assimon, V. A., Reed, R. A., Tse, E., Southworth, D. R., Zuiderweg, E. R. P., Gestwicki, J. E., and Sun, D. (2014) The molecular chaperone Hsp70 activates protein phosphatase 5 (PP5) by binding the tetratricopeptide repeat (TPR) domain. *J. Biol. Chem.* **289**, 2908-2917
31. Rudiger, S., Buchberger, A., and Bukau, B. (1997) Interaction of Hsp70 chaperones with substrates. *Nat. Struct. Mol. Biol.* **4**, 342-349
32. Mayer, M. P. (2010) Gymnastics of molecular chaperones. *Mol. Cell* **39**, 321-331
33. Chang, L., Thompson, A. D., Ung, P., Carlson, H. A., and Gestwicki, J. E. (2010) Mutagenesis reveals the complex relationships between ATPase rate and the chaperone activities of Escherichia coli heat shock protein 70 (Hsp70/DnaK). *J. Biol. Chem.* **285**, 21282-21291
34. Jeffrey Conn, P., Christopoulos, A., and Lindsley, C. W. (2009) Allosteric modulators of GPCRs: a novel approach for the treatment of CNS disorders. *Nat. Rev. Drug Discov.* **8**, 41-54
35. Leu, J. I. J., Pimkina, J., Frank, A., Murphy, M. E., and George, D. L. (2009) A Small Molecule Inhibitor of Inducible Heat Shock Protein 70. *Mol. Cell* **36**, 15-27

36. Stevens, S. Y., Cai, S., Pellecchia, M., and Zuiderweg, E. R. P. (2003) The solution structure of the bacterial HSP70 chaperone protein domain DnaK(393–507) in complex with the peptide NRLLLTG. *Protein Sci.* **12**, 2588-2596
37. Rousaki, A., Miyata, Y., Jinwal, U. K., Dickey, C. A., Gestwicki, J. E., and Zuiderweg, E. R. P. (2011) Allosteric Drugs: The Interaction of Antitumor Compound MKT-077 with Human Hsp70 Chaperones. *J. Mol. Biol.* **411**, 614-632
38. Wisen, S., Bertelsen, E. B., Thompson, A. D., Patury, S., Ung, P., Chang, L., Evans, C. G., Walter, G. M., Wipf, P., Carlson, H. A., Brodsky, J. L., Zuiderweg, E. R. P., and Gestwicki, J. E. (2010) Binding of a small molecule at a protein-protein interface regulates the chaperone activity of Hsp70-Hsp40. *ACS Chem. Biol.* **5**, 611-622
39. Balaburski, G. M., Leu, J. I. J., Beeharry, N., Hayik, S., Andrake, M. D., Zhang, G., Herlyn, M., Villanueva, J., Dunbrack, R. L., Jr., Yen, T., George, D. L., and Murphy, M. E. (2013) A modified HSP70 inhibitor shows broad activity as an anticancer agent. *Mol. Cancer Res.* **11**, 219-229
40. Schlecht, R., Scholz, S. R., Dahmen, H., Wegener, A., Sirrenberg, C., Musil, D., Bomke, J., Eggenweiler, H.-M., Mayer, M. P., and Bukau, B. (2013) Functional Analysis of Hsp70 Inhibitors. *PLoS ONE* **8**
41. Kang, Y., Taldone, T., Patel, H. J., Patel, P. D., Rodina, A., Gozman, A., Maharaj, R., Clement, C. C., Patel, M. R., Brodsky, J. L., Young, J. C., and Chiosis, G. (2014) Heat shock protein 70 inhibitors. 1. 2,5 '-Thiodipyrimidine and 5-(phenylthio)pyrimidine acrylamides as irreversible binders to an allosteric site on heat shock protein 70. *J. Med. Chem.* **57**, 1188-1207
42. Williamson, D. S., Borgognoni, J., Clay, A., Daniels, Z., Dokurno, P., Drysdale, M. J., Foloppe, N., Francis, G. L., Graham, C. J., Howes, R., Macias, A. T., Murray, J. B., Parsons, R., Shaw, T., Surgenor, A. E., Terry, L., Wang, Y., Wood, M., and Massey, A. J. (2009) Novel adenosine-derived inhibitors of 70 kDa heat shock protein, discovered through structure-based design. *J. Med. Chem.* **52**, 1510-1513
43. ModicaNapolitano, J. S., Koya, K., Weisberg, E., Brunelli, B. T., Li, Y., and Chen, L. B. (1996) Selective damage to carcinoma mitochondria by the rhodacyanine MKT-077. *Cancer Res.* **56**, 544-550
44. Wadhwa, R., Sugihara, T., Yoshida, A., Nomura, H., Reddel, R. R., Simpson, R., Maruta, H., and Kaul, S. C. (2000) Selective toxicity of MKT-077 to cancer cells is mediated by its binding to the hsp70 family protein mot-2 and reactivation of p53 function. *Cancer Res.* **60**, 6818-6821
45. Chiba, Y., Kubota, T., Watanabe, M., Otani, Y., Teramoto, T., Matsumoto, Y., Koya, K., and Kitajima, M. (1998) Selective antitumor activity of MKT-077, a delocalized lipophilic cation, on normal cells and cancer cells in vitro. *J. Surg. Oncol.* **69**, 105-110
46. Takasu, K., Inoue, H., Kim, H. S., Suzuki, M., Shishido, T., Wataya, Y., and Ihara, M. (2002) Rhodacyanine dyes as antimalarials. 1. Preliminary evaluation of their activity and toxicity. *J. Med. Chem.* **45**, 995-998
47. Koren, J., III, Miyata, Y., Kiray, J., O'Leary, J. C., III, Nguyen, L., Guo, J., Blair, L. J., Li, X., Jinwal, U. K., Cheng, J. Q., Gestwicki, J. E., and Dickey, C. A. (2012) Rhodacyanine derivative selectively targets cancer cells and overcomes tamoxifen resistance. *PLoS ONE* **7**, e35566

48. Wadhwa, R., Colgin, L., Yaguchi, T., Taira, K., Reddel, R. R., and Kaul, S. C. (2002) Rhodacyanine dye MKT-077 inhibits in vitro telomerase assay but has no detectable effects on telomerase activity in vivo. *Cancer Res.* **62**, 4434-4438
49. Petit, T., Izbicka, E., Lawrence, R. A., Nalin, C., Weitman, S. D., and Von Hoff, D. D. (1999) Activity of MKT 077, a rhodacyanine dye, against human tumor colony-forming units. *Anti-Cancer Drugs* **10**, 309-315
50. Propper, D. J., Braybrooke, J. P., Taylor, D. J., Lodi, R., Styles, P., Cramer, J. A., Collins, W. C. J., Levitt, N. C., Talbot, D. C., Ganesan, T. S., and Harris, A. L. (1999) Phase I trial of the selective mitochondrial toxin MKT 077 in chemo-resistant solid tumours. *Ann. Oncol.* **10**, 923-927
51. Colvin, T. A., Gabai, V. L., Gong, J., Calderwood, S. K., Li, H., Gummuluru, S., Matchuk, O. N., Smirnova, S. G., Orlova, N. V., Zamulaeva, I. A., Garcia-Marcos, M., Li, X., Young, Z., Rauch, J. N., Gestwicki, J. E., Takayama, S., and Sherman, M. Y. (2014) Hsp70-Bag3 interactions regulate cancer-related signaling networks. *Cancer Res.* **74**, 4731-4740
52. Abisambra, J., Jinwal, U. K., Miyata, Y., Rogers, J., Blair, L., Li, X., Seguin, S. P., Wang, L., Jin, Y., Bacon, J., Brady, S., Cockman, M., Guidi, C., Zhang, J., Koren, J., Young, Z. T., Atkins, C. A., Zhang, B., Lawson, L. Y., Weeber, E. J., Brodsky, J. L., Gestwicki, J. E., and Dickey, C. A. (2013) Allosteric heat shock protein 70 inhibitors rapidly rescue synaptic plasticity deficits by reducing aberrant tau. *Biol. Psychiatry* **74**, 367-374
53. Wang, A. M., Miyata, Y., Klinedinst, S., Peng, H.-M., Chua, J. P., Komiyama, T., Li, X., Morishima, Y., Merry, D. E., Pratt, W. B., Osawa, Y., Collins, C. A., Gestwicki, J. E., and Lieberman, A. P. (2013) Activation of Hsp70 reduces neurotoxicity by promoting polyglutamine protein degradation. *Nat. Chem. Biol.* **9**, 112-118
54. Miyata, Y., Li, X., Lee, H.-F., Jinwal, U. K., Srinivasan, S. R., Seguin, S. P., Young, Z. T., Brodsky, J. L., Dickey, C. A., Sun, D., and Gestwicki, J. E. (2013) Synthesis and Initial Evaluation of YM-08, a Blood-Brain Barrier Permeable Derivative of the Heat Shock Protein 70 (Hsp70) Inhibitor MKT-077, Which Reduces Tau Levels. *ACS Chem. Neurosci.* **4**, 930-939
55. Kawakami, M., Koya, K., Ukai, T., Tatsuta, N., Ikegawa, A., Ogawa, K., Shishido, T., and Chen, L. B. (1997) Synthesis and Evaluation of Novel Rhodacyanine Dyes That Exhibit Antitumor Activity. *J. Med. Chem.* **40**, 3151-3160
56. Kawakami, M., Koya, K., Ukai, T., Tatsuta, N., Ikegawa, A., Ogawa, K., Shishido, T., and Chen, L. B. (1998) Structure-activity of novel rhodacyanine dyes as antitumor agents. *J. Med. Chem.* **41**, 130-142
57. Li, X., Srinivasan, S. R., Connarn, J., Ahmad, A., Young, Z. T., Kabza, A. M., Zuiderweg, E. R. P., Sun, D., and Gestwicki, J. E. (2013) Analogues of the allosteric heat shock protein 70 (Hsp70) inhibitor, MKT-077, as anti-cancer agents. *ACS Med. Chem. Lett.* **4**, 1042-1047
58. Schuermann, J. P., Jiang, J., Cuellar, J., Llorca, O., Wang, L., Gimenez, L. E., Jin, S., Taylor, A. B., Demeler, B., Morano, K. A., Hart, P. J., Valpuesta, J. M., Lafer, E. M., and Sousa, R. (2008) Structure of the Hsp110:Hsc70 Nucleotide Exchange Machine. *Mol. Cell* **31**, 232-243

59. Flaherty, K. M., DeLuca-Flaherty, C., and McKay, D. B. (1990) Three-dimensional structure of the ATPase fragment of a 70K heat-shock cognate protein. *Nature* **346**, 623-628
60. Szabo, A., Langer, T., Schröder, H., Flanagan, J., Bukau, B., and Hartl, F. U. (1994) The ATP hydrolysis-dependent reaction cycle of the Escherichia coli Hsp70 system DnaK, DnaJ, and GrpE. *Proc. Natl. Acad. Sci. U. S. A.* **91**, 10345-10349
61. Sharma, S. K., De Los Rios, P., Christen, P., Lustig, A., and Goloubinoff, P. (2010) The kinetic parameters and energy cost of the Hsp70 chaperone as a polypeptide unfoldase. *Nat. Chem. Biol.* **6**, 914-920
62. Ung, P. M.-U., Thompson, A. D., Chang, L., Gestwicki, J. E., and Carlson, H. A. (2013) Identification of key hinge residues important for nucleotide-dependent allostery in *E. coli* Hsp70/DnaK. *PLoS Comput. Biol.* **9**, e1003279
63. General, I. J., Liu, Y., Blackburn, M. E., Mao, W., Gierasch, L. M., and Bahar, I. (2014) ATPase subdomain IA is a mediator of interdomain allostery in Hsp70 molecular chaperones. *PLoS Comput. Biol.* **10**, e1003624
64. Sondermann, H., Scheufler, C., Schneider, C., Höhfeld, J., Hartl, F.-U., and Moarefi, I. (2001) Structure of a Bag/Hsc70 complex: convergent functional evolution of Hsp70 nucleotide exchange factors. *Science* **291**, 1553-1557
65. Doong, H., Vrailas, A., and Kohn, E. C. (2002) What's in the 'BAG'? – a functional domain analysis of the BAG-family proteins. *Cancer Lett.* **188**, 25-32
66. Massey, A. J. (2010) ATPases as Drug Targets: Insights from Heat Shock Proteins 70 and 90. *J. Med. Chem.* **53**, 7280-7286
67. Massey, A. J., Williamson, D. S., Browne, H., Murray, J. B., Dokurno, P., Shaw, T., Macias, A. T., Daniels, Z., Geoffroy, S., Dopson, M., Lavan, P., Matassova, N., Francis, G. L., Graham, C. J., Parsons, R., Wang, Y., Padfield, A., Comer, M., Drysdale, M. J., and Wood, M. (2010) A novel, small molecule inhibitor of Hsc70/Hsp70 potentiates Hsp90 inhibitor induced apoptosis in HCT116 colon carcinoma cells. *Cancer Chemother. Pharmacol.* **66**, 535-545
68. Powers, M. V., Clarke, P. A., and Workman, P. (2008) Dual targeting of HSC70 and HSP72 inhibits HSP90 function and induces tumor-specific apoptosis. *Cancer Cell* **14**, 250-262
69. Qi, R., Sarbeng, E. B., Liu, Q., Le, K. Q., Xu, X., Xu, H., Yang, J., Wong, J. L., Vorvis, C., Hendrickson, W. A., Zhou, L., and Liu, Q. (2013) Allosteric opening of the polypeptide-binding site when an Hsp70 binds ATP. *Nat. Struct. Mol. Biol.* **20**, 900-907
70. Suh, W. C., Lu, C. Z., and Gross, C. A. (1999) Structural features required for the interaction of the Hsp70 molecular chaperone DnaK with its cochaperone DnaJ. *J. Biol. Chem.* **274**, 30534-30539
71. Wittung-Stafshede, P., Guidry, J., Horne, B. E., and Landry, S. J. (2003) The J-domain of Hsp40 couples ATP hydrolysis to substrate capture in Hsp70. *Biochemistry* **42**, 4937-4944
72. Horne, B. E., Li, T., Genevaux, P., Georgopoulos, C., and Landry, S. J. (2010) The Hsp40 J-domain stimulates Hsp70 when tethered by the client to the ATPase domain. *J. Biol. Chem.* **285**, 21679-21688

73. Kamathloeb, A. S., Lu, C. Z., Suh, W. C., Lonetto, M. A., and Gross, C. A. (1995) Analysis of three DnaK mutant proteins suggests that progession through the ATPase cycle requires conformational changes. *J. Biol. Chem.* **270**, 30051-30059
74. Fewell, S. W., Smith, C. M., Lyon, M. A., Dumitrescu, T. P., Wipf, P., Day, B. W., and Brodsky, J. L. (2004) Small molecule modulators of endogenous and co-chaperone-stimulated Hsp70 ATPase activity. *J. Biol. Chem.* **279**, 51131-51140
75. Assimon, V. A., Gillies, A. T., Rauch, J. N., and Gestwicki, J. E. (2013) Hsp70 protein complexes as drug targets. *Curr. Pharm. Desgin* **19**, 404-417
76. Huryn, D. M., Resnick, L. O., and Wipf, P. (2013) Contributions of academic laboratories to the discovery and development of chemical biology tools. *J. Med. Chem.* **56**, 7161-7176
77. Adam, C., Baeurle, A., Brodsky, J. L., Wipf, P., Schrama, D., Becker, J. C., and Houben, R. (2014) The HSP70 modulator MAL3-101 inhibits Merkel cell carcinoma. *PLoS ONE* **9**
78. Rodina, A., Patel, P. D., Kang, Y., Patel, Y., Baaklini, I., Wong, M. J. H., Taldone, T., Yan, P., Yang, C., Maharaj, R., Gozman, A., Patel, M. R., Patel, H. J., Chirico, W., Erdjument-Bromage, H., Talele, T. T., Young, J. C., and Chiosis, G. (2013) Identification of an allosteric pocket on human Hsp70 reveals a mode of inhibition of this therapeutically important protein. *Chem. Biol.* **20**, 1469-1480
79. Taldone, T., Kang, Y., Patel, H. J., Patel, M. R., Patel, P. D., Rodina, A., Patel, Y., Gozman, A., Maharaj, R., Clement, C. C., Lu, A., Young, J. C., and Chiosis, G. (2014) Heat shock protein 70 inhibitors. 2. 2,5 '-Thiodipyrimidines, 5-(phenylthio)pyrimidines, 2-(pyridin-3-ylthio)pyrimidines, and 3-(Phenylthio)pyridines as reversible binders to an allosteric site on Heat Shock Protein 70. *J. Med. Chem.* **57**, 1208-1224
80. Miyata, Y., Rauch, J. N., Jinwal, U. K., Thompson, A. D., Srinivasan, S., Dickey, C. A., and Gestwicki, J. E. (2012) Cysteine reactivity distinguishes redox sensing by the heat-inducible and constitutive forms of heat shock protein 70. *Chemistry & biology* **19**, 1391-1399
81. Wang, Y., Gibney, P. A., West, J. D., and Morano, K. A. (2012) The yeast Hsp70 Ssa1 is a sensor for activation of the heat shock response by thiol-reactive compounds. *Mol. Biol. Cell* **23**, 3290-3298
82. Liu, Q. L., Levy, E. J., and Chirico, W. J. (1996) *N*-ethylmaleimide inactivates a nucleotide-free Hsp70 molecular chaperone. *J. Biol. Chem.* **271**, 29937-29944
83. Thompson, A. D., Dugan, A., Gestwicki, J. E., and Mapp, A. K. (2012) Fine-tuning multiprotein complexes using small molecules. *ACS Chem. Biol.* **7**, 1311-1320
84. Mayer, M. P., Schroder, H., Rudiger, S., Paal, K., Laufen, T., and Bukau, B. (2000) Multistep mechanism of substrate binding determines chaperone activity of Hsp70. *Nat. Struct. Mol. Biol.* **7**, 586-593
85. Pratt, W. B., Gestwicki, J. E., Osawa, Y., and Lieberman, A. P. (2015) Targeting Hsp90/Hsp70-based protein quality control for treatment of adult onset neurodegenerative diseases. *Annu. Rev. Pharmacol. Toxicol.*, DOI: 10.1146/annurev-pharmtox-010814-124332
86. Li, X., Shao, H., Taylor, I. R., and Gestwicki, J. E. (2016) Targeting Allosteric Control Mechanisms in Heat Shock Protein 70 (Hsp70). *Current topics in medicinal chemistry* **16**, 2729-2740

FIGURES

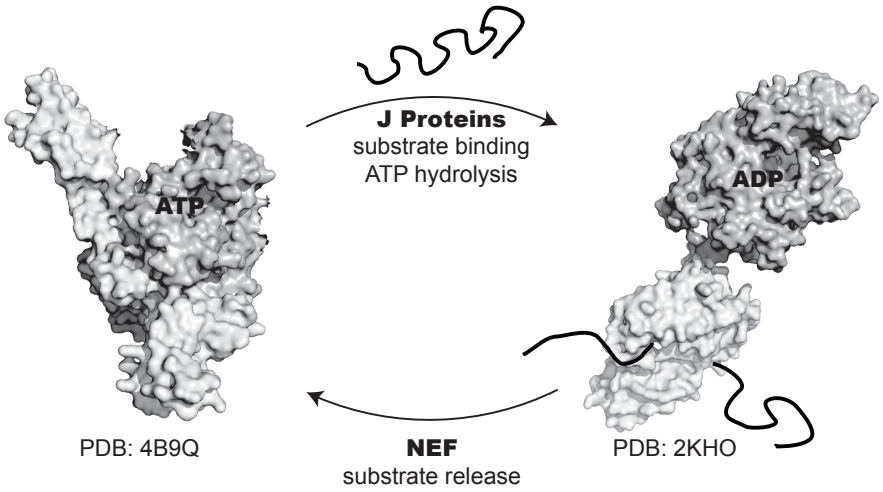

Figure 1.1: Illustration of the ATPase cycle of Hsp70. Structural insights have been made into how the NBD and SBD of Hsp70 are arranged during hydrolysis. Many of these insights have come from studies on the highly conserved prokaryotic Hsp70, DnaK. The NBD (dark gray) and SBD (light gray) are docked to each other in the ATP-bound state (left; 4B9Q) and they move independently in the ADP-bound state (right; 2KHO).

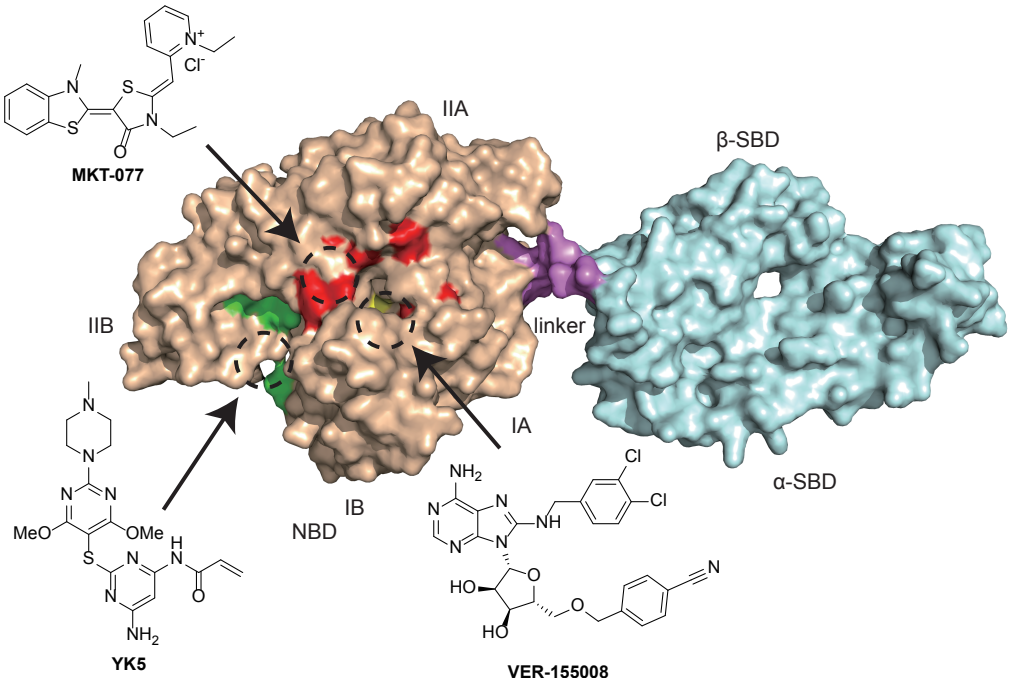

Figure 1.2: Three classes of Hsp70 inhibitors: MKT-077, VER-155008, and YK5. These molecules bind in three distinct pockets of Hsp70 (denoted by circles). For clarity, only the ADP-bound form is shown (PDB: 2KHO). The locations of the NBD, SBD and subdomains are shown.

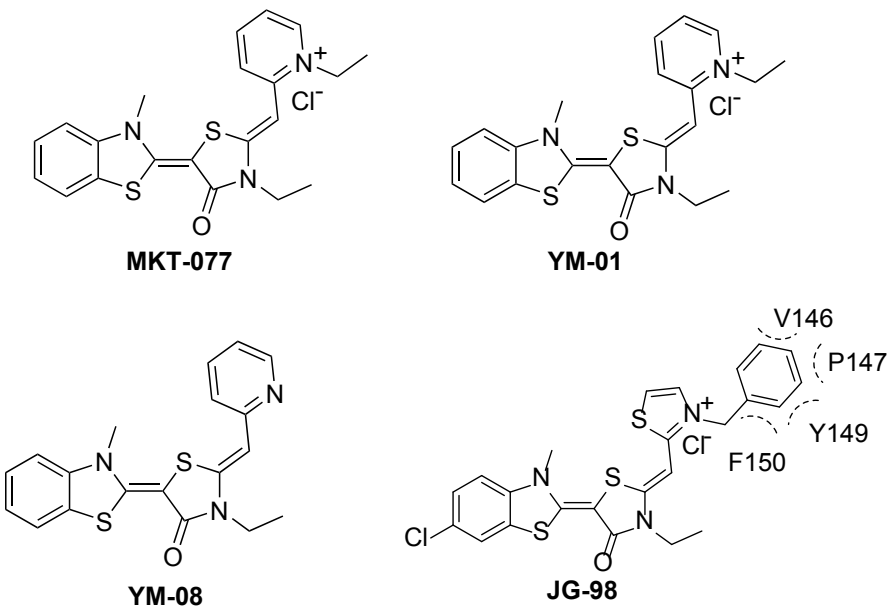

Figure 1.3: Chemical structures of MKT-077 and its analogs. The residues in Hsp70 that interact with the terminal phenyl group of JG-98 are shown.

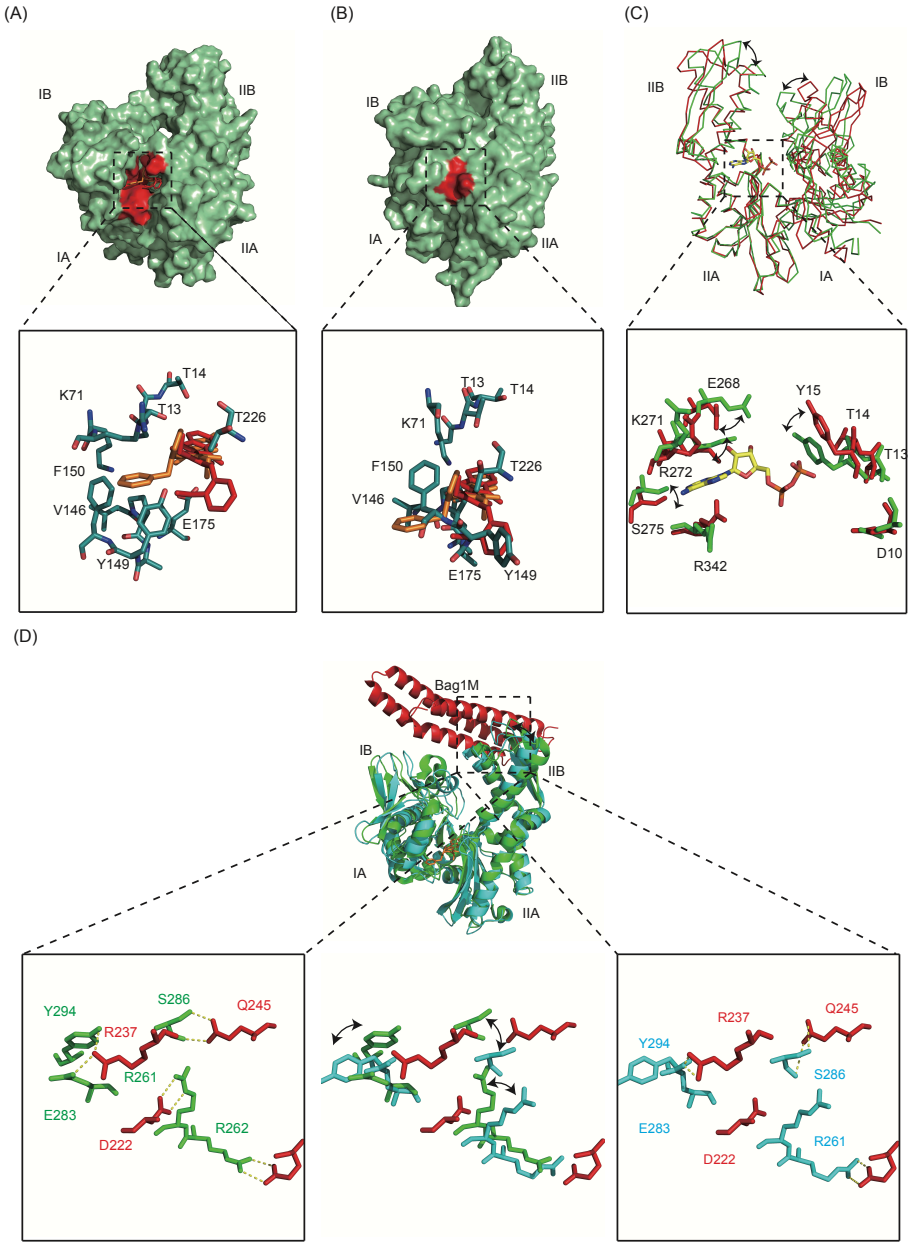

Figure 1.4: MKT-077 binds to the ADP-form of Hsp70 and disrupts binding to Bag co-chaperones. (A). MKT-077 and its analogs bind to a pocket of Hsc70's NBD in the "open" state. The gate residues are highlighted. (B) The binding site for MKT-077 and its analogs is occluded in the ATP-bound, "closed" state, with the gate residues collapsed. (C) Binding to MKT-077 induces rotations in subdomain IIB and closure of the nucleotide-binding cleft. The key motions of nearby residues in the binding site are shown compared to Hsc70's NBD in the ADP state (PDB 3C7N). (D). Binding to MKT-077 disrupts the hydrogen-bonding network that normally links Hsc70 to Bag1M. (Red: Bag1M, Green/Cyan: Hsc70 apo state (left; PDB 1HX1) or JG-98 bound Hsc70 (right).

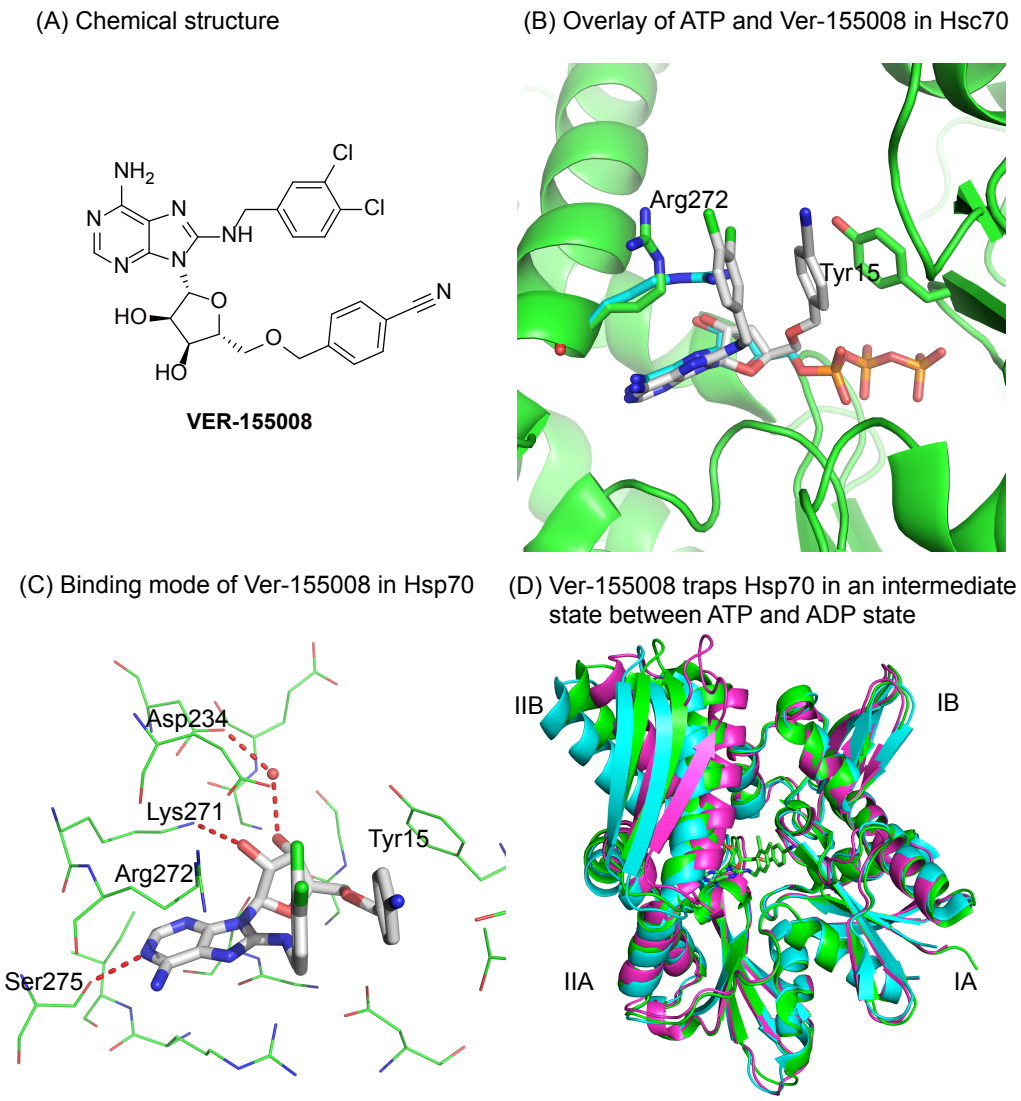

Figure 1.5: Ver-155008 is an ATP-competitive inhibitor of Hsp70 and it binds in the nucleotide-binding pocket. (A) Chemical structure of Ver-155008. (B) Overlay of the X-ray crystal structure of Hsc70 bound to ATP and Bag-1 (PDB 3FZF) with the structure of Hsc70 and Bag-1 bound to VER-155008 (PDB 3FZL). Other than a repositioning of Arg272, ATP and VER-155008 are in the same pose and Hsc70 is largely unperturbed. (C) Binding mode of VER-155008 (PDB 4IO8), with key contact residues highlighted. Hydrogen bonds are indicated by dotted lines. (D) Overlay of Hsp70's NBD bound to ATP- (PDB 1KAX), ADP- (PDB 3FZL), or VER-155008 (PDB 4I08), showing that VER-155008 keeps Hsc70 in an intermediate state between the two natural nucleotides, especially the position of the IIB subdomain.

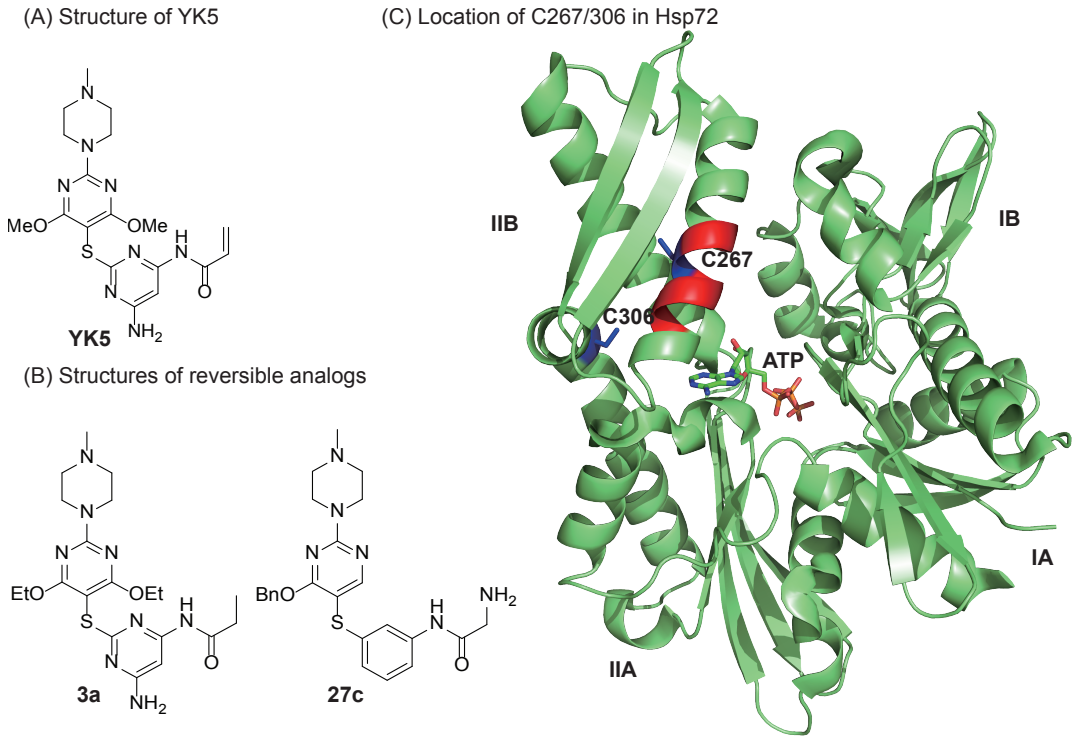

Figure 1.6: The Hsp70 inhibitor, YK5, binds to an allosteric site near Cys267. (A) Chemical structure of the irreversible inhibitor, YK5. (B) Chemical structures of reversible inhibitors, 3a and 27c, which lack the electrophile. (C) The structure of the NBD of Hsp72 (3JXU), highlighting the position of the nucleotide and C267 and C306 (Blue). The YK5-binding site $TAC_{267}ERAK$ is also shown (Red).

Chapter 2: High Throughput Screen for Inhibitors of Protein-Protein Interactions in a Reconstituted Heat Shock Protein 70 (Hsp70) Complex

INTRODUCTION

Protein-protein interactions (PPIs) are emerging as targets for both drug discovery and chemical biology (1). Indeed, 20% of the total number of PPI inhibitors have been reported in the last five years alone (2). This accelerated rate of discovery has been fueled, in part, by improvements in the design of chemical libraries (*e.g.* fragment-based collections and macrocycles) and the development of specialized HTS methodologies that are suitable for studying PPIs (*e.g.* Alpha-Lisa and split-GFP). However, not all PPIs are proving amenable to these solutions. PPIs vary dramatically in their relative affinity (K_D), polarity, and buried surface area (BSA) (3). Based on retrospective analyses of reported successes and failures, it seems that the subset of "difficult" PPIs are ones that: (a) are of weak affinity and/or (b) occur over large, shallow interfaces (4). Protein contacts with these features seem to be relatively difficult to inhibit because they lack good binding sites for drug-like (*e.g.* less than 500 Da) small molecules. In addition, "difficult" PPIs are commonly found within multi-protein complexes, which are composed of three or more components. This feature adds to the complexity of the system because, even if one can identify an inhibitor of one difficult PPI, it is often unclear how that event might influence binding to other partners. Thus, it is becoming clear that next-generation HTS approaches are needed to tackle these issues.

To explore these questions, we focused on the molecular chaperone, heat shock protein 70 (Hsp70) as a model system. Hsp70 is composed of an N-terminal, nucleotide-binding domain (NBD) and a C-terminal, substrate-binding domain (SBD). The hydrolysis of ATP in the NBD causes a dramatic conformational change that powers the chaperone cycle (5). This process is tightly regulated by binding of Hsp70 to its co-chaperones (6).

The major classes of Hsp70 co-chaperones are the J-domain proteins (also called Hsp40s or DNAJs), which stimulate the hydrolysis step, and the nucleotide exchange factors (NEFs), which bind a distinct region of Hsp70 and promote ADP release. Together, these two co-chaperones have been observed to increase Hsp70's steady state ATP hydrolysis by nearly 200-fold (7). For these reasons, the Hsp70 system is a well-studied multi-protein machine and we reasoned that it would also be a good one for studying "difficult" PPIs. Specifically, the interaction of Hsp70 with J proteins is known to be weak (micromolar) and to involve a large BSA that is highly polar (8). Similarly, the interaction of Hsp70 with the BAG family of NEFs is relatively tight (mid-nanomolar), but the contact area is large and occurs over multiple subdomains of Hsp70's NBD (9). Thus, this ternary system is emblematic of modern, multi-protein drug targets and includes multiple categories of "difficult" PPIs.

We envisioned a strategy in which measuring the ATP cycling of this three-protein system might provide a read-out for each of the PPIs. The intrinsic hydrolysis activity of Hsp70 in the absence of its co-chaperones is slow (5×10^{-4} sec^{-1}) (6,7), such that most of the measured signal would be expected to emerge as a direct result of co-chaperone interactions. In support of this idea, screens performed against a combination of the prokaryotic Hsp70 (DnaK) and one of its co-chaperones (DnaJ) had previously identified PPI inhibitors (10). However, it is not clear that a binary combination replicates the full conformational cycling of this complicated system. For example, Hsp70-NEF activity contributes to the kinetics of substrate binding and release, but is only rate-limiting in the presence of J protein activity (11). Put another way, it would be expected that only a full

complement of co-chaperones would sample the full range of conformational states that normally occur under physiological conditions.

Here, we report an HTS campaign using the human Hsp70 system: Hsp72 (HSPA1A), BAG2, and DnaJA2. There are ~13 *hsp70* genes, ~45 J-proteins and 6 BAG-domain containing NEFs in humans. From these possibilities, we chose Hsp72, DnaJA2 and BAG2 because they have been shown to be important in cancer (12-15) and because their biochemistry has been fully characterized (16). Leveraging this existing knowledge, we generated a reconstituted multi-protein complex (RMPC) of purified Hsp72, DnaJA2 and BAG2 at a carefully chosen ratio of 5:1:2.5. Then, we screened 100,000 diverse compounds for inhibitors of steady state nucleotide turnover in 384-well format. To our knowledge, this is the largest HTS campaign targeting Hsp70 that has been reported. From this screen, we identified multiple compounds that inhibit ATPase activity and we focused on two promising chemical series. Pilot medicinal chemistry campaigns, combined with secondary assays, showed that one compound targeted the Hsp70-DnaJA2 complex, while the other inhibited Hsp70-BAG2. These findings suggest that RMPCs present a tractable, biochemical approach for the discovery of inhibitors of even difficult PPIs within multi-protein systems, thus adding to the “toolbox” of methods for chemical biology.

RESULTS

High throughput ATPase screen identifies inhibitors of Hsp72-DnaJA2-BAG2.

Our search for inhibitors of PPIs within the Hsp72-DnaJA2-BAG2 system was guided by three major design ideas: (a) to avoid discovery of nucleotide-competitive molecules, we saturated the cleft using high concentrations of ATP (1 mM) in the

screening buffer, (b) DnaJA2 and BAG2 were added at concentrations that produced half-maximal stimulation of ATP hydrolysis to improve the sensitivity of the assay to potential inhibitors and activators (17) and (c) we combined all three proteins (Hsp72, DnaJA2 and BAG2) into the same wells to re-create native cycling conditions. Using these principles, we then chose inorganic phosphate release as the measure of steady state ATPase activity. Specifically, we used a modification of the malachite green (MG) assay, in which MG is replaced by quinaldine red (QR) and the measurements are made in opaque white, 384-well plates. This approach has been shown to enhance sensitivity more than 8-fold in 384-well format (10). Finally, for the chemical library, we selected a 100K diversity set from ChemDiv that is composed of lead-like molecules.

Recombinant, human Hsp72, DnaJA2, and BAG2 were each purified from *E. coli* (>95% purity, SDS-PAGE). To estimate the quality of the Hsp72 sample, we measured its intrinsic ATPase activity (~4-6 pmol/min/μg Hsp72) and found that it compared favorably to literature precedent (18). DnaJA2 and BAG2 solutions were similarly characterized by titrating them into Hsp72 and measuring their ability to stimulate hydrolysis (**Figure 2.1a**). From this characterization, we prepared a master mix that would yield final concentrations of: 0.5 μM Hsp72, 0.1 μM DnaJA2, and 0.25 μM BAG2. In 384-well plates, individual test compounds from the 100K ChemDiv collection were dispensed to the master mix, at a final concentration of ~20 to 40 μM. After a short incubation, an ATP solution (1 mM final) was added to start the reaction. After two hours, the reaction was quenched and the QR signal converted to a hydrolysis rate by comparison to an inorganic phosphate standard. Each screening plate included a negative control (a sample lacking Hsp72) and positive control containing 40 μM myricetin (19). The overall

Z-factor was calculated to be 0.65 and the co-efficient of variance was 9%. Finally, it is important to note that the screen was carried out in the presence of 0.01% Triton X-100 to minimize aggregator artifacts.

The screen revealed 1,312 molecules that appeared to inhibit the hydrolysis of ATP and 470 molecules that increased it by at least ± 1 standard deviation (SD). This list was further filtered to only include those compounds that showed effects at least ± 3SDs from the control, leaving 973 inhibitors and 74 activators (**Figure 2.1b and c**). Although it was not the focus of this study, we were potentially interested in pursuing both inhibitors and activators. However, we were also concerned that apparent activators might be fluorescence artifacts. Accordingly, both sets of active compounds were cherry-picked and tested for intrinsic fluorescence (in the absence of protein) that might interfere with the QR assay (excitation 430 nm / emission 530 nm). At the same time, we removed any compounds that were annotated as common pan-assay hits (*e.g.* PAINS) and those flagged as containing reactive functionalities. Together, these triage steps reduced the number of potential inhibitors to 471 (0.5 %) and removed all of the activators. The potential inhibitors were then subject to validation in eight-point, dose-response curves (DRCs). Molecules with EC_{50} values < 50 μM were then considered to be confirmed actives, resulting in 74 inhibitors (0.1% hit rate).

Compound R and Compound F inhibit distinct binary combinations.

Next, the top 18 inhibitors were re-purchased from ChemDiv or ChemBridge and tested in secondary DRCs. In these assays, we used both the human Hsp72-DnaJA2-BAG2 system and the highly conserved, prokaryotic orthologs: DnaK-DnaJ-GrpE. We included the prokaryotic system in the secondary screening because of its faster rate of

ATP turnover (20), which tends to produce more robust EC_{50} values. Of the 18 re-purchased compounds, five had EC_{50} values less than 50 μM (Compounds F, C, I, N and R) in the DnaK-DnaJ-GrpE system. Interestingly, these active molecules appeared to visually "bin" into two distinct groups, based on the shape of their inhibition curves (**Figure 2.2a**). The first set (Compounds I and R) inhibited ~20% of the overall activity at a saturating concentration, whereas the other molecules (Compounds C, F, and N) inhibited ATP turnover to a maximum of 80%. These two categories were immediately intriguing because our pre-screening characterization studies (see **Figure 2.1a**) had shown that ~24% (~6 pmol/μM Hsp72/min) of the overall ATPase activity was due to stimulation by BAG2, whereas 80% (~20 pmol/μM Hsp72/min) is produced by DnaJA2's contribution. Thus, it was compelling to imagine that the two categories of inhibitors might be targeting the Hsp70-NEF or Hsp70-J protein pairs. Qualitatively similar results were obtained with the human system (**Figure 2.2a**).

To explore this idea, we selected two representative compounds for further mechanistic studies. From the available compounds, F and R were particularly intriguing because they are both 2-aminothiazoles, yet they had very different activity profiles. Specifically, Compound R inhibited 21% of the total activity of DnaK-DnaJ-GrpE, with an EC_{50} of 35 μM, while Compound F inhibited 73% of the total ATP turnover, with an EC_{50} of 10 μM. To understand whether these molecules might target distinct, binary combinations, we tested them against mixtures of either DnaK-DnaJ or DnaK-GrpE alone. Consistent with the speculation, we found that Compound F inhibited the combination of DnaK and DnaJ, but that it had no activity against the DnaK-GrpE system (**Figure 2.2b**). Conversely, Compound R had no activity against the DnaK-DnaJ pair, but had modest

activity against DnaK-GrpE (**Figure 2.2c**). Thus, screening against the ternary complex seemed to yield at least one inhibitor of each "difficult" PPI.

A side product of Compound F is the active molecule and it inhibits the Hsp70-DnaJA2 interaction.

To further probe the mechanism of Compound F, we first re-synthesized the molecule (now termed IT2-21a) using a known synthetic route (**Figure 2.3a**). We were initially frustrated by the lack of activity of IT2-21a in ATPase assays, so decided to re-evaluate the chemical identity of the authentic molecule from the screening collection. By LC-MS, we found trace amounts of a side-product featuring two catechols (IT2-21c) in the original samples (**Supplemental Figure 2.S1**). We reasoned that such a side product might be expected from the undesired nucleophilic attack of the pyrazole secondary amine onto the alpha carbon of the acetophenone starting material, so we separated the two products from the crude reaction mixture by HPLC. Pure (>95%) samples of both compounds were then tested in the ATPase assay. Indeed, we found that IT2-21c was the potent inhibitor, while the molecule that is annotated in the commercial library, IT2-21a, was inactive (**Figure 2.3b**).

With the active molecule now clear, we turned to examination of structure-activity relationships (SAR). Our initial focus was on trying to eliminate the catechols, because these groups can sometimes form covalent bonds with protein nucleophiles. Briefly, it is known that catechols can be oxidized to di-*ortho*-benzoquinones, creating strong Michael acceptors (**Figure 2.3c**). Accordingly, we synthesized IT2-44a and IT2-44b, in which the catechols of IT2-21a and IT2-21c were replaced with less reactive, *para*-hydroxy substitutions (**Figure 2.3d**). We found that both IT2-44a and IT2-44b were inactive in the

ATPase assay (**Figure 2.3e**), consistent with a possible covalent mechanism. It is known that long-term storage in DMSO can exacerbate oxidation of the catechol, so we next tested "aged" DMSO stocks of IT2-21a and IT2-21c that were incubated overnight at room temperature. Consistent with the model, both samples gained activity in the ATPase assay (see **Figure 2.3e**).

Given this information, we would expect that IT2-21c might covalently modify the target (21,22). Indeed, IT2-21c still had an inhibitory effect on DnaK after the compound–treated protein was dialyzed for 24 hours (**Figure 2.3f**). To understand where this compound might bind, we titrated IT2-21c into ^{15}N labeled DnaK NBD and performed 2D NMR, HSQC experiments (**Supplemental Figure 2.S2**). Plotting the chemical shift perturbations (CSPs) onto the structure of DnaK's NBD (2KHO) showed that IT2-21c seemed to bind a conserved region that is located between the IB and IIB subdomains (**Figure 2.3g**). It is not yet clear which residue(s) is the target for covalent modification, but there are a number of possible nucleophiles, particularly lysines, in this vicinity. Interestingly, this region was previously identified as the binding site for myricetin, the positive control from our screen (19). Together, we concluded that IT2-21c was acting by a covalent mechanism and therefore not likely to be a suitable scaffold for further study. However, it binds an interesting location on the NBD, which might be exploited with structure-based drug design in the future.

Compound R analogs inhibit the Hsp70-NEF interaction.

Unlike Compound F, we found that Compound R bound reversibly and that it lacked the chemical features to make it a potential covalent inhibitor. Thus, our exploration of Compound R focused on generating analogs to better understand the

pharmacophore. A total of thirty analogs were created using a previously described synthetic route that features a Hantzsch thiazole condensation (**Figure 2.4a**) (23). These analogs largely focused on modifications of the "right" side of the molecule, as there were many commercially available anilines from which to diversify the substituted thiourea. Each of the compounds was tested for the ability to inhibit the ATPase activity of the DnaK-DnaJ-GrpE complex (**Supplemental Figure 2.S3**). Then, the active molecules (EC_{50} < 25 μM) were additionally tested against the Hsp72-DnaJA2-BAG2 combination. We did not discover any molecules that were selective for the prokaryotic or eukaryotic system, which is not surprising given the remarkably high sequence and structure conservation between these systems. From this effort, it seemed that 2,5 di-substitutions were required for activity (**Figure 2.4b**). The importance of the 2,5 di-substitution is best exemplified by comparing IT2-144 with its regio-isomers, IT2-158, IT2-159 and IT2-160; the 2,3, 2,4 and 2,6 di-fluoro derivatives, respectively. All three of these derivatives were inactive (EC_{50} > 25 μM), whereas the 2,5 di-fluoro regio-isomer, IT2-144, had an EC_{50} value of 6.9 μM. The best compound in the ATPase assay, IT2-179, replaced the fluorines for bromines and it had an EC_{50} value of ~3.6 μM against Hsp72-DnaJA2-BAG2, an approximate 3-fold improvement on Compound R. Finally, removing the ring entirely (compound IT3-70a), or extending the linker to the ring in the form of a benzyl derivative (IT2-171) abolished activity, suggesting that the positioning of this ring is a key part of the pharmacophore.

To understand possible membrane permeability, we tested the analogs in anti-proliferative MTT assays using the breast cancer cell line, MDA-MB-231. This cell line was chosen because it is known to require Hsp70 complexes for growth (13).

Encouragingly, compounds active in the ATPase assays had the expected anti-proliferative activity. For example, IT2-144 had an EC_{50} of 2.7 μM in suppressing growth of MDA-MB-231 cells; whereas the negative control, IT3-70a, was inactive (EC_{50} > 50 μM). As an initial test of potential selectivity for cancer cells, we also tested the analogs for effects on growth of normal, mouse embryonic fibroblasts (MEFs). Multiple groups have suggested that Hsp70 is selectively required in cancer cells, creating an "addiction" to this chaperone (24). Although Compound R was not selective (selectivity index ~ 0.9), the more potent analogs were significantly less toxic to MEFs. For example, IT2-144 and IT2-179 had EC_{50} values > 50 μM in these normal cells (**Figure 2.4b**). Together, these studies suggest that Compound R analogs are at least partially membrane permeable and they might be good starting points for Hsp70 inhibitors. It is important to note that their molecular selectivity has not been established and will require additional efforts.

Next, we wanted to understand whether Compound R analogs might act on other NEFs besides BAG2. This question is important because there are six members of the BAG family in mammals and, more broadly, there are at least two other, structurally distinct classes of NEFs. To explore this idea, we tested the activity of IT2-144 against a combination of Hsp70 (or DnaK) and five different, purified NEFs: human BAG1, BAG2, BAG3, Hsp105, and *E. coli* GrpE. The BAG family of NEFs bind to Hsp70's NBD through a conserved motif, termed the BAG domain (9). Thus, in addition to testing the three full-length BAG proteins (BAG1-3), we also measured activity against a truncated protein composed of only the BAG domain of BAG1. Hsp105 is a member of the Hsp110 class of NEFs, which share similar domain architecture with Hsp70 and bind in a "face-on" orientation (25). Finally, the prokaryotic GrpE makes contacts with DnaK in the IB and IIB

subdomains, similar to the BAG proteins, but also the IA subdomain, and even parts of the SBD (26). Thus, this collection of NEFs includes members that bind Hsp70 in different locations.

Because Hsp105 has intrinsic ATPase activity that is hard to resolve from Hsp70's in hydrolysis assays, we instead turned to a luciferase-refolding assay to estimate inhibition of the panel of NEFs. Luciferase refolding is commonly used to measure NEF activity, because the co-chaperone yields a characteristic concentration profile in which activity is first stimulated and then inhibited (16,27). Briefly, in this experiment, chemically denatured firefly luciferase is refolded into active enzyme by the action of Hsp70 complexes and luminescence is used to track this process (28). In control experiments, we found that IT2-144 did not inhibit native luciferase (**Supplemental Figure 2.S4**), allowing us to use this molecule in refolding assays without interference. Remarkably, we found that IT2-144 suppressed the refolding activity of Hsp70 with any of its NEFs at low micromolar concentrations (**Figure 2.5a**).

Interestingly, recent work has shown that benzothiazole-rhodacyanines, such as MKT-077 and JG-48, bind to an allosteric site on Hsp70 and interrupt binding to NEFs (29). Like IT2-144, these compounds are known to inhibit multiple categories of NEFs (27). Therefore, we wondered whether IT2-144 might bind to the same site on Hsp70. This result would be important because MKT-077 and JG-48 have strong activity in multiple disease models, but they have significant liabilities (*i.e.* photoreactivity, poor solubility) that limit their use. In other words, the benzothiazole-rhodacyanines are good proof-of-concept compounds, but a new scaffold might expand the utility of Hsp70 inhibitors.

To test this idea, we first performed extra precision (XP), induced-fit docking experiments focused on the known binding site for MKT-077 (30) (**Supplemental Figure 2.S5**). In these studies, we used the ADP-bound structure of the Hsc70 NBD (PDB 3HSC). Consistent with the biochemical studies, we found that analogs with 2,5 substitutions, such as IT2-144, had the best XP scores, whereas the 2,4 di-fluoro derivative (IT2-159) and the negative control (IT3-70a) had significantly worse XP scores (**Figure 2.5b**). The docking pose of IT2-144 suggested that the imidazo[1,2-a]pyridine was located within a deep, narrow pocket composed of Pro176, Val369, Glu175, Asp199, Ile197 and Val337. Interestingly, this group approached the magnesium that is required to chelate nucleotide. The central 2-aminothiazole then seemed to position the pendant benzyl ring to make favorable contacts with a second pocket composed of Tyr149, Gly224, Thr226, Ala223 and Thr222. The striking, overall feature of the interaction was the excellent "fit" of the molecule in a narrow channel, perhaps best exemplified by a surface rendering (**Figure 2.5b**). This docked pose also helped explain the observed structure-activity relationships (SAR) from the ATPase assays. Specifically, we noted that the fluorines at the 2- and 5-positions of IT2-144 were predicted to make favorable contacts in the second pocket. Specifically, the 2-fluorine was positioned to engage in fluorine bonding (31) with the backbone of Asp206; whereas the 5-fluorine was positioned near Tyr149. In this pose, placement of fluorine at the 3-position (as in IT2-158) would not be expected to make favorable contacts and the 4-position (as in IT2-159) would point into solvent. Together, these docking studies supported the biochemical results and suggested possible ways of improving the molecule.

To further explore the SAR, we turned to a binding assay. Specifically, we took advantage of the intrinsic fluorescence of the 2-aminothiazoles (**Figure 2.5c**) to directly measure an interaction. In this format, purified human Hsc70 was added to test compounds and the binding-induced quenching of compound fluorescence was measured at the λ_{max}. Consistent with the model, only IT2-144 had a measurable affinity for purified, human Hsc70 (**Figure 2.5d**), whereas compounds IT2-158, IT2-159 and IT2-160, as well as the negative control, IT3-70a, did not bind (K_{app} > 10 μM). Further, the apparent affinity of IT2-144 was consistent with the functional and cellular assays (K_{app} ~ 1 μM).

Another prediction of the docking study is that IT2-144 should not directly compete with ADP for binding. To test this idea, we measured the affinity of IT2-144 for human Hsc70 in the apo- and ADP-bound states. If IT2-144 was competitive for nucleotide, rather than allosteric, we would anticipate that ADP would significantly reduce the apparent affinity. However, we found that addition of ADP did not inhibit and, in fact, might have a modestly enhanced affinity (K_{app} 0.79 vs. 1.3 μM). In further support, we found that IT2-144 did not compete for binding of DnaK to a fluorophore-labeled ATP analog (**Supplemental Figure 2.S6**). Finally, we measured binding of IT2-144 to Hsc70 variants that have mutations in Thr222, a residue that docking predicted to be a potential gatekeeper to the binding site (**Figure 2.5e**). In the ADP-bound state, we found that mutation to a small amino acid (T222A) had no effect on affinity (WT K_{app} ~790 nM; T222A K_{app} ~870 nM), whereas mutation to methionine (T222M) mildly reduced affinity (K_{app} ~1.3 μM) (**Figure 2.5e**). Attempts to mutate other residues in the putative binding site affected activity or folding, so we were not able to conclusively determine their role in binding.

Although further work needs to be done, these results suggest that IT2-144 might have a mechanism-of-action that is similar to the benzothiazole-rhodacyanines, such as JG-48. Thus, IT2-144 could become an important starting point for the development of chemical probes of the Hsp70 system.

DISCUSSION

Multi-protein complexes, especially those involving "difficult" PPIs, present a challenge for HTS campaigns. Cell-based approaches can sometimes recreate the dynamics of these systems, yet it is often challenging to identify which protein is the target. As an alternative, we pursued a biochemical approach that is intended to borrow some strengths of a physiological milieu, such as multiple binding partners, with the precision of a well-defined, purified system. Specifically, we explored an HTS approach in which the enzymatic activity of the "core" protein (*i.e.* Hsp70) is measured and the effects of binding partners (*i.e.* DnaJA2 and BAG2) on turnover is used as a surrogate for their respective PPIs. We used the Hsp70 system as a model, but many other biological examples have conceptually similar architecture (*e.g.* Rho-Gap-GEF, Hsp90-p23-Aha1, RNA pol II). A key feature in these systems, including Hsp70, is that the enzyme is often weak. This allows discrimination of the effects of binding partners, such as co-chaperones, from the intrinsic activity. Indeed, a fascinating observation from our Hsp70 screen is that the potential mechanism of an inhibitor starts to become clear, even in the primary assay results. For example, Compound F inhibited the Hsp72-DnaJA2 pair and blocked ~80% of the steady state turnover. Thus, this RMPC approach may have significant advantages for a subset of targets, specifically those with slow enzymes.

HTS campaigns, including the one described here, often result in initial inhibitors with modest efficacy values (in the range of low- to mid-micromolar). Then, the active series must be advanced through a hit-to-lead, medicinal chemistry campaign to achieve high selectivity and potency. Historically, inhibitors of PPIs seem to disproportionately fail to progress through this process, likely because many PPIs have physical features, such as large BSA, which make it relatively challenging to develop competitive inhibitors. Indeed, a 2015 review of the literature found that most reported inhibitors of “difficult” PPIs have allosteric, not orthosteric, mechanisms (2). These allosteric inhibitors often take advantage of binding sites that are located far from the PPI contact, where the features of the pocket can be more favorable for tight binding. Thus, while there is no guarantee that PPI inhibitors from RMPC screens will progress through hit-to-lead campaigns, there is some reason to think that those with allosteric mechanisms, such as Compound R, should be prioritized over orthosteric ones.

Hsp70 is an emerging drug target for a number of diseases (32). Accordingly, this work might have implications beyond HTS technology development. For example, while Compound F itself is not a suitable starting point for probe development, its binding site might serve as a guide for future fragment-based tethering screens (33). Perhaps more interesting is the possibility that Compound R and its analogs might directly serve as a starting point for the development of Hsp70-NEF inhibitors. Hsp70 and its NEFs have been shown to play important roles in cancer (34) and this PPI seems to be a particularly attractive one for controlling chaperone function (27). Thus, further medicinal chemistry campaigns and mechanistic studies on IT2-144 seem warranted. Perhaps more broadly,

this RMPC approach seems to be particularly well suited to the Hsp70 system and it is intriguing to consider primary screens that add more partners, such as “client” proteins.

MATERIALS AND METHODS

Compound Library

The HTS campaign was carried out using the commercial ChemDiv 100K diversity set library, which is composed of “lead-like” molecules (e.g. molecular weight, logP, polar surface area, number of rotatable bonds, and the presence/absence of reactive or toxic structural motifs). Active compounds were confirmed with re-purchased samples from either ChemDiv or ChemBridge. Compound identity was confirmed using LC-MS and ^{1}H NMR.

Protein Purification

Human Hsp72 (HSPA1A) was purified as previously described (35) using an N-terminal 6xHis tag and Ni-NTA column, followed by overnight TEV Protease cleavage of the His tag and lastly an ATP-agarose affinity column. Human DnaJA2, and *E. coli* DnaJ were purified as previously described (16) using a N-terminal 6xHis tag and Ni-NTA column, TEV Protease cleavage of the His tag, a secondary Ni-NTA column to remove un-cleaved contaminants and finally size exclusion chromatography on a 15 mL Superdex 200 gel filtration column (GE Healthcare). Human BAG Domain, BAG1, and BAG2 were purified based on previous reports (16). Briefly, N-terminal 6xHis BAG2 was subjected to a Ni-NTA column and overnight TEV Protease cleavage of the 6xHis tag. The NEFs were then dialyzed overnight into Buffer A (25 mM HEPES, 10 mM NaCl, 15 mM β-mercaptoethanol, 0.1 mM EDTA, pH 7.6) and separated via ion-exchange chromatography on a Mono-Q HR 16/10 column (GE Healthcare). Finally, the proteins were subjected to size exclusion

chromatography on a 15 mL Superdex 200 gel filtration column (GE Healthcare). The BAG proteins were concentrated and exchanged into BAG buffer (25 mM HEPES, 5 mM $MgCl_2$, 150 mM KCl, pH 7.5). Hsp105 was purified on a Ni-NTA column, subjected to overnight TEV cleavage as described above, and then subjected to a second Ni-NTA column purification, followed by buffer exchange into BAG buffer. The prokaryotic chaperone proteins, DnaK, DnaJ, and GrpE, were purified following previously reported protocols (36). ^{15}N labeled DnaK NBD_{1-388} was expressed in M9 medium with ^{15}N ammonium chloride (Sigma) and purified on an ATP-agarose affinity column.

High Throughput ATPase Screen with Quinaldine Red

The HTS method was adapted from previously reported procedures (10). A master mix of purified Hsp72, DnaJA2 and BAG2 was prepared, such that the final concentrations would be 0.5 μM, 0.1 μM, and 0.25 μM, respectively. Solutions were added to 384-well plates using a Multidrop dispenser (Thermo Fisher Scientific, Inc.), with the exception of compound and DMSO solutions, which were added using a Biomek HDR (Beckman). Quinaldine red (QR) solution was freshly prepared each day as a 2:1:1:2 ratio of 0.05% w/v quinaldine red, 2% w/v polyvinyl alcohol, 6% w/v ammonium molybdate tetrahydrate in 6 M HCl, and water. To each well of a 384-well white, low-volume, polystyrene plate (Greiner Bio-One, Monroe, NC), was added 5 μL of a master chaperone mix. The assay buffer (100 mM Tris, 20mM KCl, 6mM $MgCl_2$, pH 7.4), was supplemented with 0.01% Triton X-100 in order to avoid identifying aggregators as false hits. The compounds, or DMSO alone, were added as 200 nL of a 1.5 mM stock, to give a final screening concentration of 43 μM, followed by 2 μL of 3.5 mM ATP to initiate the reaction. The plates were then centrifuged briefly, and subsequently incubated at 37 °C for two hours. After

incubation, 15 µL of QR solution was added, followed by 2 µL sodium citrate (32% w/v) to quench the reaction. After another 15 minute incubation period at 37 °C, fluorescence (excitation 430 nm, emission 530 nm) was read in a PHERAstar plate reader.

General Synthesis

Preparation of Substituted Thioureas

Thioureas were prepared from substituted amines according to previously described methods (23). Briefly, 1.1 molar equivalents of benzoyl isothiocyanate were added drop-wise to the commercial anilines, with stirring in acetone at room temperature. The solution was then heated to reflux for 1-3 h until completion, as monitored by thin layer chromatography (TLC). Once complete, the reaction was cooled, then poured into water/ice to precipitate the benzoyl thiourea intermediate. The intermediate was isolated by vacuum filtration and dried prior to being re-dissolved in a mixture of 20 mL methanol and 5 mL aqueous 1 M NaOH. The hydrolysis reaction was carried out at 80 °C for 1 hour, or until complete, as judged by TLC. The reaction was then cooled, and added to water/ice and neutralized by the addition of 1 M HCl. The thiourea product typically crashed out of solution upon removal of MeOH by rotary evaporation. In the cases where product did not precipitate at this stage, the product was isolated by extracting 3x with 20 mL ethyl acetate, combining the organic fractions and removing solvent by rotary evaporation. The purified thioureas were deemed at least 95% pure by LC-MS, and carried forward to make the 2-aminothiazoles.

General Preparation of 2-Aminothiazoles

Thioureas were mixed with bromo- or chloro- acetophenones dissolved in 4 mL ethanol, and refluxed with stirring for ~3 hours. Over the course of the reaction, the desired product

formed as an insoluble solid on the edge of the flask. After 3 hours, the reaction was cooled to room temperature, then placed on ice for ~30 min. Continued precipitation was observed, and this solid was collected by vacuum filtration. The product was further washed with hexanes, and then vacuum dried. Compound identity was determined by ^{1}H NMR and purity determined by LC-MS.

Compound Characterization

IT2-144: ^{1}H NMR (400 MHz, DMSO) δ 10.63 (s, 1H), 9.08 (d, J = 8.0 Hz, 1H), 8.34-8.29 (m, 1H), 7.97-7.88 (m, 2H), 7.54 (s, 1H), 7.47 (t, J = 12 Hz, 1H), 7.37-7.31 (m, 1H), 6.84 (t, J = 16 Hz, 1H), 2.63 (s, 3H). ESI-MS: calculated for $C_{17}H_{12}F_2N_4S$ 342.08; found 343.13

IT2-151: ^{1}H NMR (400 MHz, DMSO) δ 10.63 (s, 1H), 9.19 (d, J = 8.0 Hz, 1H), 8.76 (d, J = 12 Hz, 1H), 7.98-7.90 (m, 2H), 7.55 (s, 1H), 7.50 (t, J = 16 Hz, 1H), 7.33-7.28 (m, 1H), 7.23-7.19 (m, 1H), 2.66 (s, 3H). ESI-MS: calculated for $C_{17}H_{12}BrFN_4S$ 403.99; found 404.99.

IT2-159: ^{1}H NMR (400 MHz, DMSO) δ 10.30 (s, 1H), 9.08 (d, J = 8 Hz, 1H), 8.27-8.20 (q, J = 8 Hz, 1H), 7.95-7.89 (m, 2H), 7.45 (s, 1H), 7.41 (t, J = 16 Hz, 1H), 7.10 (t, J = 16 Hz, 1H), 2.62 (s, 3H).

IT2-179: ^{1}H NMR (400 MHz, DMSO) δ 10.06 (s, 1H), 9.19 (d, J = 8 Hz, 1H), 8.59 (s, 1H), 7.98-7.91 (m, 2H), 7.63 (d, J = 8 Hz, 1H), 7.55 (s, 1H), 7.51 (t, J = 16 Hz, 1H), 7.21 (d, J = 8 Hz, 1H), 2.65 (s, 3H). ESI-MS calculated for $C_{17}H_{12}Br_2N_4S$ 463.91; found 464.94.

ATPase Assays with Malachite Green

Active compounds from the primary screen were confirmed by subsequent ATPase assays using malachite green (MG), as described previously (36). Briefly, in a clear 96-well plate, compounds were incubated with Hsp72 and co-chaperones at specified

concentrations in 25 µL total volume with a final DMSO concentration of 4%. All malachite green assays were performed in an assay buffer composed of 100 mM Tris, 20 mM KCl, 6 mM $MgCl_2$, 0.01% Triton X-100, pH 7.4. The reaction was initiated by the addition of ATP at a final concentration of 1 mM, and incubated at 37 °C for 1 hour. After incubation, 80 µL of MG reagent was added, followed by 10 µL of saturated sodium citrate to quench the reaction, and absorbance of 620 nm was measured on a SpectraMax M5 platereader (Molecular Devices). ATP hydrolysis rates were calculated by comparison to a phosphate standard.

Luciferase Refolding

Luciferase refolding assays followed a previously described procedure (37). All compounds were first tested by incubation with native luciferase to determine whether they interfered with the assay (**Supplemental Figure 2.S4**). Compounds that reduced activity by >10% were excluded from further analysis in this platform. Briefly, native firefly luciferase (Promega) was denatured in 6 M guanidine hydrochloride for 1 hour at room temperature and then diluted into assay buffer (28 mM HEPES pH 7.6, 120 mM potassium acetate, 12 mM magnesium acetate, 2.2 mM dithiothreitol, 8.8 mM creatine phosphate, and 35 U/ml creatine kinase). Solutions were prepared of test compounds, chaperones, denatured luciferase (at 0.1 µM), 10 mM phosphate (for NEF-stimulation assays), and 1 mM ATP. Total volume was 25 µL (4% DMSO) in white 96-well plates (Corning) and incubation time was 1 hour at 37 °C. Steady Glo reagent was prepared fresh and added to the plate immediately prior to reading luminescence.

Cell Culture and Viability Assays

MDA-MB-231 and MEF cells were purchased from ATCC and maintained at 37 °C and 5% CO_2 in appropriate growth media (DMEM, 1% pen/strep, 10% FBS for MDA-MB-231 and 15% FBS for MEF respectively). Cell proliferation assays were carried out as described previously (34) using the MTT kit (ATCC number: 30–1010 K) with some modifications. Briefly, cells were plated in tissue culture-treated 96-well plates (5,000 cells per well for MDA-MB-231, and 2,000 cells per well for MEF) with compounds (1% DMSO) in 200 µL of growth medium for 72 hours. Cells were washed 3x with PBS, and the medium was replaced with fresh medium plus 10% MTT reagent, then subsequently incubated at 37 °C, 5% CO_2 for 4 hours. The medium was then removed, and replaced with DMSO, then read at an absorbance of 540 nm.

HSQC with ^{15}N Labeled DnaK NBD

2D HSQC experiments were carried out in order to measure binding of IT2-21c to ^{15}N-labeled DnaK NBD_{1-388}. Experiments were performed on a Bruker 800 MHz NMR at 27 °C in NMR buffer (25 mM Tris, 10 mM KCl, 5 mM $MgCl_{2,}$, 10 mM NaP_i, 5 mM ADP, 0.015% NaN_3, 5% D_2O, pH 7.2). For determining a binding site of IT2-21c, DnaK NBD concentration was held at 100 µM, and compound was titrated in at ratios of 1:1 and 1:2 (NBD:compound) at 2% DMSO. The spectra were processed with NMRPipe (38) and displayed with Sparky (39). The chemical shift assignments used were from the triple resonance data obtained by Bertelsen *et al*. (40). Compound-induced shifts that are larger than 0.01 ppm in ^{1}H and/or larger than 0.1 ppm in ^{15}N were deemed significant and were displayed on the DnaK NBD structure (2KHO).

Docking to MKT-077 Binding Site

Compound R derivatives were docked to a bovine Hsc70 crystal structure (PDB accession code: 3HSC) using both InducedFit and Glide docking software (Software Suite 2017-3, Schrodinger Inc). The nucleotide binding domain of Hsc70 is 100% identical between bovine and human. Prior to docking we optimized the protein structure using Protein Preparation Wizard. During this step water molecules, sodium and an inorganic phosphate ion from the crystal structure were removed. Only ADP and a magnesium ion were retained in the nucleotide binding pocket. Hydrogen atoms were added to the structure, protonation states of titratable residues were adjusted and overall structure was energy minimized such that heavy atoms were not allowed to move beyond 0.5 Å from their starting positions. The allosteric binding site was partially closed in the crystal structure. Therefore, we docked the allosteric inhibitor IT2-144 using an InducedFit docking algorithm. The allosteric binding pocket was defined using residues: T13, K71, Y149, E175, D199, T204 and ADP. InducedFit docking program treats both protein and ligand flexibly during docking. The lowest energy docking pose predicted by the InducedFit docking program is shown in **Figure 2.5b**. The methyl substituted imidazopyridine ring is deeply buried in the hydrophobic binding pocket and the hydrogen atom of the secondary amine makes a hydrogen bonding interaction with the backbone carbonyl oxygen of V207. The 2,5 di-fluoro phenyl ring stacks up between the beta-sheet and Y149 residue.

The allosteric binding pocket optimized, IT2-144 inhibitor-bound model was used in subsequent rigid-receptor flexible-ligand docking calculations. IT2-144 analogs were docked to the allosteric site using Glide docking with extra-precision (XP) docking scoring

function. All inhibitors were built using the Edit/Build panel of Maestro (Schrodinger Inc). They were subsequently energy minimized using LigPrep software (v4.3016, Schrodinger Inc). Inhibitor structure and docking scores are reported in **Figure 2.5b** and their binding poses are shown in **Supplemental Figure 2.S5.** 2,5 di-substituted derivatives all have similar docking scores, while the 2,4 di-substituted compound (IT2-159) and the truncated, negative compound (IT3-70a) have poorer scores. Docking poses also show a similar binding mode for all but IT2-159 and IT3-70a.

IT2-144 Binding by Fluorescence Quenching

All di-fluoro Compound R derivatives, as well as IT3-70a, were subjected to spectral characterization by determining a full scanning fluorescence spectrum at an excitation wavelength of 310 nm. These spectra were used to determine the optimal emission wavelength for each compound (IT2-144: 430 nm, IT2-158: 420 nm, IT2-159: 450 nm, IT2-160: 440 nm, IT3-70a: 460 nm). It is important to note that Compound R did not show any fluorescence in this range, and did not have an artifactual effect in the original QR assay. Only the di-fluoro derivatives appeared to give a strong enough fluorescence signature with this excitation/emission profile. Hsc70 was incubated at the indicated concentrations with nucleotide (ADP or ATP) for 30 minutes in a low-volume black 384-well plate (Corning) at room temperature (Buffer: 200 mM Tris, 40 mM KCl, 12 mM $MgCl_2$, 0.01% Triton X-100, pH 7.4). Following incubation with nucleotide, compounds were added to the wells at a constant concentration of 50 μM, and 5% DMSO. The protein/nucleotide/compound mixture was allowed to incubate at room temperature, in the dark, for 30 minutes, prior to reading fluorescence at ex: 310 nm and the appropriate emission wavelength, determined from the spectral characterization of each compound.

AUTHOR CONTRIBUTIONS

I.R.T., B.M.D., T.K., and E.R.P.Z. data curation; I.R.T., B.M.D., H.S., V.A.A., C.K., and J.E.G. formal analysis; I.R.T., B.M.D., H.S., X.R., V.A.A., C.K., J.N.R., and E.R.P.Z. investigation; I.R.T. and J.N.R. methodology; I.R.T. and J.E.G. writing-original draft; I.R.T., B.M.D., H.S., X.R., E.R.P.Z., and J.E.G. writing-review and editing; B.M.D. and J.E.G. conceptualization; M.P.J. software; M.P.J., E.R.P.Z., and J.E.G. supervision; E.R.P.Z. and J.E.G. funding acquisition; J.E.G. project administration.

ACKNOWLEDGEMENTS

The authors thank Martha Larsen and Thomas McQuade (University of Michigan; Center for Chemical Genomics) for technical assistance with the HTS campaign. We also thank Robert Briski for help in the triage of active molecules. This work was supported by NIH R01NS059690 (to J.E.G. and E.R.P.Z.) and Stand Up 2 Cancer (to J.E.G.). This work is dedicated to the memory of Tomoko Komiyama.

REFERENCES

1. Arkin, M. R., Tang, Y., and Wells, J. A. (2014) Small-molecule inhibitors of protein-protein interactions: progressing toward the reality. *Chemistry & biology* **21**, 1102-1114
2. Cesa, L. C., Mapp, A. K., and Gestwicki, J. E. (2015) Direct and Propagated Effects of Small Molecules on Protein-Protein Interaction Networks. *Frontiers in bioengineering and biotechnology* **3**, 119
3. Thompson, A. D., Dugan, A., Gestwicki, J. E., and Mapp, A. K. (2012) Fine-tuning multiprotein complexes using small molecules. *ACS chemical biology* **7**, 1311-1320
4. Scott, D. E., Bayly, A. R., Abell, C., and Skidmore, J. (2016) Small molecules, big targets: drug discovery faces the protein-protein interaction challenge. *Nature reviews. Drug discovery* **15**, 533-550
5. Chiappori, F., Merelli, I., Milanesi, L., Colombo, G., and Morra, G. (2016) An atomistic view of Hsp70 allosteric crosstalk: from the nucleotide to the substrate binding domain and back. *Scientific reports* **6**, 23474
6. Zuiderweg, E. R., Bertelsen, E. B., Rousaki, A., Mayer, M. P., Gestwicki, J. E., and Ahmad, A. (2013) Allostery in the Hsp70 chaperone proteins. *Topics in current chemistry* **328**, 99-153

7. McCarty, J. S., Buchberger, A., Reinstein, J., and Bukau, B. (1995) The role of ATP in the functional cycle of the DnaK chaperone system. *J Mol Biol* **249**, 126-137
8. Ahmad, A., Bhattacharya, A., McDonald, R. A., Cordes, M., Ellington, B., Bertelsen, E. B., and Zuiderweg, E. R. (2011) Heat shock protein 70 kDa chaperone/DnaJ cochaperone complex employs an unusual dynamic interface. *Proceedings of the National Academy of Sciences of the United States of America* **108**, 18966-18971
9. Xu, Z., Page, R. C., Gomes, M. M., Kohli, E., Nix, J. C., Herr, A. B., Patterson, C., and Misra, S. (2008) Structural basis of nucleotide exchange and client binding by the Hsp70 cochaperone Bag2. *Nat Struct Mol Biol* **15**, 1309-1317
10. Miyata, Y., Chang, L., Bainor, A., McQuade, T. J., Walczak, C. P., Zhang, Y., Larsen, M. J., Kirchhoff, P., and Gestwicki, J. E. (2010) High-throughput screen for Escherichia coli heat shock protein 70 (Hsp70/DnaK): ATPase assay in low volume by exploiting energy transfer. *J Biomol Screen* **15**, 1211-1219
11. Mally, A., and Witt, S. N. (2001) GrpE accelerates peptide binding and release from the high affinity state of DnaK. *Nature structural biology* **8**, 254-257
12. Yue, X., Zhao, Y., Liu, J., Zhang, C., Yu, H., Wang, J., Zheng, T., Liu, L., Li, J., Feng, Z., and Hu, W. (2015) BAG2 promotes tumorigenesis through enhancing mutant p53 protein levels and function. *eLife* **4**
13. Kiang, J. G., Gist, I. D., and Tsokos, G. C. (2000) Regulation of heat shock protein 72 kDa and 90 kDa in human breast cancer MDA-MB-231 cells. *Molecular and cellular biochemistry* **204**, 169-178
14. Powers, M. V., Clarke, P. A., and Workman, P. (2008) Dual targeting of HSC70 and HSP72 inhibits HSP90 function and induces tumor-specific apoptosis. *Cancer cell* **14**, 250-262
15. Whitmore, A. (2017) Targeting Human DNAJAs for Sensitization to Chemotherapeutic Agents. *The FASEB Journal* **31**, 996.995
16. Rauch, J. N., and Gestwicki, J. E. (2014) Binding of Human Nucleotide Exchange Factors to Heat Shock Protein 70 (Hsp70) Generates Functionally Distinct Complexes in Vitro. *Journal of Biological Chemistry* **289**, 1402-1414
17. Cesa, L. C., Patury, S., Komiyama, T., Ahmad, A., Zuiderweg, E. R., and Gestwicki, J. E. (2013) Inhibitors of difficult protein-protein interactions identified by high-throughput screening of multiprotein complexes. *ACS Chem Biol* **8**, 1988-1997
18. Rauch, J. N., and Gestwicki, J. E. (2014) Binding of human nucleotide exchange factors to heat shock protein 70 (Hsp70) generates functionally distinct complexes in vitro. *J Biol Chem* **289**, 1402-1414
19. Chang, L., Miyata, Y., Ung, P. M., Bertelsen, E. B., McQuade, T. J., Carlson, H. A., Zuiderweg, E. R., and Gestwicki, J. E. (2011) Chemical screens against a reconstituted multiprotein complex: myricetin blocks DnaJ regulation of DnaK through an allosteric mechanism. *Chem Biol* **18**, 210-221
20. Bonomo, J., Welsh, J. P., Manthiram, K., and Swartz, J. R. (2010) Comparing the functional properties of the Hsp70 chaperones, DnaK and BiP. *Biophysical chemistry* **149**, 58-66
21. Miyata, Y., Rauch, J. N., Jinwal, U. K., Thompson, A. D., Srinivasan, S., Dickey, C. A., and Gestwicki, J. E. (2012) Cysteine reactivity distinguishes redox sensing by

the heat-inducible and constitutive forms of heat shock protein 70. *Chem Biol* **19**, 1391-1399
22. Kang, Y., Taldone, T., Patel, H. J., Patel, P. D., Rodina, A., Gozman, A., Maharaj, R., Clement, C. C., Patel, M. R., Brodsky, J. L., Young, J. C., and Chiosis, G. (2014) Heat shock protein 70 inhibitors. 1. 2,5'-thiodipyrimidine and 5-(phenylthio)pyrimidine acrylamides as irreversible binders to an allosteric site on heat shock protein 70. *J Med Chem* **57**, 1188-1207
23. Gallardo-Godoy, A., Gever, J., Fife, K. L., Silber, B. M., Prusiner, S. B., and Renslo, A. R. (2011) 2-Aminothiazoles as therapeutic leads for prion diseases. *Journal of medicinal chemistry* **54**, 1010-1021
24. Li, X., Srinivasan, S. R., Connarn, J., Ahmad, A., Young, Z. T., Kabza, A. M., Zuiderweg, E. R., Sun, D., and Gestwicki, J. E. (2013) Analogs of the Allosteric Heat Shock Protein 70 (Hsp70) Inhibitor, MKT-077, as Anti-Cancer Agents. *ACS medicinal chemistry letters* **4**
25. Andreasson, C., Fiaux, J., Rampelt, H., Druffel-Augustin, S., and Bukau, B. (2008) Insights into the structural dynamics of the Hsp110-Hsp70 interaction reveal the mechanism for nucleotide exchange activity. *Proc Natl Acad Sci U S A* **105**, 16519-16524
26. Harrison, C. J., Hayer-Hartl, M., Di Liberto, M., Hartl, F., and Kuriyan, J. (1997) Crystal structure of the nucleotide exchange factor GrpE bound to the ATPase domain of the molecular chaperone DnaK. *Science* **276**, 431-435
27. Young, Z. T., Rauch, J. N., Assimon, V. A., Jinwal, U. K., Ahn, M., Li, X., Dunyak, B. M., Ahmad, A., Carlson, G. A., Srinivasan, S. R., Zuiderweg, E. R., Dickey, C. A., and Gestwicki, J. E. (2016) Stabilizing the Hsp70-Tau Complex Promotes Turnover in Models of Tauopathy. *Cell chemical biology* **23**, 992-1001
28. Levy, E. J., McCarty, J., Bukau, B., and Chirico, W. J. (1995) Conserved ATPase and luciferase refolding activities between bacteria and yeast Hsp70 chaperones and modulators. *FEBS Lett* **368**, 435-440
29. Li, X., Shao, H., Taylor, I. R., and Gestwicki, J. E. (2016) Targeting Allosteric Control Mechanisms in Heat Shock Protein 70 (Hsp70). *Curr Top Med Chem* **16**, 2729-2740
30. Rousaki, A., Miyata, Y., Jinwal, U. K., Dickey, C. A., Gestwicki, J. E., and Zuiderweg, E. R. (2011) Allosteric drugs: the interaction of antitumor compound MKT-077 with human Hsp70 chaperones. *J Mol Biol* **411**, 614-632
31. Gillis, E. P., Eastman, K. J., Hill, M. D., Donnelly, D. J., and Meanwell, N. A. (2015) Applications of Fluorine in Medicinal Chemistry. *Journal of medicinal chemistry* **58**, 8315-8359
32. Assimon, V. A., Gillies, A. T., Rauch, J. N., and Gestwicki, J. E. (2013) Hsp70 protein complexes as drug targets. *Curr Pharm Des* **19**, 404-417
33. Erlanson, D. A., Braisted, A. C., Raphael, D. R., Randal, M., Stroud, R. M., Gordon, E. M., and Wells, J. A. (2000) Site-directed ligand discovery. *Proceedings of the National Academy of Sciences of the United States of America* **97**, 9367-9372
34. Li, X., Colvin, T., Rauch, J. N., Acosta-Alvear, D., Kampmann, M., Dunyak, B., Hann, B., Aftab, B. T., Murnane, M., Cho, M., Walter, P., Weissman, J. S., Sherman, M. Y., and Gestwicki, J. E. (2015) Validation of the Hsp70-Bag3 protein-

protein interaction as a potential therapeutic target in cancer. *Mol Cancer Ther* **14**, 642-648
35. Chang, L., Thompson, A. D., Ung, P., Carlson, H. A., and Gestwicki, J. E. (2010) Mutagenesis reveals the complex relationships between ATPase rate and the chaperone activities of Escherichia coli heat shock protein 70 (Hsp70/DnaK). *The Journal of biological chemistry* **285**, 21282-21291
36. Chang, L., Bertelsen, E. B., Wisen, S., Larsen, E. M., Zuiderweg, E. R., and Gestwicki, J. E. (2008) High-throughput screen for small molecules that modulate the ATPase activity of the molecular chaperone DnaK. *Analytical biochemistry* **372**, 167-176
37. Wisen, S., and Gestwicki, J. E. (2008) Identification of small molecules that modify the protein folding activity of heat shock protein 70. *Anal Biochem* **374**, 371-377
38. Delaglio, F., Grzesiek, S., Vuister, G. W., Zhu, G., Pfeifer, J., and Bax, A. (1995) NMRPipe: a multidimensional spectral processing system based on UNIX pipes. *J Biomol NMR* **6**, 277-293
39. Goddard, T. D., and Kneller, D. G. (2000) SPARKY 3. *University of California, San Francisco*
40. Bertelsen, E. B., Chang, L., Gestwicki, J. E., and Zuiderweg, E. R. (2009) Solution conformation of wild-type E. coli Hsp70 (DnaK) chaperone complexed with ADP and substrate. *Proc Natl Acad Sci U S A* **106**, 8471-8476

FIGURES

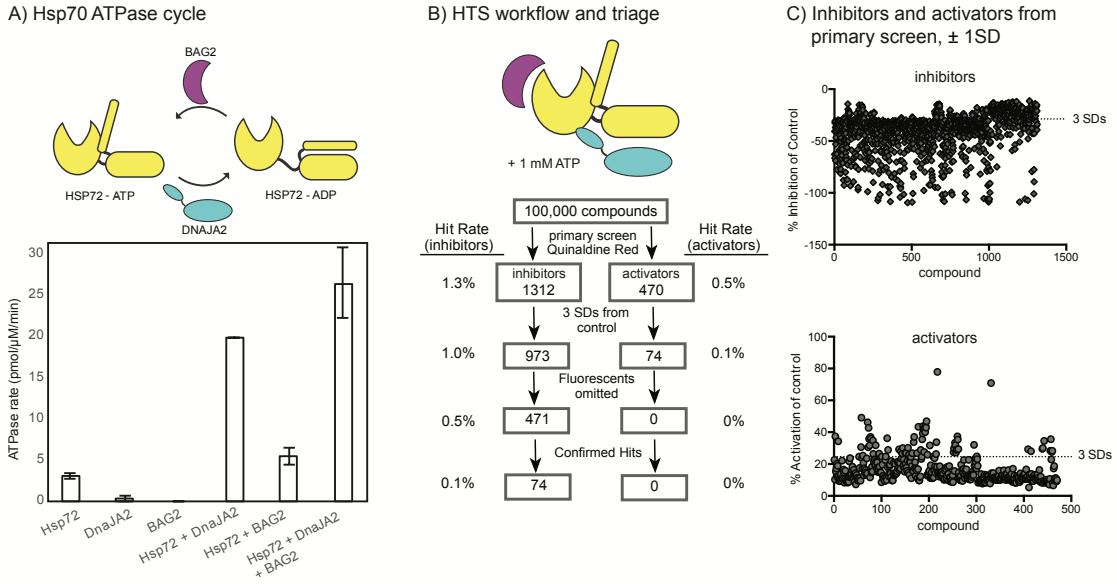

Figure 2.1: High throughput ATPase screen identifies inhibitors and activators of the Hsp72/DnaJA2/BAG2 system. A) Schematic of the Hsp72 ATPase cycle, highlighting the role of the DnaJA2 and BAG2 co-chaperones. Hsp72 (0.5 μM) has a slow hydrolysis rate in the absence of DnaJA2 (0.1 μM) or BAG2 (0.25 μM). Results are the average of triplicates and the error bars represent standard error of the mean (SEM). B) Overview of the HTS campaign. A total of 100,000 molecules were screened against the Hsp72/DnaJA2/BAG2 combination. Approximately 1.8 % of the molecules had inhibitor or activator activity at ± 1 SD and 1.1% were inhibitors or activators at ± 3 SD. After triage for fluorescent artifacts and dose response curves (EC_{50} < 50 μM), 74 molecules were predicted to be inhibitors. See the text and Methods sections for details. C) Overview of the compounds with activity at ± 1 SD and ± 3 SD from the controls, highlighting the distribution of the top active molecules.

A) Re-purchased active compounds repeat in dose response

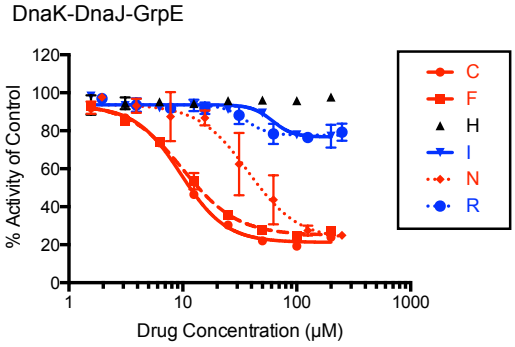

Hsp72-DnaJA2-BAG2

Compound	EC50 (μM)	$Max_{inhibition}$
C	26.2	60
F	28.2	52
H	15.5	18
I	10.9	16
N	NA	NA
R	NA	NA

B) Compound F inhibits J protein stimulated ATP hydrolysis

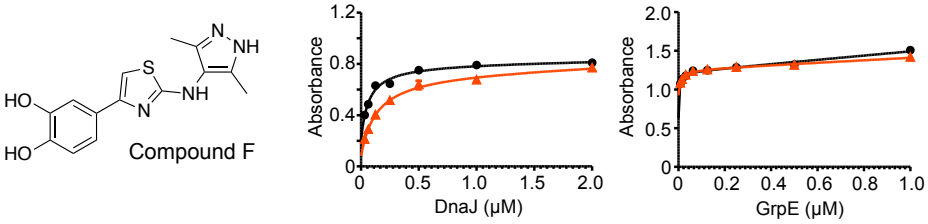

C) Compound R inhibits NEF stimulated ATP hydrolysis

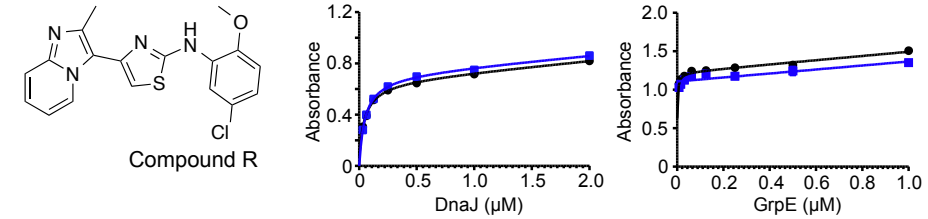

D) Compound F inhibition of DnaK-DnaJ E) Compound R inhibition of DnaK-GrpE

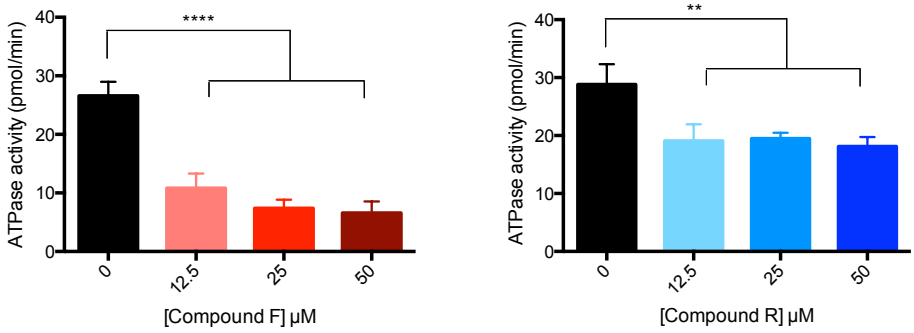

Figure 2.2: Confirmation of active molecules reveals that they are either inhibitors of J protein or NEF co-chaperones. A) The top 18 active molecules were re-purchased and subject to DRCs in the prokaryotic and human Hsp70 systems. Compounds not shown were inactive or not sufficiently soluble for testing. B) Compound F inhibits DnaJ-mediated stimulation, but has little effect on GrpE-mediated stimulation in ATPase assay. Absorbance is measured at 620 nm C) Compound R has no activity against DnaK-DnaJ, but modestly inhibits DnaK-GrpE. Results in B and C are the average of at least three experiments performed in triplicate each and the error bars represent SEM. D) Compound F inhibits a combination of DnaK and DnaJ dose-dependently at low micromolar concentrations (****, $P < 0.0001$). E) Compound R showed significant inhibition of a combination of DnaK, DnaJ, and GrpE at low micromolar concentrations (**, $P = 0.005$). Results are the average of triplicate values and error bars represent SEM.

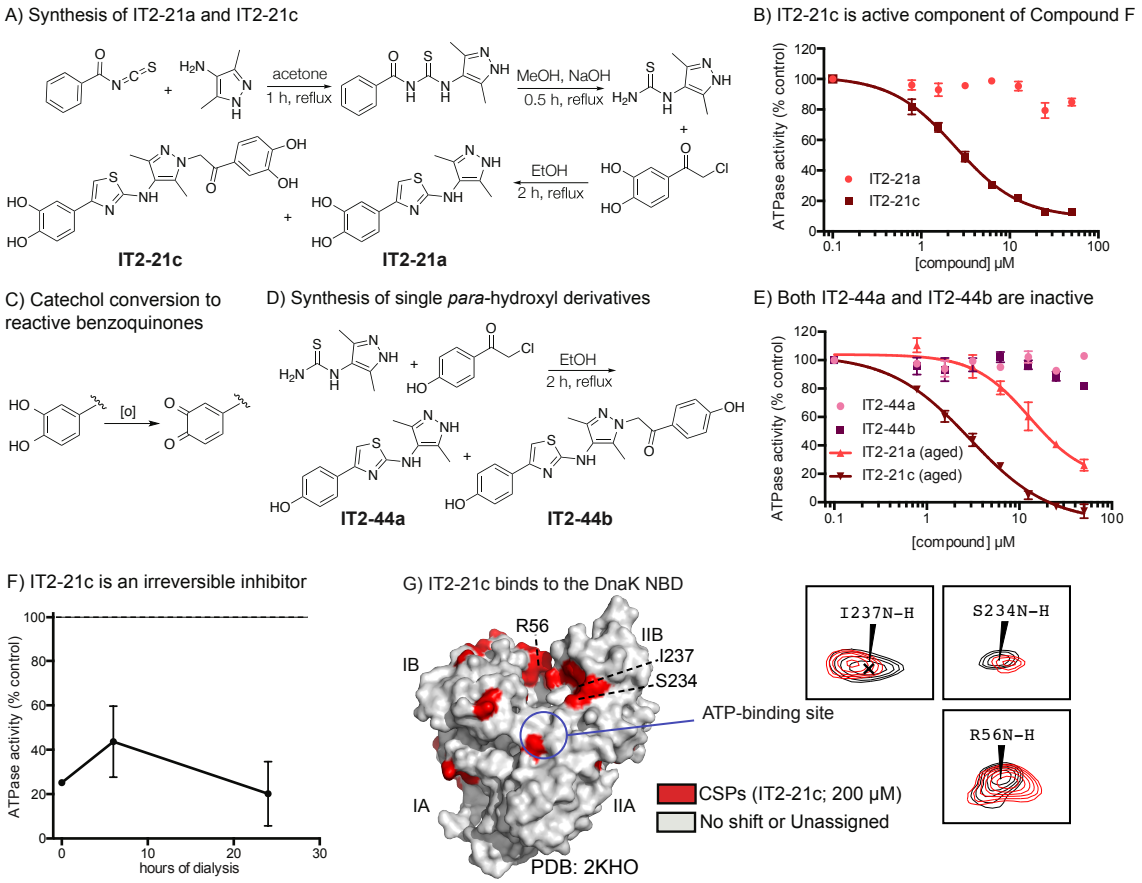

Figure 2.3: A side product of Compound F synthesis is an irreversible inhibitor of Hsp70 systems. A) Synthesis of IT2-21a and IT2-21c by Hantzsch thiazole condensation. Compounds IT2-21c and IT2-21a were separated by HPLC. B) IT2-21c, not IT2-21a, is an inhibitor of DnaK/DnaJ/GrpE ATPase activity. Results are the average of triplicates and error bars represent SEM. C) Known oxidation of catechol rings to yield reactive benzoquinones. D) Synthesis of IT2-44a and IT2-44b. Compounds were separated by HPLC. E) Neither of the *para*-phenolic analogs were active in the ATPase assay using DnaK/DnaJ/GrpE. Results are the average of triplicates and error bars represent SEM. "Aging" DMSO stocks of IT2-21a and IT2-21c by overnight incubation at room temperature improved their activity, consistent with an oxidative mechanism. F) IT2-21c (100 μM) was incubated with DnaK (2.5 μM), then subjected to dialysis. Samples were removed from dialysis after 6 and 24 hours and the ATPase assay performed with added DnaJ. Even 24 hours of dialysis was not able to reverse compound activity. G) A potential binding site of IT2-21c was revealed by HSQC experiments with ^{15}N labeled DnaK NBD. Chemical shift perturbations (CSPs; > 0.01 ppm in ^{1}H and/or > 0.1 ppm in ^{15}N) in the presence of IT2-21c were localized to the IB and IIB subdomains (red). See the methods section for details. Peaks shifting for select residues are highlighted with NBD + 2% DMSO in grey and NBD + 200 μM IT2-21c in red.

A) Synthetic route for Compound R derivatives

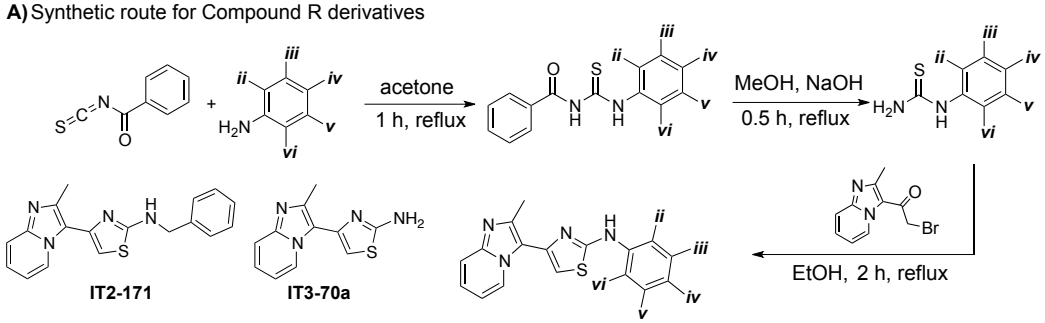

B) Inhibition of ATPase activity and cell viability by Compound R derivatives

Compound						ATPase EC_{50} (μM)	MDA-MB-231 EC_{50} (μM)	MEF EC_{50} (μM)	Selectivity Index (SI)
	ii	*iii*	*iv*	*v*	*vi*				
R	OMe	H	H	Cl	H	9.5 ± 4.9	5.8 ± 1.0	5.3 ± 1.1	0.9
IT2-144	F	H	H	F	H	6.9 ± 3.9	2.7 ± 1.0	>50	>50
IT2-149	F	H	H	Me	H	>25†	NA	NA	NA
IT2-151	F	H	H	Br	H	4.7 ± 7.3	2.9 ± 0.8	9.3 ± 4.0	3.2
IT2-179	Br	H	H	Br	H	3.6 ± 1.5	3.1 ± 1.3	>50	>50
IT2-158	F	F	H	H	H	>25†	NA	NA	NA
IT2-159	F	H	F	H	H	>50	8.5 ± 1.8	5.4 ± 0.7	0.8
IT2-160	F	H	H	H	F	>25†	NA	NA	NA
IT2-171						>25†	NA	NA	NA
IT3-70a						>50	>50	>50	-

† Tested with DnaK/DnaJ/GrpE
NA Not tested

Figure 2.4: Synthesis and activity of Compound R derivatives. A) Synthesis of Compound R analogs. Structures of IT2-171 and IT3-70a are shown here. B) Activity of analogs in ATPase assays (Hsp72, DnaJA2, and BAG2 at 0.5 μM, 0.1 μM, and 0.25 μM, respectively). Results are the average of three independent experiments, each performed in triplicate ± SD. In addition, compounds were tested for membrane permeability using cell growth assays in MDA-MB-231 breast cancer cells and normal mouse embryonic fibroblasts (MEFs). EC_{50}s in cell experiments are the result of two independent experiments, each in triplicate ± SD. The selectivity index is the EC_{50} in MDA-MB-231 cells divided by the EC_{50} in MEF cells.

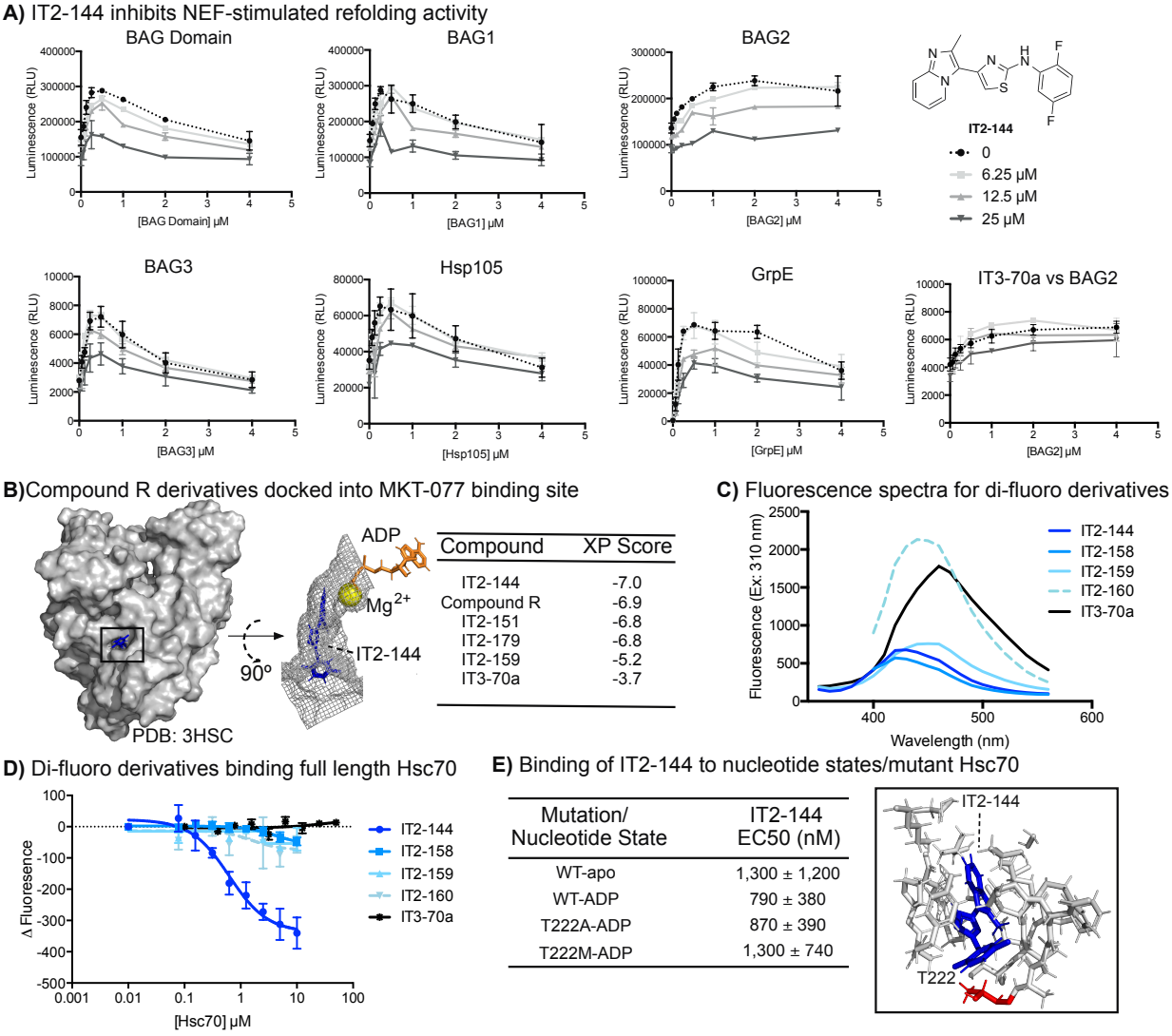

Figure 2.5: IT2-144 inhibits NEF mediated activity and potentially binds in the MKT-077 binding pocket A) IT2-144 inhibits a wide range of Hsp70-NEF combinations in luciferase refolding assays. Hsp72 (1 µM) was used with all of the NEFs except for GrpE, which used DnaK (1 µM). Likewise, DnaJA2 (0.5 µM) was used for all of the NEFs except for GrpE, which used DnaJ (0.5 µM). Denatured luciferase (0.1 µM) and potassium phosphate (10 mM) were also added. Results are the average of triplicate values and the error bars represent SEM. B) IT2-144 docked to the MKT-077 binding site of Hsc70 (3HSC). Top-view of the binding pocket (residues within 5 angstroms of IT2-144) highlights IT2-144 as well as ADP and magnesium in the adjacent nucleotide binding cassette. C) Scanning fluorescence spectra for all di-fluoro derivatives and the negative compound IT3-70a, with excitation wavelength set at 310 nm. D) Change in fluorescence intensity with increasing Hsc70 concentration. Compounds were held at 50 µM and fluorescence emission was read at optimal wavelengths, determined in spectral scans (see part C). E) Full length Hsc70 was incubated with or without ADP and then tested for ability to bind IT2-144 (ex: 310 nm, em: 430 nm). EC_{50} was determined from two independent experiments in triplicate. Full length Hsc70 with mutations at position T222 were also tested for ability to bind IT2-144. T222 is highlighted in structure of IT2-144 docked to Hsc70.

SUPPLEMENTAL FIGURES

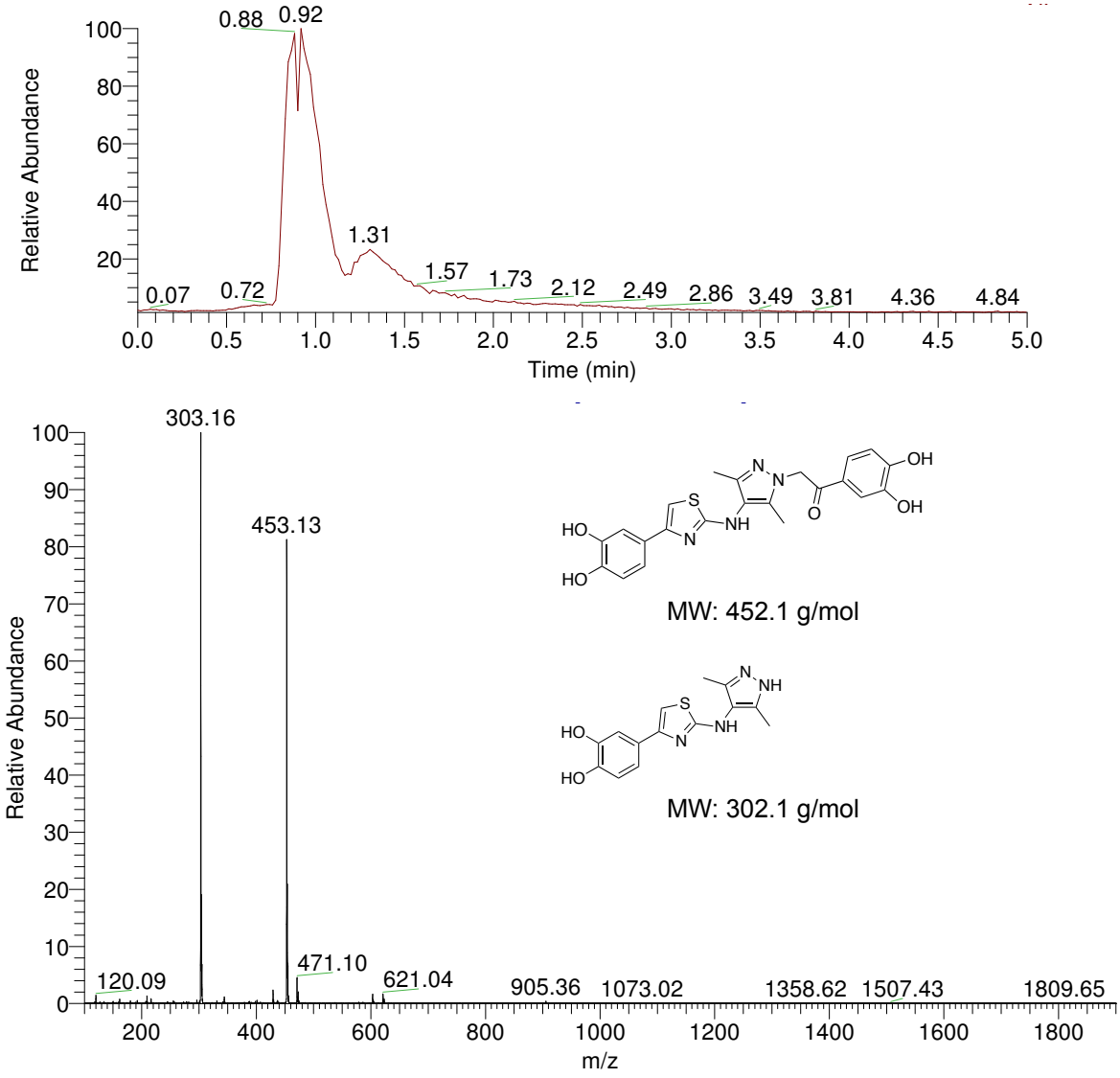

Figure 2.S1: LCMS of Compound F purchased stock molecule

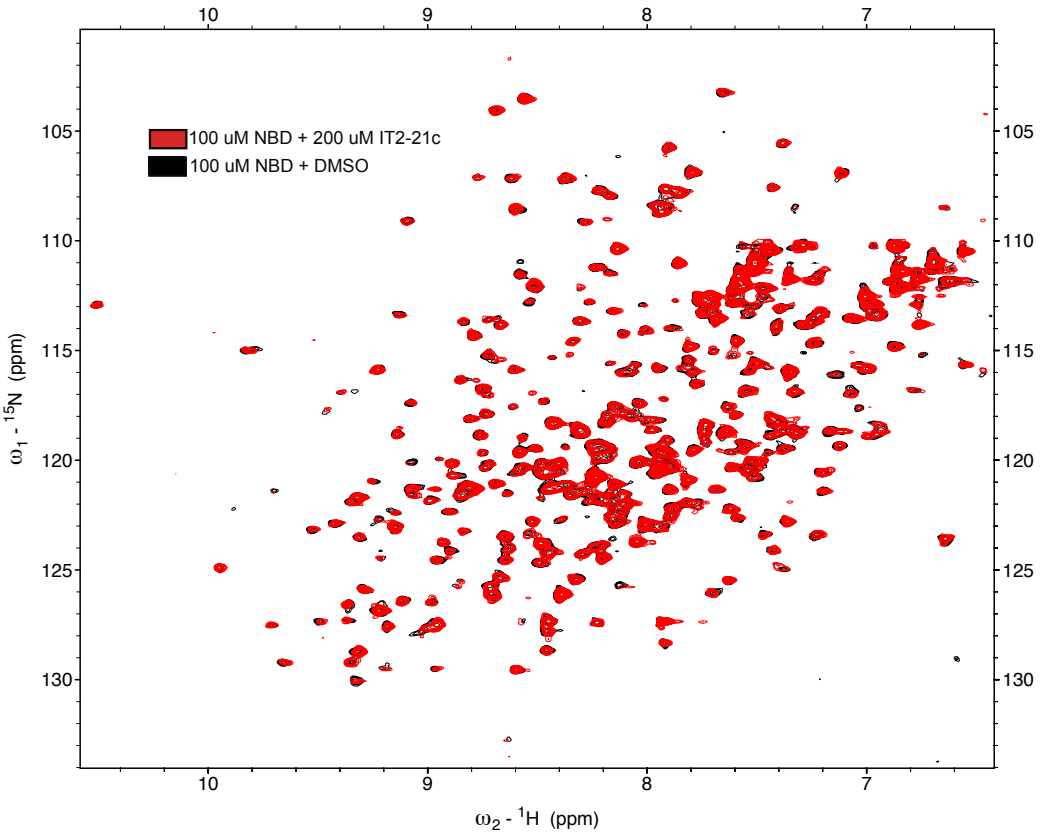

Figure 2.S2: Overlay of DnaK NBD HSQC spectra, in the presence and absence of IT2-21c.

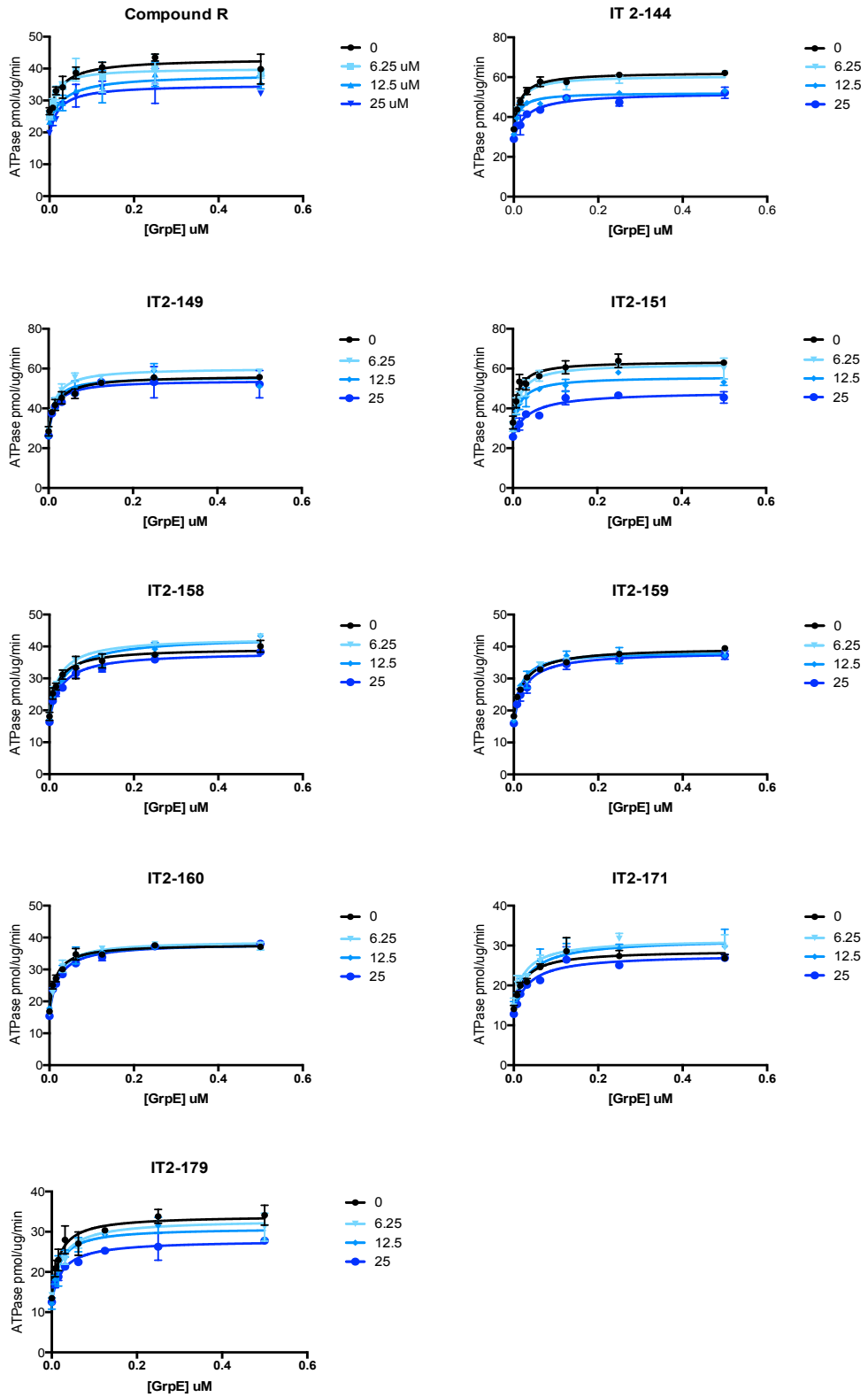

Figure 2.S3: Compound R derivatives against GrpE-stimulated DnaK ATP turnover. DnaK is held at1 μM and DnaJ at 0.125 μM. Any molecules that exhibited an inhibitory effect against DnaK-DnaJ-GrpE were further tested in dose-reponse against the Hsp72-DnaJA2-BAG2 complex.

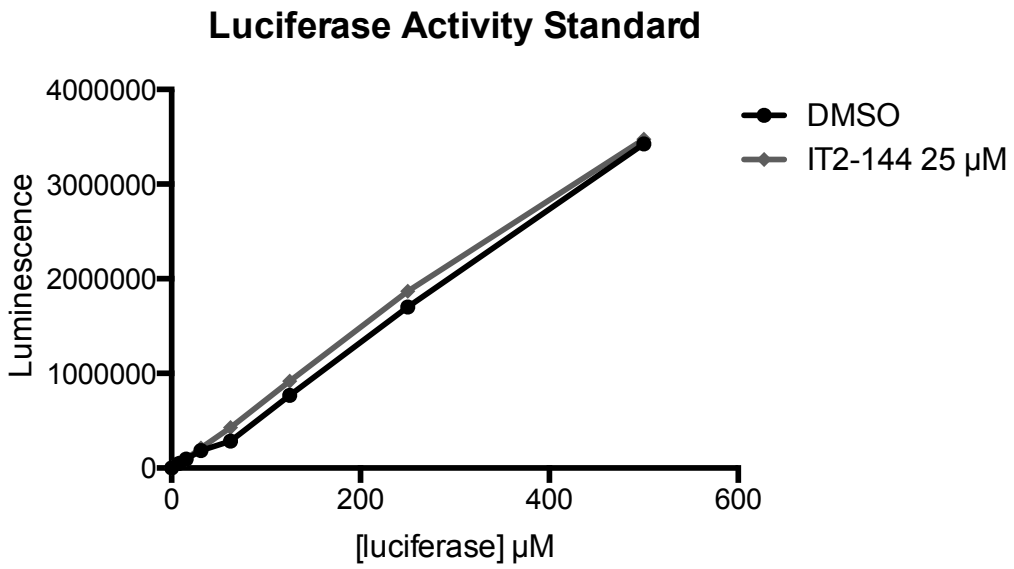

Figure 2.S4: IT2-144 does not inhibit activity of recombinant luciferase at 25 μM.

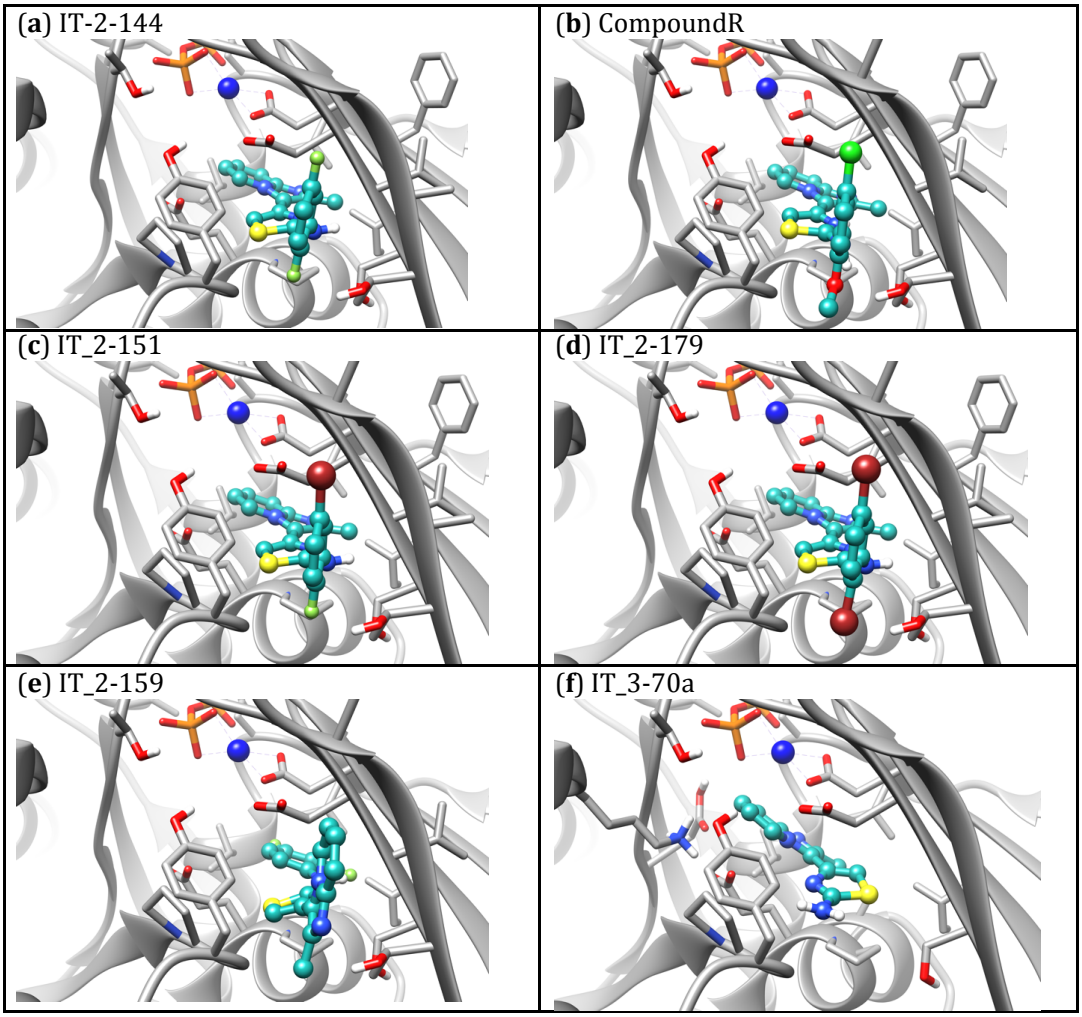

Figure 2.S5: Docking pose of allosteric inhibitors. Carbon atoms of protein and inhibitors are shown in gray and cyan colors respectively. Oxygen, nitrogen, hydrogen and phosphorus are shown in red, blue, white and orange colors respectively. Mg2+ ion is shown in blue color.

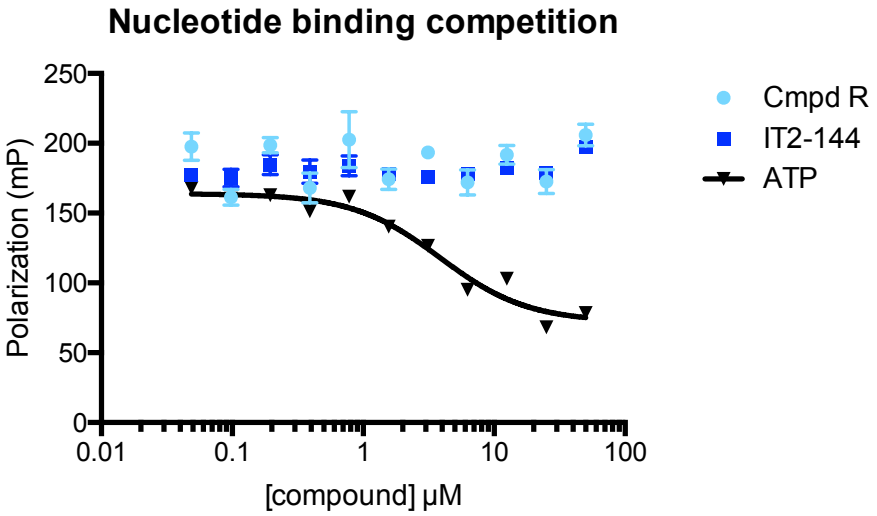

Figure 2.S6: Neither Compound R nor IT2-144 competes with ATP for binding DnaK

Chapter 3: Discovering Weak Links in the Proteostasis Network of Castration Resistant Prostate Cancer (CRPC)

INTRODUCTION

The androgen receptor (AR) is a highly disordered protein that acts as a hormone-activated transcription factor to drive the aberrant propagation of prostate cancer (PCa) cells. Accordingly, for the past ~30 years, prostate cancer therapeutics have largely been focused on inhibiting AR signaling (1). This is achieved both by targeting the synthesis of androgens, as well as through direct antagonism of AR. While these therapies, collectively referred to as androgen deprivation therapy (ADT), have proven successful in treating early stage disease and prolonging lifespan of prostate cancer patients, it is becoming increasingly clear that patients who receive the treatment invariably progress to castration resistant prostate cancer (CRPC). This stage of disease is incurable and responsible for the death of approximately 40,000 men each year, in the US alone (2). Because of this, there has been a recent push to understand the underlying mechanisms of progression to CRPC, in order to design new therapies (3).

With the progression to CRPC, prostate cancer cells become resistant to ADT. At the molecular level, this resistance is associated with amplification or mutation of the AR gene, alternative splicing of AR mRNA to give rise to truncated proteins, and non-canonical activation of AR target genes by the glucocorticoid receptor (GR) (4). Each of these mechanisms provides relative resistance by either increasing the concentration of AR or using alternative methods for driving AR-responsive gene transcription. This theme is exemplified by the AR truncations that emerge in CRPC. It has been observed that the majority of AR splice variants largely remove the canonical ligand-binding domain, making the receptor immune to antagonists that bind in this site, while sparing the DNA-binding domain (DBD) (5). One splice variant, denoted ARv7, has been identified to form an active

protein that can translocate into the nucleus and activate transcription independently of androgen. ARv7 has been associated with particularly poor prognosis in a subset of CRPC patients, who show no response to continued ADT (6). It is, therefore, reasoned that androgen deprivation therapies, such as enzalutamide and abiraterone, are not suitable for patients who have developed CRPC, especially those with ARv7 positive disease.

AR is a member of the steroid hormone receptor (SHR) class of transcription factors. A hallmark of the SHRs is that they are obligate clients of the molecular chaperones, such as heat shock protein 70 (Hsp70) and heat shock protein 90 (Hsp90) (7,8). Pioneering work in reconstituted systems has shown that SHRs are dependent on chaperones for both folding and function (9,10). Briefly, work on both GR and AR has shown that the unfolded protein is first bound by Hsp70 and Hsp40 to form the “early complex” (11), followed by recruitment of Hsp90 through the co-chaperone HOP to form the “mature complex”. Hsp90 and its co-chaperones stabilize the ligand-binding cleft, making it competent for ligand binding. Recent structures of the GR-Hsp90-HOP complex show how this system prevents aggregation of the LBD, by keeping it in an open configuration (12). Moreover, yeast studies and biochemical work with rabbit reticulocyte lysates have further refined the key chaperones involved in this process, the order in which they bind, and how they also control nuclear translocation and SHR turnover (10,13).

However, many important questions still remain. Modern functional genomics, including optimized shRNA screens, have allowed, for the first time, large scale screening of entire protein networks (14). There are more than 180 chaperones expressed in

humans and only a subset of these have ever been explored for potential effects on SHR homeostasis or function. In addition, it isn't clear whether the canonical chaperones that are required for folding full length AR would also be required for folding AR truncations, such as ARv7. This question is especially important because the molecular chaperone network may represent opportunities for therapeutic intervention in order to inhibit the proper folding and function of AR and its variants (7,15).

Here, we designed a focused shRNA library targeting 139 chaperone and co-chaperone encoding genes. We used this library, in combination with inhibitors of Hsp70 and Hsp90, to perform functional genomics and synthetic lethality screens in prostate cancer cell lines with defined AR status. This effort confirmed a central, and cooperative, role for Hsp70 and Hsp90 in PCa cell survival and supported recent evidence that Hsp70, but not Hsp90, plays a key role in ARv7 processing (16). Furthermore, the screens also revealed unexpected vulnerabilities in CRPC cells, including an increased reliance on Hsp60. Knockdown of this chaperone suppressed growth in the CRPC cell line, 22Rv1, but was not required in the prostate cancer cell lines, PC-3 and LNCaP. These results suggest that Hsp60 is a required chaperone for CRPC and a putative, new drug target for this disease. This study provides a path to justify new high throughput screening (HTS) modalities, patterned after those described in Chapter 2, to target the protein-protein interactions of Hsp60.

RESULTS

Design of an shRNA collection targeting the chaperone network

As models of prostate cancer in its various AR states, we selected three cell lines: PC-3 (17), an AR-negative cell line derived from a bone metastasis, LNCaP (18), an AR-

positive, androgen-responsive cell line derived from a lymph node metastasis, and 22Rv1 (19), an AR/AR splice variant-positive cell line that developed resistance to ADT in a mouse xenograft model (**Figure 3.1a**) (20). These cell lines were chosen to model the spectrum of androgen signaling dependence that is observed in prostate cancer, with a special focus on full length AR (AR-FL) and ARv7. Moreover, PC-3 cells are the least aggressive form of prostate cancer represented on this panel, while the 22Rv1 cells represent a state that is associated with the worst prognosis (6). 22Rv1 cells express the AR splice variant, ARv7, and are therefore unresponsive to ADT.

To explore the chaperone dependence of these cell lines, we assembled a focused library of shRNAs targeting 139 chaperone-encoding genes. This relatively small library size gave us room to design-in high coverage by having 25 shRNA sequences targeting each gene transcript. In addition to these targeting shRNA sequences, the library contains 500 non-gene targeting sequences to serve as negative controls. Although CRISPR-Cas9 methods are powerful tools for functional genomics, this shRNA collection does not require creation of a stable Cas9-expressing cell, so it has the versatility to be rapidly applied to multiple cell types.

The collection includes each isoform of the major Hsp70, Hsp90, and small heat shock protein (sHsp) families (**Figure 3.1c**). In addition, it was of particular interest to include a near complete collection of shRNAs targeting the known co-chaperones of these systems. For example, this called for a large collection of genes from the Hsp40 (J-domain protein) family. This class of co-chaperones to the Hsp70 system is extensive, and while many members are predicted to have redundant functions, it is also believed that the Hsp40 proteins confer substrate specificity to the Hsp70 chaperone system (21).

The Hsp40 class of co-chaperones, therefore, was the most well-represented class in our shRNA library, which included 42 targeted genes of this class. We also considered the abundance of literature that supports the role of peptidyl-prolyl isomerases (PPIases) and tetratricopeptide repeat (TPR) domain co-chaperones in the folding and regulation of AR. Several key members of these classes were included in the library. Notable members of these classes are HOP (STIP1), the key connector of the Hsp70 and Hsp90 systems, CHIP (STUB1), an important E3 ubiquitin ligase associated with Hsp70 and Hsp90, and SGTA1, FKBP51, and FKBP52 which have all been heavily implicated in AR function (22-24).

The remainder of genes included in this library were chosen from previous publications describing the various branches of the chaperone network (25), as well as from our own knowledge of the network and its druggable interactions (26). While the library size only covered a modest number of genes and was not comprehensive of the entire chaperone network as it exists in cells, we aimed to include all of the key connectors between the main chaperone "hubs". With this, our goal was to be able to establish not only reliance on individual genes, but any reliance on the interplay between the proteins that make up this network. In other words, we aimed to identify synthetic lethal interactions between molecular chaperones, or "weak links".

Inhibitors of Hsp70 and Hsp90 cause differential destabilization of AR-FL and ARv7

In order to reveal synthetic lethal interactions in PCa cells, we turned to established inhibitors of the major chaperones, Hsp70 and Hsp90 (**Figure 3.2**). The Hsp70 inhibitor, JG231, is a newer generation molecule inspired by the MKT-077 scaffold (see Chapter 1). While this molecule is predicted to have an increased ER (endoplasmic reticulum)

signature over other molecules from this same series (unpublished data), it has shown little specificity for particular isoforms of Hsp70. Full dose-response curves were generated for this molecule in order to establish IC_{50} values in each of our PCa cell lines prior to screening (**Table 3.2**). In comparison, AUY922 is a third-generation Hsp90 inhibitor inspired by the natural product, radicicol, that has been evaluated in clinical trials as a potential therapeutic for a range of cancer types, including multi-drug resistant lung cancer and metastatic breast cancer (27). This molecule is a competitive inhibitor targeting the ATP binding pocket of Hsp90 and binds the protein with a K_d of ~1.7 nM (28). An important feature to note about this molecule is that it potently kills PCa cells at low nanomolar concentrations, however it only kills cells after exposure for at least 48 hours. We found, empirically, that we could treat each of our PCa cell lines with 100 nM AUY922 for just 24 hours and achieve approximately 50% reduction in cell growth. This was the treatment regime we followed for all cell lines in our synthetic lethality screens with AUY922.

It is known that Hsp70 and Hsp90 inhibitors reduce the stability of AR and ARv7 in PCa cells (16,29). Prior to screening, we decided to assess the effect of JG231 and AUY922 on AR stability in the cell lines intended for our shRNA screens by Western blot. Strikingly, we noticed that Hsp70 and Hsp90 inhibition had profound, and differential effects on protein levels (**Figure 3.2**). AR has a notably short half-life in cells (30,31) and therefore we treated 22Rv1 and LNCaP cells with the chaperone inhibitors for just 6 hours, and immediately collected lysate. We saw that while AUY922 potently reduced levels of full-length AR in both cell types, it was virtually unable to reduce levels of ARv7 in 22Rv1 cells. On the other hand, JG231 was significantly less potent against full length

AR, yet extremely effective in reducing ARv7. This observation is consistent with three ideas: 1) that the activity of these two chaperones is required for the stability of AR in cells, 2) that Hsp90 interacts primarily with the ligand binding domain of AR, whereas Hsp70 interacts at multiple sites throughout the N-terminal domain and DNA-binding domain, and 3) that Hsp90 acts to finish the folding process, whereas Hsp70 chaperones the early stages of folding for these proteins. This third idea seemed consistent with the observation that Hsp90 inhibition was a more potent strategy in lowering levels of full length AR, since loss of Hsp90 activity may be a "deciding" factor in sending unfoldable AR to the proteasomal degradation pathway.

Another notable observation from these drug treatment assays was that treatment with AUY922 caused a robust increase in levels of Hsp70 (using a non-specific antibody that recognizes both Hsc70 and the stress-inducible Hsp72). This observation is consistent with extensive previous work characterizing inhibitors of Hsp90 (32). It is well-known, particularly from clinical characterization of this inhibitor class, that small molecule inhibition of Hsp90 causes an acute, HSF1-regulated, stress response in cells, which can be measured by changes in protein level of Hsp72. This observation has served as a clinical biomarker in patient serum samples for the activity of Hsp90 inhibitors (33). We observed that, in 22Rv1 and LNCaP cells, this response is reversible upon removing AUY922 from the media and continued cell culture (not shown).

Chemical-genetic interactions identified in prostate cancer cell lines

Taking our small molecule chaperone modulators and shRNA library, we set out to determine chemical-genetic interactions within the chaperone network for our panel of PCa cell lines. We did this by periodically dosing cells carrying the shRNA library with

each of our chaperone inhibitors (JG231 and AUY922) at approximately the IC_{50} throughout the growth period (**Figure 3.1b**).

The results of all three screens (untreated, JG231-, and AUY922-treated) across our cell line panel are shown in **Figures 3.3**-**3.5**. In PC-3 cells, relatively few chaperone-encoding genes showed growth phenotypes in the presence and absence of drug (**Figure 3.3**). This suggests that these cells show remarkably low reliance on the chaperone network for survival. LNCaP and 22Rv1 cells, on the other hand, show several significant growth phenotypes with knockdown across the network. It is worth noting that many of the hit genes that appeared in LNCaP cells showed similar phenotype scores across all three screens (**Figure 3.4**). This was not the case for many significant hits identified in the 22Rv1 cells, as several genes showed significant growth phenotypes in one screen compared to the others (**Figure 3.5**). For example, it was notable that a few genes in the Hsp90 system (HSP90AB1, PTGES3, and STIP1) showed synthetic lethality with Hsp70 inhibition. In the reverse experiment, a few of the prominent Hsp40 class members (DNAJA1, DNAJA2, DNAJC2) showed synthetic lethality with Hsp90 inhibition. We hypothesize that this relationship points to a cooperativity between the Hsp70/40 and Hsp90 systems that is particularly important for the survival of this ARv7 positive cell line. Recent work from the Neckers lab has suggested that Hsp70 and Hsp40 inhibition in combination presents a promising therapeutic strategy for the treatment of CRPC (16). We suggest that Hsp70 and Hsp90 inhibition should additionally be explored as a viable combination therapy for this disease.

In addition to identifying synthetic lethality in this network, we were also interested in patterns that emerged across multiple cell lines in response to a particular drug. We

hypothesize that identifying these more general patterns could point to the underlying biology, and/or direct targets of these inhibitors in cells. Treatment with AUY922 produced a very distinct pattern of synergistic, as well as resistant knockdown phenotypes in both of our AR positive cell lines (**Figure 3.6a**). Specifically, it was observed in both LNCaP and 22Rv1 cells treated with AUY922 that knockdown of Hsp90β (HSP90AB1), p23 (PTGES3), and HOP (STIP1) showed negative growth phenotypes, whereas knockdown of Hsp90α (HSP90AA1) and CHIP (STUB1) showed positive growth phenotypes.

We set out to validate select hits using individual shRNAs in 22Rv1 cells, continuously cultured with AUY922 (**Figure 3.6b**). Knockdown of p23 and HOP were confirmatory of a synergistic growth defect in combination with AUY922 treatment. Notably, HOP knockdown was only weakly sensitizing, whereas p23 knockdown was more strongly sensitizing in the presence of AUY922. While knockdown of CHIP was unable to confirm a resistance phenotype, compared to the nontargeting control shRNA (1165), it is clear that this shRNA sequence conferred only partial knockdown by Western blot. Further optimization, and possibly use of alternative shRNA sequences, will be necessary to confirm the CHIP knockdown, as well as other resistance phenotypes. Despite this, we believe it is significant that these positive growth phenotypes were only observed in the AR positive cell lines. In particular, it is striking that knockdown of CHIP, in the screening format, was protective to Hsp90 inhibition (as well as Hsp70 inhibition, as observed in LNCaP) since it is hypothesized to be a key facilitator of chaperone-guided ubiquitination and degradation of AR (34).

Selective vulnerabilities in prostate cancer cell lines

In addition to identifying synthetic lethal relationships amongst the chaperone network, we were interested in identifying which members of this group of proteins were essential for cell survival, in the absence of any drug. By screening this library across our prostate cancer cell panel, as well as in various additional cancer cell lines, we identified that TCP1 and other components of the TRiC chaperonin complex (the CCT genes) were broadly essential. The AAA+ ATPase, VCP, was also a common hit across diverse cell types, as was the mitochondrial Hsp70 isoform, mortalin (HSPA9). Beyond this list of genes, there were few additional chaperones or co-chaperones with broadly essential phenotypes, with the notable exception of Hsp10 (HSPE1). While these broadly essential genes served as good positive controls, the primary goal of these screens was to identify chaperones that were selectively essential in CRPC, compared to non-ADT resistant cells. We were, indeed, able to identify genes for which knockdown caused negative growth phenotypes in 22Rv1 cells, but not the other representative cell lines. The most unexpected finding from these screens was the reliance of the 22Rv1 cells on Hsp60 (HSPD1).

Hsp60 is a mitochondrial chaperonin that forms a tetradecameric barrel structure, with a heptameric ring of Hsp10 (HSPE1) serving as its “lid” (35). Interestingly, while Hsp60 only appeared as a hit in 22Rv1 cells, Hsp10 was broadly essential across all of our representative prostate cancer lines, as well as cell lines derived from non-cancerous breast tissue (data not shown). One possible explanation for this could be that Hsp10 plays a role in mediating the assembly of Hsp60 (36), though this theory has not been thoroughly investigated. It is possible that Hsp10 plays an alternative, essential role in cells that is independent of Hsp60.

Hsp60 is a selective vulnerability in 22Rv1 cells

In response to observing Hsp60's unique essentiality in 22Rv1 cells, we next focused efforts on validating this result with individual knockdown models. Two collections of cell lines were created carrying individual shRNAs targeting Hsp60 and Hsp10, as well as a nontargeting control sequence (denoted 1165). In 22Rv1, these shRNA sequences were introduced in an inducible system, where both the production of the shRNA and a TurboRFP reporter, were under control of a Tet-on promoter, so that knockdown in these cells could be controlled via the addition of doxycycline (dox). These cells were grown for a period of ~20 days, in the presence of 1 μg/mL dox, and the percent RFP positive population was monitored by flow cytometry over this period. In this system, we observed that knockdown of Hsp60 had a detrimental effect on growth, however this phenotype was not observed until ~2 weeks of exposure to dox (**Figure 3.7**). Hsp10 knockdown also showed a negative growth phenotype, on a faster time scale. It was additionally determined from this time course experiment that decreases in Hsp60 and Hsp10 protein could not be observed until 96 hours of treatment with dox, therefore all subsequent experiments with inducible knockdown were carried out after at least 96 hours of dox exposure.

Individual knockdowns were also tested in PC-3 cells in a similar fashion, with the exception that they were introduced in a non-inducible system. Therefore, no treatment with doxycycline was necessary to induce knockdown of Hsp60 and Hsp10 in these cells. Over the course of ~16 days of continued monitoring by flow cytometry, the knockdown of Hsp60 had no effect on the growth of PC-3 cells (**Figure 3.8**). On the other hand, one sequence targeting Hsp10 (Hsp10_1) was particularly lethal in these cells, preventing the

collection of some data points due to profoundly slow cell growth. While the other Hsp10-targeting shRNA (Hsp10_2) was not lethal in these cells, this was, in fact, consistent with the phenotypes observed for these two sequences in the library screen. It is interesting, however, that both sequences are effective in slowing the growth of 22Rv1 cells.

Quantifying the knockdown for these particular shRNA sequences revealed that the Hsp60-targeting sequences could consistently achieve approximately 50% knockdown in both cell lines (maximally, in the case of the inducible knockdown in 22Rv1 cells). The inducible Hsp60 knockdown system (with sequence Hsp60_2) was further used in combination with some small molecule modulators in order to observe the effects on AR and ARv7 homeostasis in 22Rv1 cells (**Figure 3.9**). Interestingly, knockdown of Hsp60 seemed to have no effect, synergistic or resistant, on AR homeostasis in combination with an Hsp70 inhibitor, JG231. In combination with an Hsp90 inhibitor (AUY922) however, Hsp60 knockdown seemed to increase the levels of ARv7. A similar effect was also quantified for the combination of Hsp60 knockdown with proteasome inhibition (bortezomib) and AR agonism (R1881). In the case of R1881 treatment, it is notable that drug treatment also appeared to reduce the detectable levels of actin, indicating that even low nanomolar concentrations of the compound, at short time intervals, drastically affected the overall health of 22Rv1 cells.

DISCUSSION

The chaperone network is a complex and highly interconnected system, the function of which is driven by many transient protein-protein interactions and coordinated hand-offs of client proteins. In order to study such a system, and attempt to understand the folding pathway of a given client protein, the application of diverse toolsets is crucial.

Functional genomic techniques provide the breadth to be able to study large numbers of genes, requiring little or no prior knowledge of their function in a cell. Small molecule modulators provide an alternative power of being able to selectively, and acutely, disrupt (or promote) activities of their targets. Combining the breadth of a functional genomic platform with the controlled use of small molecule modulators allows for the identification of both key interactions within a cell and any cell line-selective vulnerabilities. It is for these reasons that we developed a focused functional genomic platform, specifically intended for studying the chaperone network, in order to add to our arsenal of tools to probe chaperone function in cells.

Prostate cancer, and specifically CRPC, is a unique disease model for which there is a known target, that transitions from being easily treated to highly problematic and "undruggable". Considering this, as well as the established dependence of AR on the chaperone network, we decided to focus on prostate cancer cell models for testing the utility of our combined functional genomic and chemical toolsets. There is strong precedent for the concept of harnessing protein homeostasis in order to eliminate "undruggable" targets. To date, efforts in this realm have primarily been made towards repurposing the cellular degradation machinery for the guided clearance of these difficult targets (37). We believe that AR, and the truncated forms of AR that arise in CRPC, can alternatively be sentenced for degradation by disabling the folding machinery responsible for the receptor's stability. This idea has been encouraged by a long-standing observation that inhibiting Hsp70 or Hsp90 can lead to decreased levels of AR in cells. We confirm in this study that inhibiting Hsp70 and Hsp90 both lead to degradation of AR, and that these chaperone systems can be simultaneously targeted to clear full length and truncated AR.

Furthermore, the cooperativity between Hsp70 and Hsp90 is important for the proliferation of CRPC cells. These findings encourage the use of combined Hsp70 and Hsp90 inhibition for treating CRPC.

One of the most fascinating findings of this study was that there were certain chaperones that CRPC cells showed a heightened reliance on for survival. The chaperonin, Hsp60, is one example of this. While Hsp60 is known to be upregulated in prostate cancer (38), there has been little evidence, to date, to suggest that it plays a role in disease progression to a hormone refractory state (39,40). While the mechanism of the selective vulnerability to Hsp60 knockdown is unclear, studies are currently underway to further characterize this phenomenon. This includes, but is not limited to, determining the metabolic profile of our cell lines with and without Hsp60 knockdown, subcellular localization of Hsp60, and characterizing whether Hsp60 is required for signaling of AR/ARv7. Furthermore, in collaboration with the Neckers Lab, we are currently validating the effect of Hsp60 knockdown on tumor growth in a mouse xenograft model.

Regardless of the role in CRPC cell survival, Hsp60 offers an exciting starting point for a new drug discovery campaign. Like Hsp70, Hsp60 is an ATP-dependent chaperone that relies on a partner protein, Hsp10, in order to refold denatured substrates. So far, there have been a handful of small molecules published as Hsp60 inhibitors (41), however these are early days in the discovery of chemical tools for this particular chaperone. Furthermore, none of the molecules published to this day have been evaluated for their effect on the Hsp60-Hsp10 interaction. In the spirit of Chapter 2 of this thesis, we propose that the Hsp60-Hsp10 complex would be an ideal candidate for the discovery of new inhibitors, using a reconstituted multiprotein complex (RMPC) approach, and that any

such inhibitors to emerge from a screen would be well-suited for evaluation as novel CRPC therapeutics.

METHODS

Cell line maintenance

PC-3, LNCaP, and 22Rv1 cells were purchased from ATCC and grown in RPMI 1640 medium supplemented with 10% non-heat-inactivated fetal bovine serum (Gibco 16000044) and 1% penicillin/streptomycin. All cell lines were maintained in regular tissue culture-treated flasks, with the exception of the low-adherent LNCaPs, which were kept in carboxyl-coated flasks (Corning 354778). All cells were grown at 37 °C and 5% CO_2.

Reagents

JG231 was prepared in house, while AUY922 was purchased from Advanced ChemBlocks Inc. (cat # 10274), and R1881 was purchased from Sigma Aldrich (R0908). The chaperone shRNA library was cloned into the lentiviral backbone plasmid, pMK1275, and individual shRNAs were cloned into either the dox-inducible backbone, pMK1201 (derived from pINDUCER10 of the Elledge Lab) or pMK1200. All backbone plasmids were generously provided by Dr. Martin Kampmann.

Immunoblotting

Target	Company/Cat #	Dilution used	Host
AR	Abcam (ab133273)	1:1,000	Rabbit
Hsc/p70	Santa Cruz (sc33575)	1:200	Rabbit
Hsp27	Santa Cruz (sc59562)	1:200	Mouse
Hsp60	Cell Signaling (D6F1)	1:1,000	Rabbit
Hsp10	Santa Cruz (sc376313)	1:1,000	Mouse

HOP	Enzo Life Sciences (ADI-SRA-1500)	1:1,000	Mouse
p23	Abgent (AP14751c)	1:1,000	Rabbit
actin	Sigma (A5441)	1:200	Mouse
α-mouse 2° (HRP)	Cell Signaling (7076S)	1:10,000	Goat
α-rabbit 2° (HRP)	Cell Signaling (7074S)	1:10,000	Goat

Table 3.3: List of antibodies used.

For quantifying the effect of chaperone inhibitors on destabilization of AR-FL and ARv7, cells were grown in a 6-well plate to near 100% confluency. At this point, the growth medium was replaced with fresh medium containing the drug in 1% DMSO. The drug was left on the cells and incubated at 37°C and 5% CO_2 for six hours, immediately followed by harvesting and lysing in M-PER supplemented with protease inhibitors. Lysate concentrations were quantified by a bicinchoninic acid assay (BCA, ThermoFisher 23227) and then run on 4-15% gradient SDS polyacrylamide gels at 5-10 µg of total protein per sample. All blot quantification was performed in Image Lab™ software (BioRad).

MTT cell viability assay

Cell Line	IC_{50} of JG231 (μM)
PC-3	7.1 ± 2.0
LNCaP	0.8 ± 1.1
22Rv1	1.5 ± 0.4

Table 3.2: IC_{50} values for JG231 in PCa cell lines (24 hour treatment)

Cell viability post-treatment with chaperone inhibitors was determined following a previously described method (42) with some modifications using MTT (3(4, 5-dimethylthiazolyl 2)2, 5diphenyltetrazolium bromide) (ATCC® kit 30-1010K™). Briefly, cells were seeded at optimal densities for assessment of viability after 24 hours according

to trials with each cell type (PC-3 and LNCaP: 5,000 cells per well, 22Rv1: 10,000 cells per well). The cells were treated with a range of chaperone inhibitor concentrations (final DMSO concentration at 1%) after they were allowed to adhere to the plates overnight, and then incubated at 37 °C for 24 hours in 100 µL of growth medium. Subsequently, 10 µL of MTT reagent was added to each well and then incubated at 37 °C for 4 hours to allow for reduction of the yellow tetrazolium dye to an insoluble, purple formazan. The medium was removed, 75 µL of DMSO was added to each well, and the solubilized formazan was quantified by measuring OD_{540} on a Molecular Devices Spectramax M5 plate reader.

Lentiviral production and infection

All lentiviruses were prepared by transfection into HEK293T cells using Lipofectamine 2000 and packaging plasmids pMol, pRSV, and pVSV-g. Viral particles were allowed to form for 48 hours post transfection, and then the viral supernatant was collected, passed through a 0.45 µm filter, and stored at 4 °C for no longer than one week prior to use. Viral supernatant was added to suspended cells immediately following trypsinization, along with 8 µg/mL polybrene (Santa Cruz sc-134220). The cells were allowed to adhere to the flasks, then the medium was replaced with regular growth medium after 6-8 hours. After 48 hours, the cells successfully infected with the lentiviral plasmids were selected with 1 µg/mL puromycin (Gibco A11138-03) for an additional 48 hours. Flow cytometry was used to determine infection and selection efficiency via the expression of fluorescent markers encoded by the lentiviral vectors (generally BFP for pooled shRNA screens, and mCherry or TurboRFP for individual shRNA constructs).

Pooled shRNA screens

Lentivirus was prepared as described above of the pooled shRNA library and used to infect the prostate cancer cell lines. Most cell lines were initially infected at ~50-60% efficiency, monitored by BFP intensity, and then were further selected with puromycin to ~100%. Immediately following the selection T_0 samples, of ~4 million cells each, were collected and stored at -80 °C until genomic DNA was isolated for sequencing. The cells were continually cultured, maintaining at least 4 million cells with each passage, for a period of ~10 doublings. For screens with chaperone inhibitors, the cells were dosed three times at around the IC_{50} of each drug, for a duration of 24 hours each time. At the end of the growth period, samples of ~4 million cells were collected for the T_{final} sample.

Genomic DNA isolation, indexing and PCR purification

Genomic DNA was extracted using the MN NucleoSpin® Blood Kit (Macherey-Nagel 740951) for ~4-6 million cells per sample. Whole genomic DNA samples were carried forward into indexing PCRs using Q5® High-Fidelity polymerase (New England BioLabs M0492S). PCR amplified, and indexed, fragments of approximately 280 bp were purified by a two-step SPRI bead purification (43), and concentrations were determined on a Qubit Fluorometer before pooling for deep sequencing on a HiSeq 4000.

REFERENCES

1. Crawford, E. D., Schellhammer, P. F., McLeod, D. G., Moul, J. W., Higano, C. S., Shore, N., Denis, L., Iversen, P., Eisenberger, M. A., and Labrie, F. (2018) Androgen Receptor-Targeted Treatments for Prostate Cancer: 35 Years' Progress with Antiandrogens. *The Journal of urology*
2. Scher, H. I., Solo, K., Valant, J., Todd, M. B., and Mehra, M. (2015) Prevalence of Prostate Cancer Clinical States and Mortality in the United States: Estimates Using a Dynamic Progression Model. *PloS one* **10**, e0139440
3. Chi, K. N., Bjartell, A., Dearnaley, D., Saad, F., Schroder, F. H., Sternberg, C., Tombal, B., and Visakorpi, T. (2009) Castration-resistant prostate cancer: from new pathophysiology to new treatment targets. *European urology* **56**, 594-605

4. Watson, P. A., Arora, V. K., and Sawyers, C. L. (2015) Emerging mechanisms of resistance to androgen receptor inhibitors in prostate cancer. *Nature reviews. Cancer* **15**, 701-711
5. Lallous, N., Dalal, K., Cherkasov, A., and Rennie, P. S. (2013) Targeting alternative sites on the androgen receptor to treat castration-resistant prostate cancer. *International journal of molecular sciences* **14**, 12496-12519
6. Antonarakis, E. S., Lu, C., Wang, H., Luber, B., Nakazawa, M., Roeser, J. C., Chen, Y., Mohammad, T. A., Chen, Y., Fedor, H. L., Lotan, T. L., Zheng, Q., De Marzo, A. M., Isaacs, J. T., Isaacs, W. B., Nadal, R., Paller, C. J., Denmeade, S. R., Carducci, M. A., Eisenberger, M. A., and Luo, J. (2014) AR-V7 and resistance to enzalutamide and abiraterone in prostate cancer. *The New England journal of medicine* **371**, 1028-1038
7. Cano, L. Q., Lavery, D. N., and Bevan, C. L. (2013) Mini-review: Foldosome regulation of androgen receptor action in prostate cancer. *Molecular and cellular endocrinology* **369**, 52-62
8. Freeman, B. C., and Yamamoto, K. R. (2002) Disassembly of transcriptional regulatory complexes by molecular chaperones. *Science (New York, N.Y.)* **296**, 2232-2235
9. Echeverria, P. C., and Picard, D. (2010) Molecular chaperones, essential partners of steroid hormone receptors for activity and mobility. *Biochimica et biophysica acta* **1803**, 641-649
10. Pratt, W. B., and Toft, D. O. (1997) Steroid receptor interactions with heat shock protein and immunophilin chaperones. *Endocrine reviews* **18**, 306-360
11. Morgner, N., Schmidt, C., Beilsten-Edmands, V., Ebong, I. O., Patel, N. A., Clerico, E. M., Kirschke, E., Daturpalli, S., Jackson, S. E., Agard, D., and Robinson, C. V. (2015) Hsp70 forms antiparallel dimers stabilized by post-translational modifications to position clients for transfer to Hsp90. *Cell reports* **11**, 759-769
12. Kirschke, E., Goswami, D., Southworth, D., Griffin, P. R., and Agard, D. A. (2014) Glucocorticoid receptor function regulated by coordinated action of the Hsp90 and Hsp70 chaperone cycles. *Cell* **157**, 1685-1697
13. Sahasrabudhe, P., Rohrberg, J., Biebl, M. M., Rutz, D. A., and Buchner, J. (2017) The Plasticity of the Hsp90 Co-chaperone System. *Molecular cell* **67**, 947-961.e945
14. Kampmann, M., Bassik, M. C., and Weissman, J. S. (2013) Integrated platform for genome-wide screening and construction of high-density genetic interaction maps in mammalian cells. *Proceedings of the National Academy of Sciences of the United States of America* **110**, E2317-2326
15. Azad, A. A., Zoubeidi, A., Gleave, M. E., and Chi, K. N. (2015) Targeting heat shock proteins in metastatic castration-resistant prostate cancer. *Nature reviews. Urology* **12**, 26-36
16. Moses, M. A., Kim, Y. S., Rivera-Marquez, G. M., Oshima, N., Watson, M. J., Beebe, K., Wells, C., Lee, S., Zuehlke, A. D., Shao, H., Bingman, W. E., Kumar, V., Malhotra, S., Weigel, N. L., Gestwicki, J. E., Trepel, J., and Neckers, L. M. (2018) Targeting the Hsp40/Hsp70 chaperone axis as a novel strategy to treat castration-resistant prostate cancer. *Cancer research*

17. Kaighn, M. E., Narayan, K. S., Ohnuki, Y., Lechner, J. F., and Jones, L. W. (1979) Establishment and characterization of a human prostatic carcinoma cell line (PC-3). *Investigative urology* **17**, 16-23
18. Horoszewicz, J. S., Leong, S. S., Kawinski, E., Karr, J. P., Rosenthal, H., Chu, T. M., Mirand, E. A., and Murphy, G. P. (1983) LNCaP model of human prostatic carcinoma. *Cancer research* **43**, 1809-1818
19. Sramkoski, R. M., Pretlow, T. G., 2nd, Giaconia, J. M., Pretlow, T. P., Schwartz, S., Sy, M. S., Marengo, S. R., Rhim, J. S., Zhang, D., and Jacobberger, J. W. (1999) A new human prostate carcinoma cell line, 22Rv1. *In vitro cellular & developmental biology. Animal* **35**, 403-409
20. McLean, D. T., Strand, D. W., and Ricke, W. A. (2017) Prostate cancer xenografts and hormone induced prostate carcinogenesis. *Differentiation; research in biological diversity* **97**, 23-32
21. Kampinga, H. H., and Craig, E. A. (2010) The HSP70 chaperone machinery: J proteins as drivers of functional specificity. *Nature reviews. Molecular cell biology* **11**, 579-592
22. Paul, A., Garcia, Y. A., Zierer, B., Patwardhan, C., Gutierrez, O., Hildenbrand, Z., Harris, D. C., Balsiger, H. A., Sivils, J. C., Johnson, J. L., Buchner, J., Chadli, A., and Cox, M. B. (2014) The cochaperone SGTA (small glutamine-rich tetratricopeptide repeat-containing protein alpha) demonstrates regulatory specificity for the androgen, glucocorticoid, and progesterone receptors. *The Journal of biological chemistry* **289**, 15297-15308
23. Ni, L., Yang, C. S., Gioeli, D., Frierson, H., Toft, D. O., and Paschal, B. M. (2010) FKBP51 promotes assembly of the Hsp90 chaperone complex and regulates androgen receptor signaling in prostate cancer cells. *Molecular and cellular biology* **30**, 1243-1253
24. Yong, W., Yang, Z., Periyasamy, S., Chen, H., Yucel, S., Li, W., Lin, L. Y., Wolf, I. M., Cohn, M. J., Baskin, L. S., Sanchez, E. R., and Shou, W. (2007) Essential role for Co-chaperone Fkbp52 but not Fkbp51 in androgen receptor-mediated signaling and physiology. *The Journal of biological chemistry* **282**, 5026-5036
25. Taipale, M., Tucker, G., Peng, J., Krykbaeva, I., Lin, Z. Y., Larsen, B., Choi, H., Berger, B., Gingras, A. C., and Lindquist, S. (2014) A quantitative chaperone interaction network reveals the architecture of cellular protein homeostasis pathways. *Cell* **158**, 434-448
26. Assimon, V. A., Gillies, A. T., Rauch, J. N., and Gestwicki, J. E. (2013) Hsp70 protein complexes as drug targets. *Current pharmaceutical design* **19**, 404-417
27. Jhaveri, K., Ochiana, S. O., Dunphy, M. P., Gerecitano, J. F., Corben, A. D., Peter, R. I., Janjigian, Y. Y., Gomes-DaGama, E. M., Koren, J., 3rd, Modi, S., and Chiosis, G. (2014) Heat shock protein 90 inhibitors in the treatment of cancer: current status and future directions. *Expert opinion on investigational drugs* **23**, 611-628
28. Eccles, S. A., Massey, A., Raynaud, F. I., Sharp, S. Y., Box, G., Valenti, M., Patterson, L., de Haven Brandon, A., Gowan, S., Boxall, F., Aherne, W., Rowlands, M., Hayes, A., Martins, V., Urban, F., Boxall, K., Prodromou, C., Pearl, L., James, K., Matthews, T. P., Cheung, K. M., Kalusa, A., Jones, K., McDonald, E., Barril, X., Brough, P. A., Cansfield, J. E., Dymock, B., Drysdale, M. J., Finch, H., Howes, R., Hubbard, R. E., Surgenor, A., Webb, P., Wood, M., Wright, L., and Workman, P.

(2008) NVP-AUY922: a novel heat shock protein 90 inhibitor active against xenograft tumor growth, angiogenesis, and metastasis. *Cancer research* **68**, 2850-2860
29. He, S., Zhang, C., Shafi, A. A., Sequeira, M., Acquaviva, J., Friedland, J. C., Sang, J., Smith, D. L., Weigel, N. L., Wada, Y., and Proia, D. A. (2013) Potent activity of the Hsp90 inhibitor ganetespib in prostate cancer cells irrespective of androgen receptor status or variant receptor expression. *International journal of oncology* **42**, 35-43
30. Wilson, S., Cavero, L., Tong, D., Liu, Q., Geary, K., Talamonti, N., Xu, J., Fu, J., Jiang, J., and Zhang, D. (2017) Resveratrol enhances polyubiquitination-mediated ARV7 degradation in prostate cancer cells. *Oncotarget* **8**, 54683-54693
31. Lee, D. K., and Chang, C. (2003) Endocrine mechanisms of disease: Expression and degradation of androgen receptor: mechanism and clinical implication. *The Journal of clinical endocrinology and metabolism* **88**, 4043-4054
32. Armstrong, H. K., Koay, Y. C., Irani, S., Das, R., Nassar, Z. D., Selth, L. A., Centenera, M. M., McAlpine, S. R., and Butler, L. M. (2016) A Novel Class of Hsp90 C-Terminal Modulators Have Pre-Clinical Efficacy in Prostate Tumor Cells Without Induction of a Heat Shock Response. *The Prostate* **76**, 1546-1559
33. Dakappagari, N., Neely, L., Tangri, S., Lundgren, K., Hipolito, L., Estrellado, A., Burrows, F., and Zhang, H. (2010) An investigation into the potential use of serum Hsp70 as a novel tumour biomarker for Hsp90 inhibitors. *Biomarkers : biochemical indicators of exposure, response, and susceptibility to chemicals* **15**, 31-38
34. Wang, A. M., Miyata, Y., Klinedinst, S., Peng, H. M., Chua, J. P., Komiyama, T., Li, X., Morishima, Y., Merry, D. E., Pratt, W. B., Osawa, Y., Collins, C. A., Gestwicki, J. E., and Lieberman, A. P. (2013) Activation of Hsp70 reduces neurotoxicity by promoting polyglutamine protein degradation. *Nature chemical biology* **9**, 112-118
35. Okamoto, T., Ishida, R., Yamamoto, H., Tanabe-Ishida, M., Haga, A., Takahashi, H., Takahashi, K., Goto, D., Grave, E., and Itoh, H. (2015) Functional structure and physiological functions of mammalian wild-type HSP60. *Archives of biochemistry and biophysics* **586**, 10-19
36. Bottinger, L., Oeljeklaus, S., Guiard, B., Rospert, S., Warscheid, B., and Becker, T. (2015) Mitochondrial heat shock protein (Hsp) 70 and Hsp10 cooperate in the formation of Hsp60 complexes. *The Journal of biological chemistry* **290**, 11611-11622
37. Gu, S., Cui, D., Chen, X., Xiong, X., and Zhao, Y. (2018) PROTACs: An Emerging Targeting Technique for Protein Degradation in Drug Discovery. *BioEssays : news and reviews in molecular, cellular and developmental biology* **40**, e1700247
38. Cornford, P. A., Dodson, A. R., Parsons, K. F., Desmond, A. D., Woolfenden, A., Fordham, M., Neoptolemos, J. P., Ke, Y., and Foster, C. S. (2000) Heat shock protein expression independently predicts clinical outcome in prostate cancer. *Cancer research* **60**, 7099-7105
39. Castilla, C., Congregado, B., Conde, J. M., Medina, R., Torrubia, F. J., Japon, M. A., and Saez, C. (2010) Immunohistochemical expression of Hsp60 correlates with tumor progression and hormone resistance in prostate cancer. *Urology* **76**, 1017.e1011-1016

40. Johansson, B., Pourian, M. R., Chuan, Y. C., Byman, I., Bergh, A., Pang, S. T., Norstedt, G., Bergman, T., and Pousette, A. (2006) Proteomic comparison of prostate cancer cell lines LNCaP-FGC and LNCaP-r reveals heatshock protein 60 as a marker for prostate malignancy. *The Prostate* **66**, 1235-1244
41. Meng, Q., Li, B. X., and Xiao, X. (2018) Toward Developing Chemical Modulators of Hsp60 as Potential Therapeutics. *Frontiers in molecular biosciences* **5**, 35
42. Li, X., Colvin, T., Rauch, J. N., Acosta-Alvear, D., Kampmann, M., Dunyak, B., Hann, B., Aftab, B. T., Murnane, M., Cho, M., Walter, P., Weissman, J. S., Sherman, M. Y., and Gestwicki, J. E. (2015) Validation of the Hsp70-Bag3 protein-protein interaction as a potential therapeutic target in cancer. *Molecular cancer therapeutics* **14**, 642-648
43. Fisher, S., Barry, A., Abreu, J., Minie, B., Nolan, J., Delorey, T. M., Young, G., Fennell, T. J., Allen, A., Ambrogio, L., Berlin, A. M., Blumenstiel, B., Cibulskis, K., Friedrich, D., Johnson, R., Juhn, F., Reilly, B., Shammas, R., Stalker, J., Sykes, S. M., Thompson, J., Walsh, J., Zimmer, A., Zwirko, Z., Gabriel, S., Nicol, R., and Nusbaum, C. (2011) A scalable, fully automated process for construction of sequence-ready human exome targeted capture libraries. *Genome biology* **12**, R1

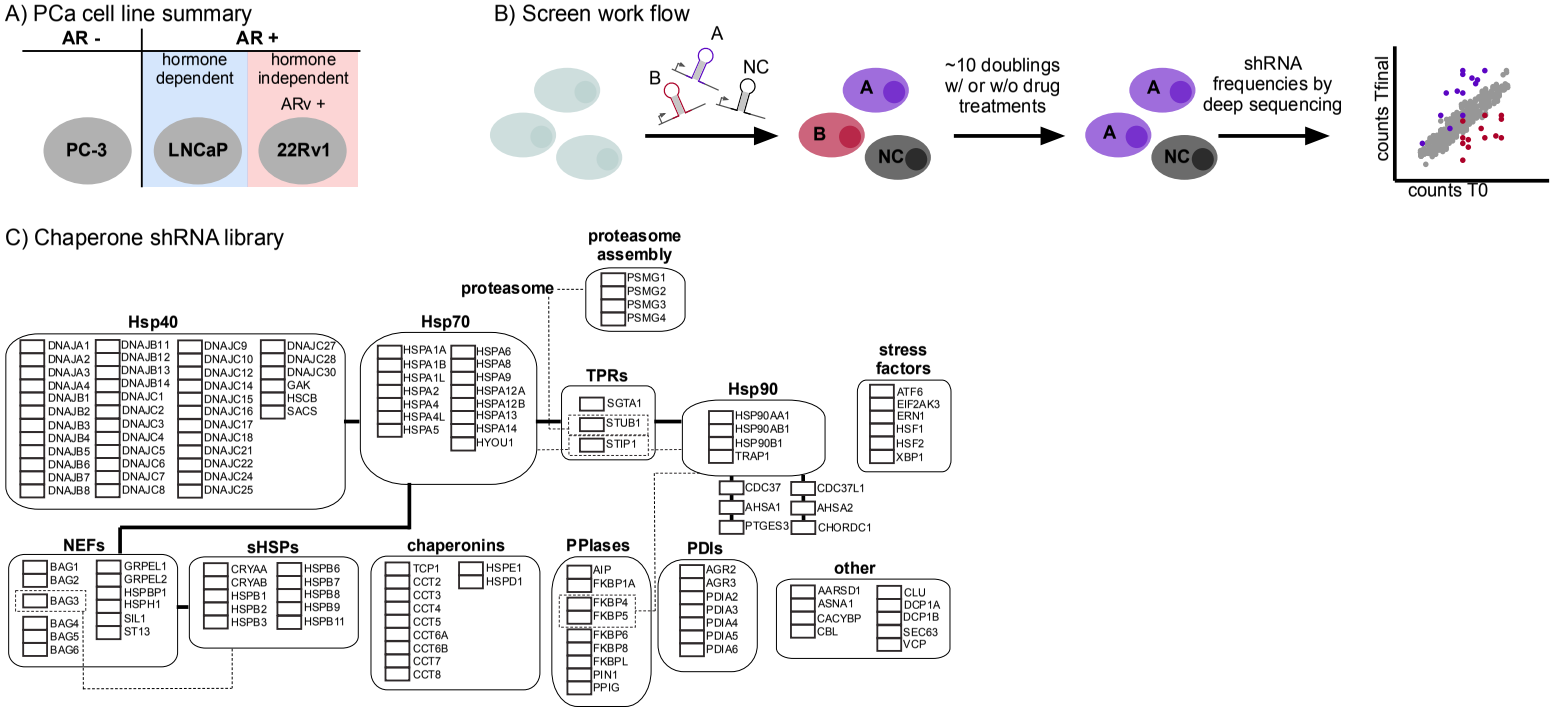

Figure 3.1: Functional genomics screens in PCa cell lines. A) Cell lines used in this study, annotated with their AR status. B) Screen workflow. A population of cells is infected with lentivirus of the pooled shRNA library where each shRNA sequence targets a chaperone- encoding gene (A and B), or is a non-targeting negative control sequence (NC). The cells are puro-selected to create a T0 population, a portion of which is collected, while the remainder are continuously cultured. The cells are grown for a period of ~10 doublings, with or without periodic 24h drug treatments, resulting in a Tfinal population. The frequency of each shRNA is compared in T0 and Tfinal by deep sequencing. C) Custom chaperone shRNA library. Each gene in the library has 25 unique shRNA sequences targeting the corresponding mRNA. This library also features 500 different negative control sequences. Every gene targeted in the library is shown on this network map, where solid bold lines represent known connections between chaperone classes, and dotted lines represent either connections between individual genes and whole classes, or connections to the proteasomal degradation pathway (proteasome components not included in library).

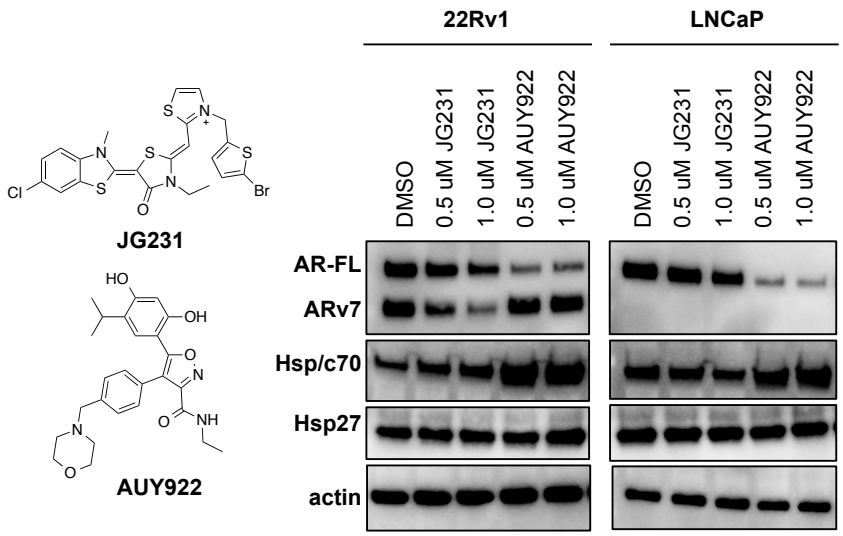

Figure 3.2: Chaperone inhibitors JG231 and AUY922 have differential effects on AR/ARv7 homeostasis in cells. An Hsp70 inhibitor (JG231) and an Hsp90 inhibitor (AUY922) were applied to 22Rv1 and LNCaP (the two AR positive cell lines) cells. Cells were incubated with the drug for six hours, then harvested and lysed.

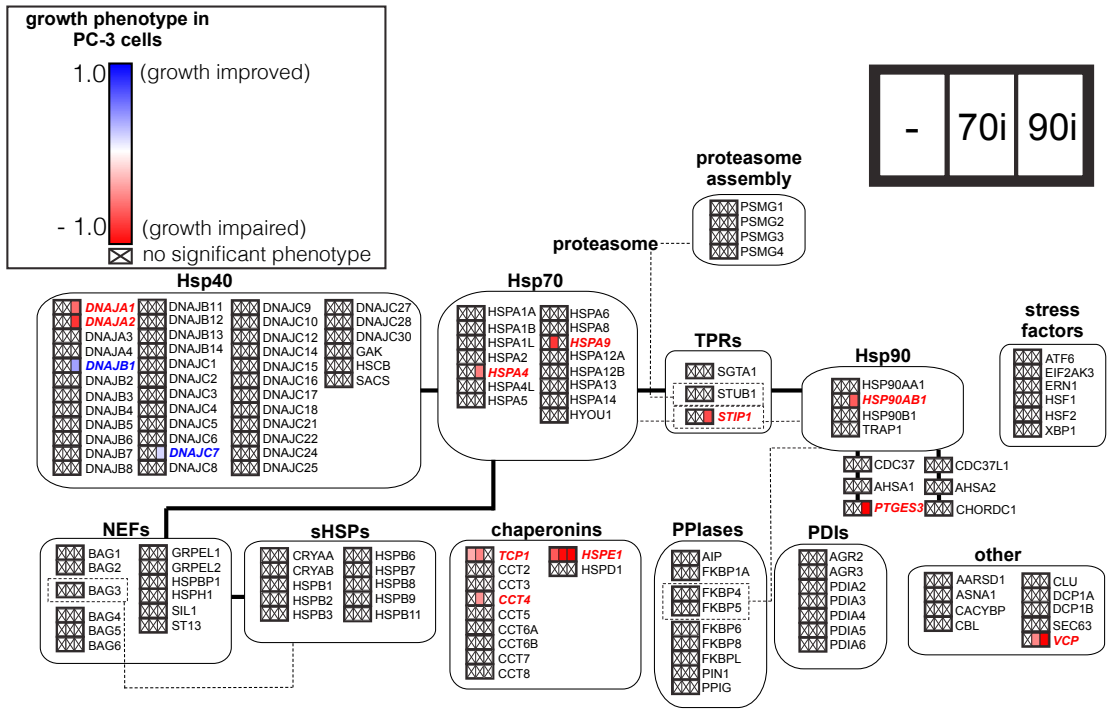

Figure 3.3: Screen results in PC-3 cells. All highlighted phenotypes have a p value ≤ 0.005. Results of the untreated, JG231-treated (70i) and AUY922-treated (90i) screens are shown.

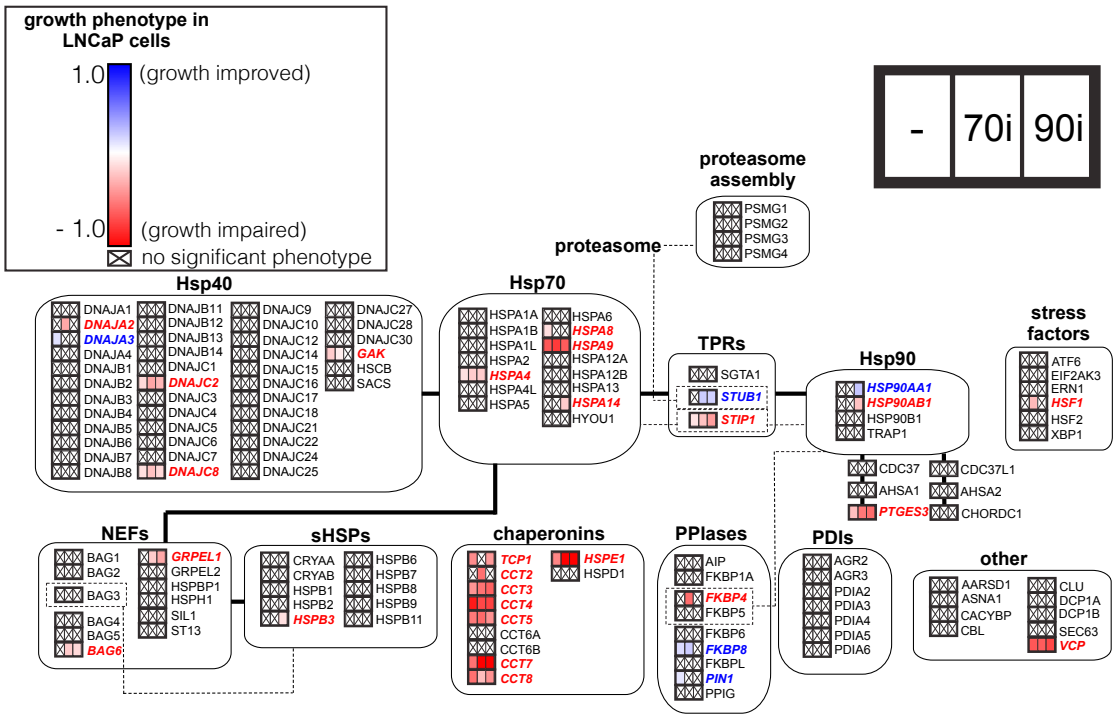

Figure 3.4: Screen results in LNCaP cells. All highlighted phenotypes have a p value ≤ 0.005. Results of the untreated, JG231-treated (70i) and AUY922-treated (90i) screens are shown.

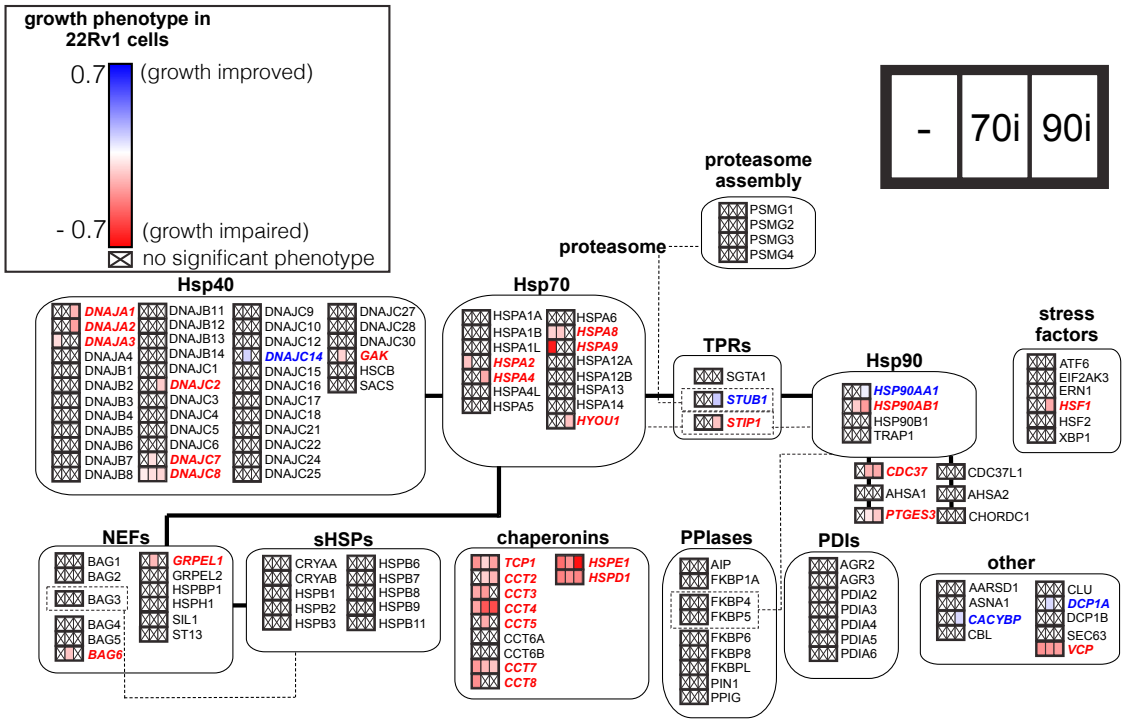

Figure 3.5: Screen results in 22Rv1 cells. All highlighted phenotypes have a p value ≤ 0.005. Results of the untreated, JG231-treated (70i) and AUY922-treated (90i) screens are shown.

A) Emergent phenotypes with AUY922 treatment

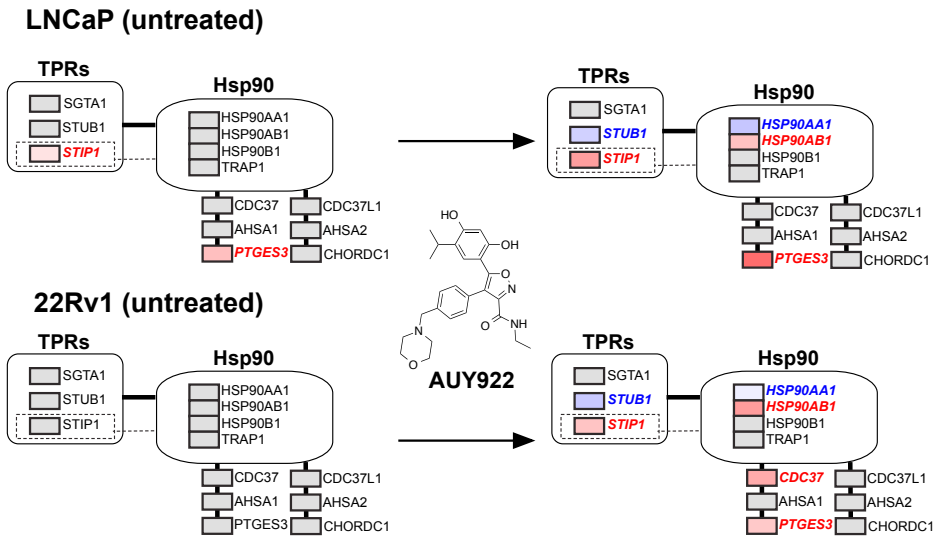

B) Validation of phenotypes with AUY922 treatment

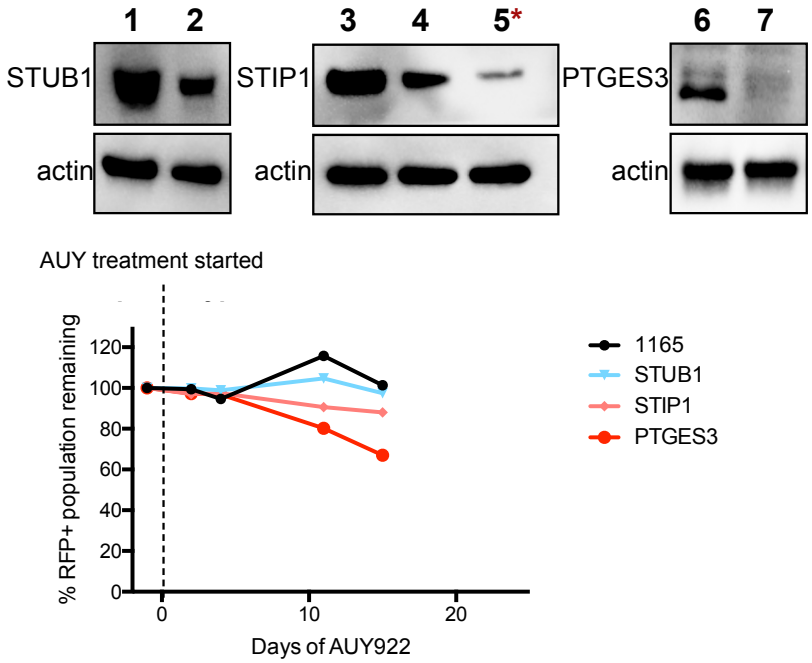

Figure 3.6: Chemical genetic interactions with AUY922. A) A distinct pattern of phenotypes emerge in cells treated with AUY922. All highlighted phenotypes (not in grey) had a p value ≤ 0.005 in the shRNA screens. B) Individual shRNAs were introduced to 22Rv1 cells in order to validate phenotypes for AUY922 treatment in the functional genomic screens. Knockdown was confirmed by Western blot of sh22Rv1 lysates: lanes 1, 3, and 6) 1165 (control shRNA) lysates, lane 2) STUB1 knockdown, lanes 4 and 5) two different STIP1 shRNAs (cell line in lane 5 was used in growth phenotype validation experiment) lane 7) PTGES3 knockdown. 22Rv1 cells with these constitutive shRNAs were grown in the presence of 5 nM AUY922 for 15 days and the % RFP positive population was monitored by flow cytometry with passaging.

A) Growth phenotype validation with inducible knockdowns in 22Rv1

B) Knockdown validation in puro-selected cell lines

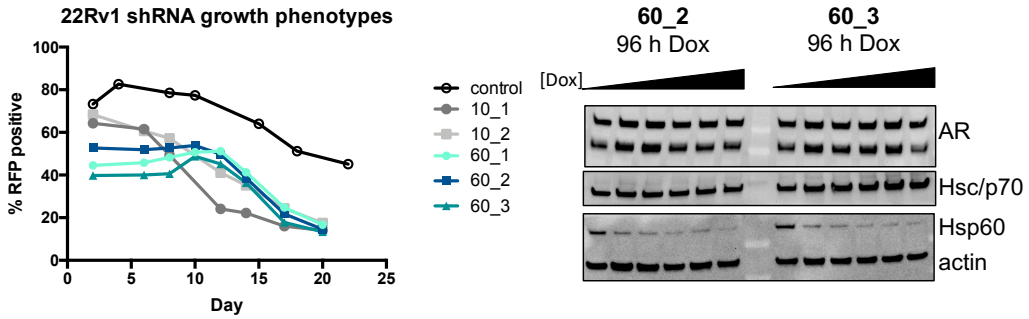

Figure 3.7: Hsp60 and Hsp10 knockdown validation in inducible 22Rv1 cells. A) Cells with shRNAs in pMK1201 background were grown in the presence of 1 μg/mL dox and RFP was monitored by flow cytometry to approximate growth phenotype of shRNA positive population. B) 60_2 and 60_3 cell lines were further puro-selected to near 100% RFP positive and tested for dox dose responsive knockdown of Hsp60. Top concentration of dox tested was 1 μg/mL with 2-fold dilutions to 0 μg/mL. Knockdown of Hsp60 was quantified to be ~40-60%, and had no significant effect on Hsp70 or AR/ARv7 levels.

A) Growth phenotype validation with constitutive knockdowns in PC-3

B) Knockdown validation in PC-3 lysates

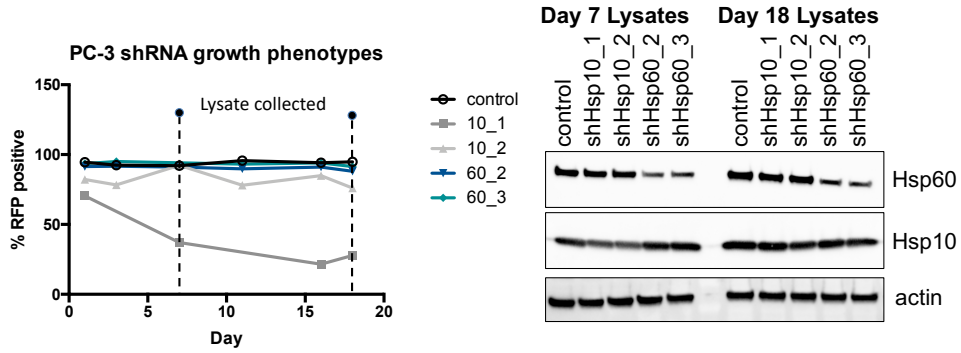

Figure 3.8: Hsp60 and Hsp10 knockdown validation in constitutive PC-3 cells. A) Cells with shRNAs in pMK1200 background were initially puro-selected to near 100% RFP (mCherry) positive, and were then monitored by flow cytometry to approximate the growth phenotype of the shRNA positive population. Lysates were collected with each split in order to test knockdown efficiency. B) The lysates from day 7 and day 18 of the growth validation experiment were assessed for knockdown efficiency, compared to the control (empty vector) cells. Hsp60 knockdown was quantified to be approximately 50%, which was consistent through the course of the experiment. Hsp10 knockdown was observed, and estimated to be more efficient for 10_1 than 10_2 (calculating for the substantial decrease in the % RFP positive population).

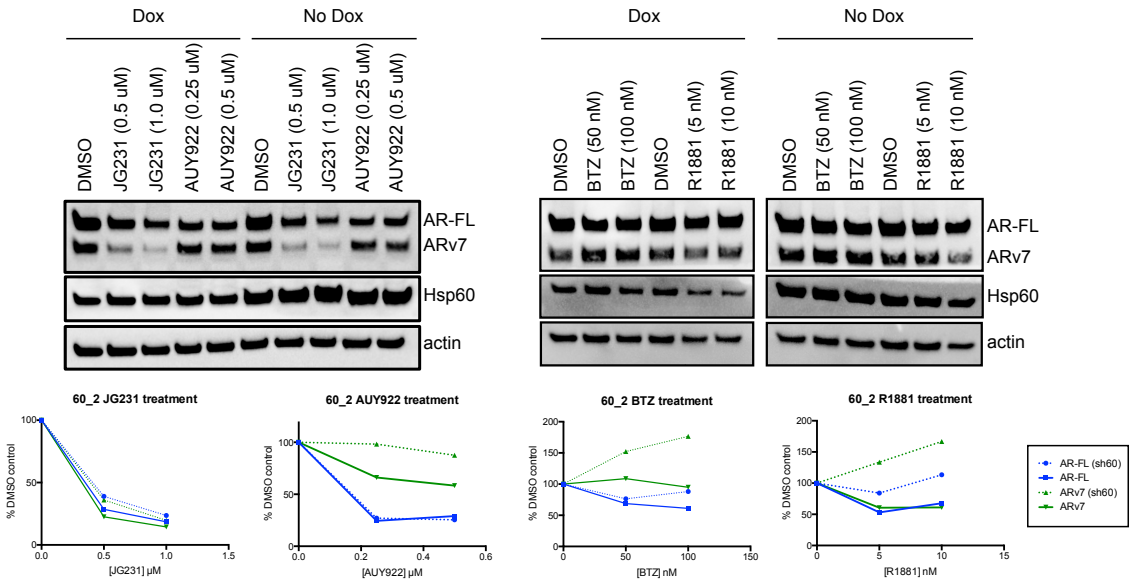

Figure 3.9: Effect of Hsp60 knockdown on AR/ARv7 levels in response to small molecule treatment. Cells were grown in the presence ("Dox") or absence ("No Dox") of 1 μg/mL dox for 96 hours. After the 96-hour knockdown period, the medium was replaced with fresh medium supplemented with the indicated drugs in 1% DMSO. After six hours of drug treatment, cells were harvested and lysed, and the lysates were probed by Western blot. Bands were quantified in Image Lab™ and normalized to actin.

Chapter 4: Conclusions and Future Directions

INTRODUCTION

Molecular chaperones are a class of proteins that deserve attention as drug targets for a wide range of diseases. However, they present many challenges that traditional drug discovery methods are simply not built to handle. The central issue that makes chaperones such difficult targets is that they are highly cooperative machines, both in their structure and immediate protein-protein interactions, and in the sense that they each play, as-of-yet, poorly defined roles in the greater proteostasis network. In order to really know how to “drug” the chaperone network, we still need to have a much deeper understanding of how these proteins function together in the context of a cell.

Although the clinical success stories about proteostasis modulators are few and far between, the lessons we’ve learned thus far have suggested that there may be a “right” way to treat each disease by targeting different branches of proteostasis. For instance, it has become clear that inhibiting the proteasome is a remarkably successful strategy for treating multiple myeloma, where other cancer types are less receptive to these same drugs (1,2). Similarly, while Hsp90 inhibitor programs have been terminated for several cancer types, they have shown promising efficacy in HER2+ breast cancer, and a few candidate molecules are still being evaluated for other clinical applications (3,4). There has even been evidence to suggest that the complexes formed by Hsp90 (and Hsp70) are molecularly distinct from one cancer cell type to another (5). So not only do we lack the complete knowledge of which chaperones are needed for folding a given client protein, but the relevant complexes that form may differ from one cell type to another. This calls for a return to the basics, so to speak, as we must develop more precise tools to answer these questions.

Allosteric Inhibitors of Hsp70

The small molecule series inspired by MKT-077, VER-155008, and YK5 have served as great tools to manipulate Hsp70's function in various settings (5-7). While they represent some of the most thoroughly developed chemical matter targeting Hsp70, these molecules are only a subset of the series that have been explored as Hsp70 inhibitors to date. Furthermore, several alternative binding sites exist on the protein that can be targeted. It will be important to use all of these emerging tools moving forward in the pursuit of understanding Hsp70's complex activity through chemical biology.

One such example of a chemical scaffold that binds a distinct site on the NBD of Hsp70 is MAL3-101 (**Figure 4.1**). This molecule binds the IIA subdomain of Hsp70's NBD at the interface of the protein's interaction with the J domain of the Hsp40 co-chaperones. Recent work with this molecule has pointed to a compelling application in the treatment of both Merkel cell carcinoma and rhabdomyosarcoma (8,9), and furthermore has been able to identify particular members of the Hsp70 class that are important for survival of these cells. The success of MAL3-101's use as a tool compound to date is especially encouraging of further efforts to target its binding site, as there is increasing structural characterization becoming available to inform those efforts (10). It is even possible to design molecules that promote, rather than disrupt, the interaction of the J domain at this site, as this has been observed for a series of molecules inspired by MAL3-101 (11). MAL3-101 and its derivatives will serve as valuable tools in dissecting the role of the Hsp70-Hsp40 interaction and can expand our understanding of the specificity imparted by the various Hsp40 family members in human cells.

While many targetable sites have been identified on the NBD of Hsp70, efforts to design molecules targeting the SBD have been far more limited. Targeting the SBD of Hsp70 is an intriguing idea, as it is the site of the most sequence variation among the Hsp70 homologs (12). Therefore, the discovery that a fungal metabolite, novolactone (**Figure 4.1**), covalently binds the E444 residue of Hsp72 was novel and potentially the gateway for discovery of a whole new breed of Hsp70 inhibitor (13). The site of this covalently modified glutamic acid is at a portion of the SBD that is solvent-exposed in the ADP-state, but becomes masked by docking of the SBD to the NBD in the ATP-state. Furthermore, while this residue is conserved in the cytosolic and ER Hsp70 isoforms, it is replaced by a glutamine in the ribosome-associated and mitochondrial isoforms. This suggests that the site might be able to be selectively targeted by covalent modulators, and therefore a starting point for the development of useful tool compounds.

MAL3-101 and novolactone illustrate the existence of even more ways to target Hsp70's function with small molecules, and the list of identified compounds and binding sites will likely continue to grow in the coming years. As these molecules and modes of inhibition are published, it will be extremely useful to continue characterizing how these molecules affect the interaction of Hsp70 with its co-chaperones. Further studies of this nature will be able to increase our understanding of Hsp70's interactions both on the molecular level, and in the context of the chaperone network.

New Inhibitors of Hsp70's Protein-Protein Interactions

One of the most exciting aspects of discovering Compound R as an inhibitor of the Hsp70-NEF interaction was the idea that it could serve as a "scaffold hop" from the molecule series inspired by MKT-077. While MKT-077 and its derivatives have been

extremely useful tools to the understanding of Hsp70's biology, it is a problematic scaffold for further drug development due to its rhodacyanine core and the charge localized to the pyridinium ring of most of the active derivatives. It has been of great interest to our group that neutral molecules with alternative core scaffolds be developed from this series. The discovery of Compound R presented that opportunity, as it is likely to bind the same site as MKT-077 and carry out a similar mechanism of inhibition.

While further structural characterization of this binding event will be necessary, we can continue to drive potency through further chemical modification of the Compound R scaffold. Particularly, the newer generation, and most potent, MKT-077 derivatives feature an additional ring system appended to the pyridinium ring that makes extended interactions with an adjacent pocket on the NBD. Currently, the Compound R derivatives we have now are predicted to be buried in the site that is occupied by the benzothiazole-rhodacyanine core upon MKT-077 binding. By extending the Compound R scaffold with new derivatives featuring additional ring systems, we could potentially take advantage of the added affinity observed in the newer generation MKT-077 derivatives.

Another possibility for future work in this area of Hsp70 inhibitor development is in the design of new screening campaigns centered on other reconstituted complexes. While this screening strategy has been explored previously by our group, those efforts have focused primarily on the prokaryotic Hsp70 (DnaK) system, and have also made use of natural product compound libraries, rather than diversity sets (14,15). No such efforts, to date, have focused on human-derived Hsp70 complexes containing a client protein. Additionally, as we learn more about which protein-protein interactions are relevant for certain diseases, we can design new RMPC screening strategies around

alternative chaperone/co-chaperone complexes. This type of work is already underway for the Hsp60-Hsp10 complex, under the leadership of Hao Shao in our group.

Weak Links in the Proteostasis Network of Castration Resistant Prostate Cancer

The work presented in this thesis is a starting point for the identification of selective vulnerabilities in the chaperone network of castration resistant prostate cancer cells. While there is still a shortage of appropriate cell models for studying the many possible transformations that can occur to give rise to CRPC, we are currently working to expand the panel of cell lines in our functional genomic screens. The same screens using our chaperone shRNA library, in combination with JG231 and AUY922, are now being carried out in an additional CRPC cell line, C4-2 (16) (**Figure 4.2a**). This cell line will serve as a valuable addition to these studies, as it is derived from LNCaP cells that received ADT in a mouse xenograft model. Therefore, the comparison of vulnerabilities in C4-2 to those in LNCaP will be greatly informative as to what chaperone requirements emerge with progression to CRPC. Furthermore, the C4-2 cell line represents a mechanism of resistance to ADT that is alternative to splicing of the androgen receptor. In preparation for screening in this cell line, the chaperone inhibitors were each tested for effects on AR homeostasis, in the fashion presented in Chapter 3. Unsurprisingly, the results were almost identical to what was observed in LNCaP cell lysate (compare **Figure 4.2b** to **Figure 3.2**).

While these immortalized cell models have been so useful in our functional genomic platform for identifying synthetic lethal interactions and selective vulnerabilities, it will be important to identify the significance of these screening hits in more clinically relevant models and datasets. Towards this goal, we are now working to further

characterize the underlying biology of the heightened sensitivity of 22Rv1 cells to Hsp60 knockdown. In collaboration with the Neckers lab, future steps will include testing knockdown of Hsp60 for the ability to slow tumor growth in a mouse xenograft model, as well as continued combination studies with various pathway inhibitors. One intriguing possibility is that the knockdown of Hsp60 may perturb cellular metabolism in a way that CRPC cells are especially sensitive to. Recent work has highlighted an observed differentiation of metabolic pathways in AR-driven CRPC cells, compared to AR-negative cell types (17). This work has fueled our interest in thoroughly characterizing the metabolic profiles of each of our cell lines with and without knockdown of Hsp60. Metabolic profiling may be able to inform future experiments combining Hsp60 knockdown with small molecule modulators of the natural metabolic pathways.

We've recently turned to bioinformatics using clinically-derived datasets as another avenue for following up on the hits identified in our functional genomic screens. Many datasets exist and are publicly available, such as those in the cBioPortal database (18,19). From a preliminary analysis using the datasets available in this portal, we learned that across ~50,000 individual cases, Hsp60 and Hsp10 expression is altered at frequencies of 1.3% and 0.7%, respectively. The analysis identified that those alteration frequencies were increased to 6-10% in prostate cancer-specific datasets. And while no conclusion could be made about whether there was a significant correlation with ADT-resistance, it was also noted that there was a significant frequency of co-occurrent alterations in Hsp60 or Hsp10 with AR (log odds ratio for 60/AR = 1.519, and 10/AR = 1.260). This preliminary analysis is encouraging of future investigations to determine the

frequency of alterations for several molecular chaperones in more CRPC-focused datasets.

As part of a larger effort to identify the cellular folding machinery for AR and ARv7, our group plans to carry out future functional genomic screens with phenotypic read-outs other than cell growth. For instance, if we could identify a chaperone that is necessary for both maintaining high levels of AR, and preserving its transcriptional activity, we could hypothesize that that chaperone is a key part of AR's proper folding trajectory. And if we could do the same thing for ARv7, then we would be able to identify the key differences in how these two proteins fold in a cell. For these efforts, it will be necessary to construct new reporter cell lines that can be used for FACS-based binning of cells with either high/low AR protein levels or high/low expression of AR-target genes. We are currently working in close collaboration with both the Kampmann lab, and the Neckers lab, to assemble the tools necessary for this endeavor.

REFERENCES

1. Dou, Q. P., and Zonder, J. A. (2014) Overview of proteasome inhibitor-based anti-cancer therapies: perspective on bortezomib and second generation proteasome inhibitors versus future generation inhibitors of ubiquitin-proteasome system. *Current cancer drug targets* **14**, 517-536
2. Kisselev, A. F., van der Linden, W. A., and Overkleeft, H. S. (2012) Proteasome inhibitors: an expanding army attacking a unique target. *Chemistry & biology* **19**, 99-115
3. Neckers, L., and Workman, P. (2012) Hsp90 molecular chaperone inhibitors: are we there yet? *Clinical cancer research : an official journal of the American Association for Cancer Research* **18**, 64-76
4. Yuno, A., Lee, M. J., Lee, S., Tomita, Y., Rekhtman, D., Moore, B., and Trepel, J. B. (2018) Clinical Evaluation and Biomarker Profiling of Hsp90 Inhibitors. *Methods in molecular biology (Clifton, N.J.)* **1709**, 423-441
5. Rodina, A., Wang, T., Yan, P., Gomes, E. D., Dunphy, M. P., Pillarsetty, N., Koren, J., Gerecitano, J. F., Taldone, T., Zong, H., Caldas-Lopes, E., Alpaugh, M., Corben, A., Riolo, M., Beattie, B., Pressl, C., Peter, R. I., Xu, C., Trondl, R., Patel, H. J., Shimizu, F., Bolaender, A., Yang, C., Panchal, P., Farooq, M. F., Kishinevsky, S., Modi, S., Lin, O., Chu, F., Patil, S., Erdjument-Bromage, H., Zanzonico, P., Hudis,

C., Studer, L., Roboz, G. J., Cesarman, E., Cerchietti, L., Levine, R., Melnick, A., Larson, S. M., Lewis, J. S., Guzman, M. L., and Chiosis, G. (2016) The epichaperome is an integrated chaperome network that facilitates tumour survival. *Nature* **538**, 397-401

6. Yaglom, J. A., Wang, Y., Li, A., Li, Z., Monti, S., Alexandrov, I., Lu, X., and Sherman, M. Y. (2018) Cancer cell responses to Hsp70 inhibitor JG-98: Comparison with Hsp90 inhibitors and finding synergistic drug combinations. *Scientific reports* **8**, 3010
7. Wang, W. F., Yan, L., Liu, Z., Liu, L. X., Lin, J., Liu, Z. Y., Chen, X. P., Zhang, W., Xu, Z. Z., Shi, T., Li, J. M., Zhao, Y. L., Meng, G., Xia, Y., Li, J. Y., and Zhu, J. (2017) HSP70-Hrd1 axis precludes the oncorepressor potential of N-terminal misfolded Blimp-1s in lymphoma cells. *Nature communications* **8**, 363
8. Adam, C., Baeurle, A., Brodsky, J. L., Wipf, P., Schrama, D., Becker, J. C., and Houben, R. (2014) The HSP70 modulator MAL3-101 inhibits Merkel cell carcinoma. *PloS one* **9**, e92041
9. Sabnis, A. J., Guerriero, C. J., Olivas, V., Sayana, A., Shue, J., Flanagan, J., Asthana, S., Paton, A. W., Paton, J. C., Gestwicki, J. E., Walter, P., Weissman, J. S., Wipf, P., Brodsky, J. L., and Bivona, T. G. (2016) Combined chemical-genetic approach identifies cytosolic HSP70 dependence in rhabdomyosarcoma. *Proceedings of the National Academy of Sciences of the United States of America* **113**, 9015-9020
10. Kityk, R., Kopp, J., and Mayer, M. P. (2018) Molecular Mechanism of J-Domain-Triggered ATP Hydrolysis by Hsp70 Chaperones. *Molecular cell* **69**, 227-237.e224
11. Wisen, S., Bertelsen, E. B., Thompson, A. D., Patury, S., Ung, P., Chang, L., Evans, C. G., Walter, G. M., Wipf, P., Carlson, H. A., Brodsky, J. L., Zuiderweg, E. R., and Gestwicki, J. E. (2010) Binding of a small molecule at a protein-protein interface regulates the chaperone activity of hsp70-hsp40. *ACS chemical biology* **5**, 611-622
12. Chiappori, F., Fumian, M., Milanesi, L., and Merelli, I. (2015) DnaK as Antibiotic Target: Hot Spot Residues Analysis for Differential Inhibition of the Bacterial Protein in Comparison with the Human HSP70. *PloS one* **10**, e0124563
13. Hassan, A. Q., Kirby, C. A., Zhou, W., Schuhmann, T., Kityk, R., Kipp, D. R., Baird, J., Chen, J., Chen, Y., Chung, F., Hoepfner, D., Movva, N. R., Pagliarini, R., Petersen, F., Quinn, C., Quinn, D., Riedl, R., Schmitt, E. K., Schitter, A., Stams, T., Studer, C., Fortin, P. D., Mayer, M. P., and Sadlish, H. (2015) The novolactone natural product disrupts the allosteric regulation of Hsp70. *Chemistry & biology* **22**, 87-97
14. Cesa, L. C., Patury, S., Komiyama, T., Ahmad, A., Zuiderweg, E. R., and Gestwicki, J. E. (2013) Inhibitors of difficult protein-protein interactions identified by high-throughput screening of multiprotein complexes. *ACS chemical biology* **8**, 1988-1997
15. Chang, L., Miyata, Y., Ung, P. M., Bertelsen, E. B., McQuade, T. J., Carlson, H. A., Zuiderweg, E. R., and Gestwicki, J. E. (2011) Chemical screens against a reconstituted multiprotein complex: myricetin blocks DnaJ regulation of DnaK through an allosteric mechanism. *Chemistry & biology* **18**, 210-221

16. Wu, T. T., Sikes, R. A., Cui, Q., Thalmann, G. N., Kao, C., Murphy, C. F., Yang, H., Zhau, H. E., Balian, G., and Chung, L. W. (1998) Establishing human prostate cancer cell xenografts in bone: induction of osteoblastic reaction by prostate-specific antigen-producing tumors in athymic and SCID/bg mice using LNCaP and lineage-derived metastatic sublines. *International journal of cancer* **77**, 887-894
17. Zacharias, N., Lee, J., Ramachandran, S., Shanmugavelandy, S., McHenry, J., Dutta, P., Millward, S., Gammon, S., Efstathiou, E., Troncoso, P., Frigo, D. E., Piwnica-Worms, D., Logothetis, C. J., Maity, S. N., Titus, M. A., and Bhattacharya, P. (2018) Androgen Receptor Signaling in Castration-Resistant Prostate Cancer Alters Hyperpolarized Pyruvate to Lactate Conversion and Lactate Levels In Vivo. *Molecular imaging and biology : MIB : the official publication of the Academy of Molecular Imaging*
18. Gao, J., Aksoy, B. A., Dogrusoz, U., Dresdner, G., Gross, B., Sumer, S. O., Sun, Y., Jacobsen, A., Sinha, R., Larsson, E., Cerami, E., Sander, C., and Schultz, N. (2013) Integrative analysis of complex cancer genomics and clinical profiles using the cBioPortal. *Science signaling* **6**, pl1
19. Cerami, E., Gao, J., Dogrusoz, U., Gross, B. E., Sumer, S. O., Aksoy, B. A., Jacobsen, A., Byrne, C. J., Heuer, M. L., Larsson, E., Antipin, Y., Reva, B., Goldberg, A. P., Sander, C., and Schultz, N. (2012) The cBio cancer genomics portal: an open platform for exploring multidimensional cancer genomics data. *Cancer discovery* **2**, 401-404

FIGURES

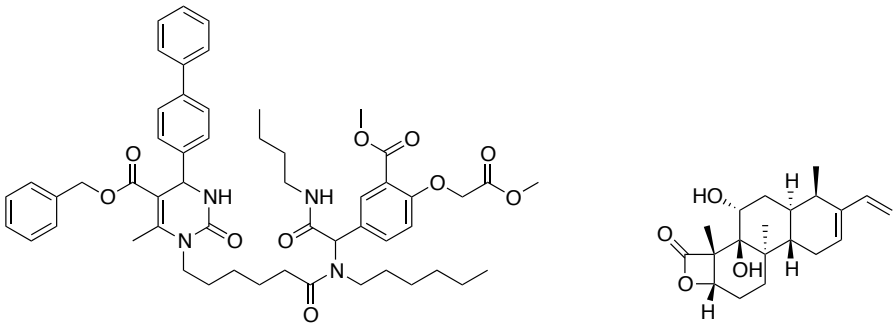

Figure 4.1: Chemical structures of MAL3-101 and novolactone

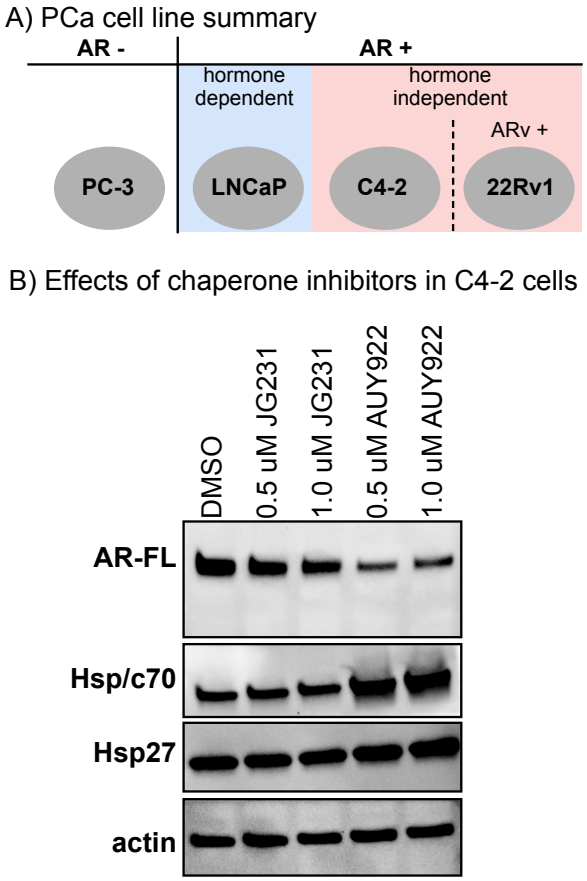

Figure 4.2: Expanded PCa cell line panel includes C4-2 cells. A) C4-2 is an AR positive cell line that is not responsive to hormone and does not express splice variants of AR. B) 6-hour treatment with JG231 and AUY922 in C4-2 cells leads to differential destabilization of AR and, in the case of AUY922, activation of a stress response.

Publishing Agreement

It is the policy of the University to encourage the distribution of all theses, dissertations, and manuscripts. Copies of all UCSF theses, dissertations, and manuscripts will be routed to the library via the Graduate Division. The library will make all theses, dissertations, and manuscripts accessible to the public and will preserve these to the best of their abilities, in perpetuity.

Please sign the following statement:

I hereby grant permission to the Graduate Division of the University of California, San Francisco to release copies of my thesis, dissertation, or manuscript to the Campus Library to provide access and preservation, in whole or in part, in perpetuity.

Isabelle Taylor
Author Signature

6/5/18
Date